AD NUMBER
AD479806
LIMITATION CHANGES
TO: **Approved for public release; distribution is unlimited.**
FROM: **Distribution authorized to U.S. Gov't. agencies and their contractors; Administrative/Operational Use; 1962. Other requests shall be referred to U.S. Naval Postgraduate School, Monterey, CA 93943.**
AUTHORITY
USNPS ltr, 23 Sep 1971

TWO-STORY STRUCTURE SUBJECTED TO IMPULSIVE LOADING

JOHN M. BAUMAN

TWO-STORY STRUCTURE

SUBJECTED TO IMPULSIVE LOADING

* * * * *

John M. Bauman

TWO-STORY STRUCTURE

SUBJECTED TO IMPULSIVE LOADING

by

John M. Bauman

Lieutenant, United States Navy

Submitted in partial fulfillment of
the requirements for the degree of

MASTER OF SCIENCE
IN
MECHANICAL ENGINEERING

United States Naval Postgraduate School
Monterey, California

1 9 6 2

TWO-STORY STRUCTURE SUBJECTED TO IMPULSIVE LOADING

by

John M. Bauman

This work is accepted as fulfilling
the thesis requirements for the degree of
MASTER OF SCIENCE
IN
MECHANICAL ENGINEERING
from the
United States Naval Postgraduate School

ABSTRACT

Experimental and analytical studies are made of the elastic and elastic-plastic response of a three degree of freedom dynamical system composed of three rigid and compact masses connected by slender columns, the bottom (heaviest) mass being suspended as a ballistic pendulum and subjected to an initial velocity step. Such a system is related to the behavior of machinery mounted in a ship subjected to an underwater explosion.

The analytical work was performed on a high speed digital computer and employed mathematical description of the structural members in which force-deflection relations depended upon previous plastic strain history.

Comparisons are made between experimental and analytical responses on the basis of the velocity-time history of the two smaller masses. Good agreement is shown.

ACKNOWLEDGMENT

The author wishes to express special appreciation to Dr. J. E. Brock, thesis adviser, for his encouragement and advice throughout the progress of this thesis.

Appreciation is also extended to the personnel of the Shock Branch, Structural Mechanics Laboratory, of the David Taylor Model Basin for their advise and assistance in the experimental portion of this thesis. Specifically, the author wishes to thank Mr. Robert L. Bort for the suggestion of the thesis topic and his assistance in the experimental development.

TABLE OF CONTENTS

1. Introduction

The present interest in the response of structures subjected to rapidly applied dynamic loads has produced an increasing amount of literature in the area of dynamic loading. The literature covers the behavior of structural metals, the response of simple structures, and the response of ships subjected to explosions. [1] , [2] , [3]*

A recent investigation conducted by Kurzenhauser [1] at the U. S. Naval Postgraduate School, Monterey, California, dealt with the behavior of a simple plane structure in which the horizontal (roof) member was of great stiffness compared to the columns and in which the greatest part of the mass and weight was in the roof. The loading was an impact in the plane of the structure and at the roof level. This system could be adequately approximated by a single degree of freedom model and a simple theoretical analysis, based essentially on energy considerations, was able to make good predictions of experimental behavior.

In the case of a similar multi-story structure, the energy is divided between the various roof and floor masses and it is not possible to use energy considerations alone to obtain a theoretical prediction of dynamic behavior. Thus, analysis of a system above a single degree of freedom requires evaluation of the various equations of motion of the system. If the structure passes into the plastic region, a suitable assumption must be made to compute the behavior in this region. The numerical manipulations required in solving such a problem become enormous and the use of a high speed digital computer becomes necessary.

This thesis deals with a small two-story structure mounted on a large movable mass. The entire system was reduced to a three degree of

*Numbers in [ ] refer to Bibliography.

freedom system. This particular system can be likened to a piece of equipment mounted to a ship's hull. The ship is then subjected to an underwater explosion and the system's response is studied. Reference [3] gives examples of equipment and machinery damage and response, wherein illustrations of actual shipboard foundation failures are presented along with a typical velocity history for a mild shock. The ability to predict the response of such a system would aid in the original design of such structures.

A mathematical model was evolved for the above system and a comparison made between the response predicted by the mathematical model and a test structure.

It is felt necessary to mention the fact that the experimental portion of the project was carried out prior to the evaluation of the mathematical model and certain complications arose in the mathematical evolution that would have been eliminated had the sequence been reversed. The values obtained from the mathematical model will be referred to as the "theoretical results" throughout; however, these results cannot be truly classified as "theoretical" since a large amount of experimentation with the mathematical model was necessary before a suitable comparison could be made.

The experimental portion of the thesis was conducted entirely at the David Taylor Model Basin, Carderock, Md., during the period 30 June to 19 July 1961. The theoretical investigation and reduction of data was carried out at the U. S. Naval Postgraduate School, Monterey, California, during the period 1 January 1962 to 1 April 1962, utilizing the Control Data Corporation 1604 computer.

The experimental investigation will be discussed before the theoretical considerations due to the fact that this was the order in which they were actually conducted. A better understanding of the complications introduced in the theoretical considerations will be obtained if the factors responsible for the complications are presented first.

2. Experimental Investigation

Test Structure

The test structure consisted of two rectangular hot rolled steel bars measuring 2" x 2" x 12", separated and supported by two sets of 1/8" x 2" hot rolled steel columns. Figure (1a) shows a sketch of th structure without the attached measuring equipment. The only variation made to the test structure was the introduction of 3003-H14 aluminum columns for ten (10) of the twenty-six (26) test runs. These columns also measured 1/8" x 2".

The length of the supporting columns, prior to mounting was 12". Holes measuring 3/8" in diameter were drilled on the centerline one inch from each end of the supporting columns to accommodate a 3/8"-NC bolt for clamping the supports to the base and bars mentioned above.

The rectangular bars and base were drilled and tapped for 3/8"-NC threads 3/4" deep at both ends, to receive the securing bolts. Holes measuring 3/8" in diameter were also drilled in the sides of the bars for attachment of the velocity meters used in the test. Small metal bases, fitted to receive the accelerometers used in the test, were welded to the upper surfaces of each of the rectangular bars.

The entire clamping of the supporting columns was accomplished by the single 3/8"-NC bolt along with a 1/8" x 2" x 2" clamping plate, see figure (1b). The spacing between the base to the center bar and the distance between the center bar to the upper bar was approximately 8".

The single screw attachment of the columns to the base and bars proved to be weak as far as giving good fixity at these junctions. This poor fixity caused the effective length of the columns to be somewhat in excess of the actual free length of 8". Figure (2) is a picture of the

fully instrumented test structure. The velocity meter coils are on the side seen on the picture. The accelerometers are on the upper surfaces facing toward the left.

The base of the structure contained two 2" x 2" x 2" hot rolled steel blocks to be used for attachment of the supporting columns. The base was designed to fit a mounting block already attached to the ballistic pendulum used in the tests.

Since the width of the supporting columns was large in comparison with the thickness, the structure's motion was limited to a single plane.

Ballistic Pendulum

The ballistic pendulum was used as the means for producing the impulsive loading on the structure. A picture of the pendulum is shown in figure (3).

The ballistic pendulum consisted of four major components: 1. The anvil, upon which the test structure was mounted. 2. The hammer, which transferred its energy to the anvil producing the impulsive load. 3. The hammer hold-back and release mechanism. 4. The anvil hold-back and catching system.

The hammer consisted of a solid steel cylinder, 8" in diameter and 48" in length. Four smaller cylinders were mounted on the sides to receive the supporting wires from the overhead. These cylinders were 4" in diameter and 6-1/2" in length. The total weight of the hammer was 785.1 lbs.

The anvil was likewise 8" in diameter; however, its length was 36". The four supporting cylinders measured 3.5" in diameter and 7" in length. The supporting cables were 8 ft in length $\pm$1". The total weight of the anvil was 598.6 lbs.

The hammer hold-back and release mechanism consisted of an electric hoist to pull the hammer back to an elevated position, the initial position depending upon the impact desired. The release mechanism consisted of an electro-magnetic latch which could be operated from a remote station near the recording instruments.

The anvil hold-back and catching system consisted of a ratchet pulley and a tie-back line. The line was attached to the anvil at one end, passed through the pulley and carried a 25 lb. weight at the free end. Upon impact the anvil was forced back and elevated. The 25 lb. weight pulled the line through the ratchet pulley and the anvil was prevented from returning upon reaching its maximum elevation.

The ratchet catching system was used to prevent interference between the anvil supporting wires and the test structure. The proximity of the test structure and the anvil supporting wires, when the anvil was in its equilibrium position, was such that the structure came into contact with the supporting wires upon impact. To eliminate this, the anvil was pulled back approximately 8-1/2" horizontally prior to impact.

Since the experimental testing was conducted prior to a thorough theoretical investigation, the significance of this initial anvil position was not realized, and the exact initial horizontal location of the anvil was not recorded. Upon examination of the theoretical aspects it was found that this initial position was quite significant and complicated the theoretical solution of the problem. More will be said concerning this later.

Measuring Equipment

The test structure was instrumented with three bar-magnet velocity meters manufactured and calibrated by the David Taylor Model Basin. One

velocity meter was mounted on each of the three concentrated masses of the structure. The meter mounted on the anvil had a sensitivity of 146 mv/fps, the meter on the center mass (lower rectangular bar) had a sensitivity of 167 mv/fps, and the third meter, mounted on the upper mass (upper rectangular bar), had a sensitivity of 151 mv/fps. From tests conducted by the David Taylor Model Basin, it was determined that the sensitivities varied approximately $\pm 3\%$ over a 4 inch stroke.

Two Statham accelerometers were mounted, one each, on the upper and center masses of the test structure.

The output from the velocity meters went to the Velocity Meter Control Unit (Attenuator), manufactured by the David Taylor Model Basin. No amplification was possible with this unit, the maximum output being one times the input. This unit also permitted a convenient switching arrangement for obtaining a calibration trace on the oscillograph.

The output from the Control Unit was picked up by a Consolidated Electrodynamics Corporation Recording Oscillograph. The oscillograph utilized galvanometers of the fluid damped type for recording the velocity response on the oscillograph record. The galvanometers had a natural frequency of 1000 cps.

Outputs from the accelerometers were amplified by Consolidated Engineering Corporation 3-KC Carrier Amplifiers. The power supply for the above amplifiers consisted of a Consolidated Engineering Corporation Oscillator-Power Supply. The amplified accelerometer signals were then received by the above mentioned oscillograph.

A General Radio Company, 1000 cycle, Vacuum-Tube Fork was used to produce a time reference trace on the oscillograph record. The oscillograph also produced a time reference; however, it was felt that the 1000

cycle trace would provide a good check on the oscillograph's time scale.

Since difficulty was encountered with the interference between the test structure and the anvil supporting wires, an extra galvanometer was utilized for recording an indication of contact between the wires and the structure. This consisted of a simple battery circuit, using the point of probable contact as the switch. When wires and structure made contact, a pulse was recorded on the oscillograph record, the duration of this pulse gave the period of contact. Figure (4) shows a sketch of the instrumentation.

Appendix VI gives a tabulation of the various instrument serial and model numbers.

Test Procedure

The following steps were followed for a typical test run

1. The structure's columns (springs) were placed in position and securely fastened.

2. The anvil was elevated to a position where interference between the structure and supporting wires would not be encountered.

3. The velocity meter magnets were adjusted to insure free passage as the anvil moved away.

4. The hammer was elevated to a predetermined position, depending upon the step input desired, using the electric hoist.

5. The recording oscillograph was operated at a paper speed of 4 in./sec. and velocity meter and accelerometer calibration traces were recorded.

6. All calibration settings for the various instruments were recorded.

7. The instruments were then set for the predetermined settings for the actual run, and all values recorded.

8. The recording oscillograph was operated at a paper speed of 40 in./sec. and the hammer released.

9. The oscillograph was secured when the velocity meter magnets were free from the coils or, for the lower input runs, when it was felt sufficient data were recorded.

List of Symbols

a - initial horizontal anvil displacement

b - width of rectangular supporting column

E - modulus of elasticity

F_i - force produced by flexure of columns ($i = 1,2$)

g - acceleration of gravity (32.2 ft/sec^2)

h - thickness of rectangular supporting columns

H - (subscript) denotes horizontal component

I - moment of inertia of the cross section

k - spring constant in elastic range

k^* - spring constant in plastic range

ℓ - column length

L - length of anvil supporting cable

M_i - mass ($i = 1,2,3$)

M_u - fully plastic bending moment

Q - axial load on columns produced by structures weight

R - tension in hold-back line

T - tension in supporting cables

V - (subscript) denotes vertical component

x_i - horizontal displacement of M_i

x_u - relative spring displacement at which the fully plastic bending moment is realized

y_i - vertical displacement of anvil

$\bar{\sigma}$ - dynamic yield strength

3. Theoretical Considerations

Mathematical Model

The mathematical model of the two-story structure can be visualized as a mass - spring system as shown in figure (5a). This idealization reduces the structure to a three degree of freedom system. Figure (5b) shows the free body diagram for the system. The M_i symbols denote the masses of the anvil, center mass, and upper mass respectively, the F_i symbols denote the forces produced by the flexure of the columns, and the X_i denote displacements of the respective masses.

Summing forces for each mass results in the following equations of motion,

$$\ddot{X}_1 = -\frac{F_1 + T_H}{M_1} \tag{1}$$

$$\ddot{X}_2 = \frac{F_1 - F_2}{M_2} \tag{2}$$

$$\ddot{X}_3 = \frac{F_2}{M_3} \tag{3}$$

where the force T_H is the horizontal component of the force in the supporting cables.

Letting "L" denote the length of the anvil supporting wire, "a" the horizontal distance that the anvil is initially displaced, "x_1", the displacement of the anvil from the initial position "a", and "y_1", the vertical displacement of the anvil, we have from figure (6a),

$$L^2 = (a + x_1)^2 + (\mathcal{L} - y_1)^2$$

where,

$$\mathcal{L} = \sqrt{L^2 - a^2}$$

In figure (6b) "W" is the total weight of the anvil plus structure (W = 656 lbs.). The symbol "T" denotes the tension in the supporting cables.

The symbol "R" denotes the hold-back wire reaction which immediately reduces to zero upon impact. From figure (6b) we may write,

$$T_V = 656 + \frac{656}{g}\ddot{y}_1 \tag{4}$$

$$\frac{T_H}{T_V} = \frac{\sin\theta}{\cos\theta} = \frac{a + x_1}{\mathcal{L} - y_1} \tag{5}$$

from figure (6a),

$$y_1 = \mathcal{L} - \sqrt{L^2 - (a + x_1)^2} \tag{6}$$

$$\dot{y}_1 = \frac{(a + x_1)\,\dot{x}_1}{\mathcal{L} - y_1} \tag{7}$$

$$\ddot{y}_1 = \frac{(a + x_1)\,\ddot{x}_1 + \dot{x}_1^2 + \dot{y}_1^2}{\mathcal{L} - y_1} \tag{8}$$

By substitution of equation (8) into equation (4) and then combining with equation (5), we arrive at a value for T_H in terms of known or computed variables. Substituting this value of T_H back into equation (1) and solving for $\ddot{x}_1$ produces,

$$\ddot{x}_1 = \frac{-F_1 - \left(\frac{a + x_1}{\mathcal{L} - y_1}\right) 656 \left[1 + \frac{\dot{x}_1^2 + \dot{y}_1^2}{9(\mathcal{L} - y_1)}\right]}{M_1 + \left(\frac{a + x_1}{\mathcal{L} - y_1}\right)^2 \cdot \frac{656}{9}} \tag{9}$$

The three equations describing the response of the model are equations (2), (3), and (9).

Basic Considerations

The test structure followed closely to the portal frame used by Kurzenhauser in his tests, the major differences being in the number of degrees of freedom and the method of loading. The portal frame had a fixed base and the loading took place through the upper mass of the structure. The two-story structure used in these tests was loaded through its

base, which was attached to a movable mass.

When deformations beyond the elastic limit were encountered, it became necessary to deviate from Hooke's Law and to study the behavior in the plastic region. Since the entire system was reduced to a spring - mass system it became necessary to assume a force versus deflection relationship that would satisfy the behavior of the structure as it passed from the elastic region into the plastic region. Figure (7) shows the assumed force versus relative deflection response.

The structure's columns behaved elastically up to the relative deflection corresponding to X_u, whereupon the behavior departed from Hooke's Law. The simplest way to represent the complicated response in the elastic-plastic deformation, is to assume two linear spring constants, (slope of the lines represented by the force deflection curve) one for the elastic range and a second for the plastic range. The elastic spring constant is represented by k and the plastic spring constant by k*. Upon loading, the columns follow the elastic spring constant (k) until yielding of the columns takes place, then they follow the plastic spring constant (k*). When unloaded, the columns follow the displaced elastic spring constant (k), forming an hysteresis loop as indicated in the figure.

It is assumed that the transition from the elastic bending moment to the fully plastic bending moment in the column cross-sections, occurs instantaneously at the deflection corresponding to X_u.

For rectangular cross-sections, the fully plastic bending moment is defined by the relation,

$$M_u = \frac{\bar{\sigma} b h^2}{4}$$

where $\bar{\sigma}$ is the yield point or yield strength of the material involved, b is the width of the column, and h is the thickness of the column.

A force analysis of one of the columns in the elastic region will permit evaluation of the elastic spring constant. Referring to figure (8a), and utilizing the cantilever beam deflection equations gives the following results,

$$\frac{X}{2} = \frac{\left(\frac{F}{2}\right)\left(\frac{\ell}{2}\right)^3}{3EI}$$

$$X = \frac{F\ell^3}{24EI}$$

Where: F = total forcing function on two supporting columns
E = modulus of elasticity
I = moment of inertia

Considering the influence of the compressive force Q, where Q denotes the total compressive force on two columns and Q_e is the critical Euler column loading for two columns, we have,

$$K = \frac{F}{X} = \frac{24EI}{\ell^3}\left[1 - \frac{Q}{Q_e}\right] \qquad (10)$$

where,

$$Q_e = \frac{2\pi^2 EI}{\ell^2}$$

It has been shown that the approximation used in equation (10) "is sufficiently accurate almost up to the critical value of the load." [6]

A force analysis of one of the supporting columns, figure (8b), when M_u is achieved, gives the following for small deflections,

$$\Sigma M_A = 0$$
$$2M_u = \frac{Q}{2}X + \frac{F}{2}\ell$$
$$F = -\frac{Q}{\ell}X + \frac{4M_u}{\ell} \qquad (11)$$

Equation (11) is the equation of the straight line representing the plastic region shown on the force-deflection diagram of figure (7). The

spring constant k* for the plastic region is therefore the slope of this line,

$$K^{*} = -\frac{Q}{\ell} \tag{12}$$

It will be noted from figure (7) that, at the deflection x_u, the spring force represented by equation (10) for the elastic region is equal to the force represented by equation (12) for the plastic region. Equating these two produces the following,

$$\frac{24 E I X_u}{\ell^3}\left[1 - \frac{Q}{Q_e}\right] = -\frac{Q}{\ell}X_u + \frac{4 M_u}{\ell} \tag{13}$$

The value for x_u can be easily obtained from equation (13).

Complications Introduced by Experimental Set-up

The two major problems that arose from the experimental model were the failure to record the initial anvil displacement prior to impact and the lack of fixity of the supporting columns.

Since the initial anvil displacement was not recorded, it became necessary to determine this value from the available information. This was accomplished by plotting the sum of the system's total momentum versus time for both the experimental and theoretical values. The initial displacement "a" used in equation (9) was varied through a reasonable range until agreement with the experimental points was obtained. Figure (9) is a representative plot. The above mentioned comparison between theoretical and experimental was made for each run where sufficient values of anvil velocity were available. Since the length of the velocity trace depended upon the time the magnet departed the velocity meter coil, the values for

the anvil velocity for the plastic runs were not available beyond about 50 to 100 M (millis conds). The value obtained for the initial anvil displacement utilizing the above method was consistently 0.7 ft. The value arrived at for this displacement should have been fixed for all runs, as indicated from the plots, since the anvil was moved to the same position for each run during the actual tests.

The value (a = 0.7') was therefore used for all runs with the exception of two of the low input steel runs, which definitely indicated a lower value for "a".

The lack of fixity of the supporting columns introduced a problem as to the value for effective length in the formulae for determing k and k*. The effective length was varied until phase agreement (peaking at the same time) was achieved. The effective lengths found necessary were 9.0 inches for steel and 8.75 inches for aluminum.

4. Numerical Solution

Reduction of Equations for Computer

The first step in reducing the equations to a suitable form for introduction into the computer was to reduce the three second order equations (2), (3), and (9) to six first order equations. Introducing the following dummy variables,

$$\xi = \dot{X}_1$$
$$\eta = \dot{X}_2$$
$$\gamma = \dot{X}_3$$

then,

$$\dot{\xi} = \ddot{X}_1$$
$$\dot{\eta} = \ddot{X}_2$$
$$\dot{\gamma} = \ddot{X}_3$$

the six first order equations then become,

$$\dot{X}_1 = \xi \tag{14}$$

$$\dot{X}_2 = \eta \tag{15}$$

$$\dot{X}_3 = \gamma \tag{16}$$

$$\dot{\xi} = \frac{-F_1 - \left(\frac{a+x_1}{\ell - y_1}\right) 656 \left[1 + \frac{\xi^2 + \dot{y}_1^2}{g(\ell - y_1)}\right]}{M_1 + \left(\frac{a+x_1}{\ell - y_1}\right)^2 \cdot \frac{656}{g}} \tag{17}*$$

$$\dot{\eta} = \frac{F_1 - F_2}{M_2} \tag{18}$$

$$\dot{\gamma} = \frac{F_2}{M_3} \tag{19}$$

---

* Note that $\ell - y_1$, and $\dot{y}_1$ are given by algebraic relations involving x_1 and ξ ; see Equations (6) and (7), page 12 .

Letting the symbol D denote the dependent variable, Y denote the independent variable, and introducing the following equivalent symbols,

$D_1 = \ddot{\xi}$ $\quad Y_1 = X_1$ $\quad CC = a + X_1$

$D_2 = \ddot{\eta}$ $\quad Y_2 = X_2$ $\quad CK = \mathcal{L} - Y_1$

$D_3 = \ddot{\gamma}$ $\quad Y_3 = X_3$ $\quad YV = \dot{Y}_1$

$D_4 = \dot{\xi}$ $\quad Y_4 = \xi$

$D_5 = \dot{\eta}$ $\quad Y_5 = \eta$

$D_6 = \dot{\gamma}$ $\quad Y_6 = \gamma$

produces the following equations written in the Fortran language,

```
D(1) = Y(4)
D(2) = Y(5)
D(3) = Y(6)
D(4) = (-F(1) - (CC/CK) * 656. * (1. + ( Y(4)**2 + YV**2)/
       (32.20 *CK)))/(18.9+656./32.20)*(CC/CK) **2 )
D(5) = (F(1) - F(2))/ 0.711
D(6) = F(2) / 0.705
```

Appendix I contains the Main Flow Chart, the Force versus Relative Deflection Flow Chart, and the actual Fortran program. The program traces the time history of the displacements, velocities, and accelerations* of the three masses M_1, M_2, and M_3 starting with the initial conditions $x_1 = x_2 = x_3 = 0$; $V_2 = V_3 = 0$, $V_1 = \text{STEP}$.

---

*Accelerations are given in the actual computer print-out, however, they were not used in the analysis and have been trimmed off the sheets shown in Appendix V. Also, the print statement shown in Appendix I does not produce displacements. Displacements were, however, printed in an earlier version and it would be very easy to restore them.

Numerical Integration System

The numerical integration system used was the Runge-Kutta method. The two major advantages of this system, as stated by Milne [8], are:

1. No special starting procedure is required.
2. The length of the time interval may be altered during the computation.

The reasons for utilizing the Runge-Kutta method are: first of all the fact that the integration relies upon the last computed point, as listed in advantage number one above, secondly, the routine was already available for immediate use in the U. S. Naval Postgraduate School computer center.

The system, as with many numerical integration systems, is based on the Taylor Series. For a single first order differential equation $y' = f(t, y)$ the following computations are completed to arrive at a value $y(t + \Delta t)$,

$$K_1 = \Delta t\, f(t, y)$$

$$K_2 = \Delta t\, f\left(t + \frac{\Delta t}{2},\ y + \frac{1}{2} K_1\right)$$

$$K_3 = \Delta t\, f\left(t + \frac{\Delta t}{2},\ y + \frac{1}{2} K_2\right)$$

$$K_4 = \Delta t\, f(t + \Delta t,\ y + K_3)$$

$$y(t + \Delta t) = y_t + \frac{1}{6}\left[K_1 + 2K_2 + 2K_3 + K_4\right]$$

The same basic procedure as above can be applied to a system of first order equations such as the six equations shown previously.

5. Graphical Comparison of Results

This section shows a graphical comparison of the experimental results, represented by the circled points, and the theoretical response predicted by the mathematical model, represented by the smooth curves.

The first section displays the results of sixteen runs using steel columns. The first seven plots contain a single theoretical curve since these columns experienced no plastic deformation. The next nine plots display three theoretical curves corresponding to dynamic yield strengths of 40,000 psi, 50,000 psi, and 60,000 psi. The last two plots repeat two of the runs extending the time cut-off to 200 MS.

The second section displays the results of ten runs using aluminum columns. The first three runs are in the elastic region and therefore display the single theoretical curve. The remaining seven runs display two theoretical curves for dynamic yield strengths of 20,000 psi and 30,000 psi. The theoretical curves shown on pages 44 , 45 , and 46 actually merge, within plotting error, from approximately 90 MS to 100 MS.

The term "Step" denotes the initial anvil velocity upon impact (ft/sec). It was determined from the velocity meter mounted on the anvil.

Section One - Steel

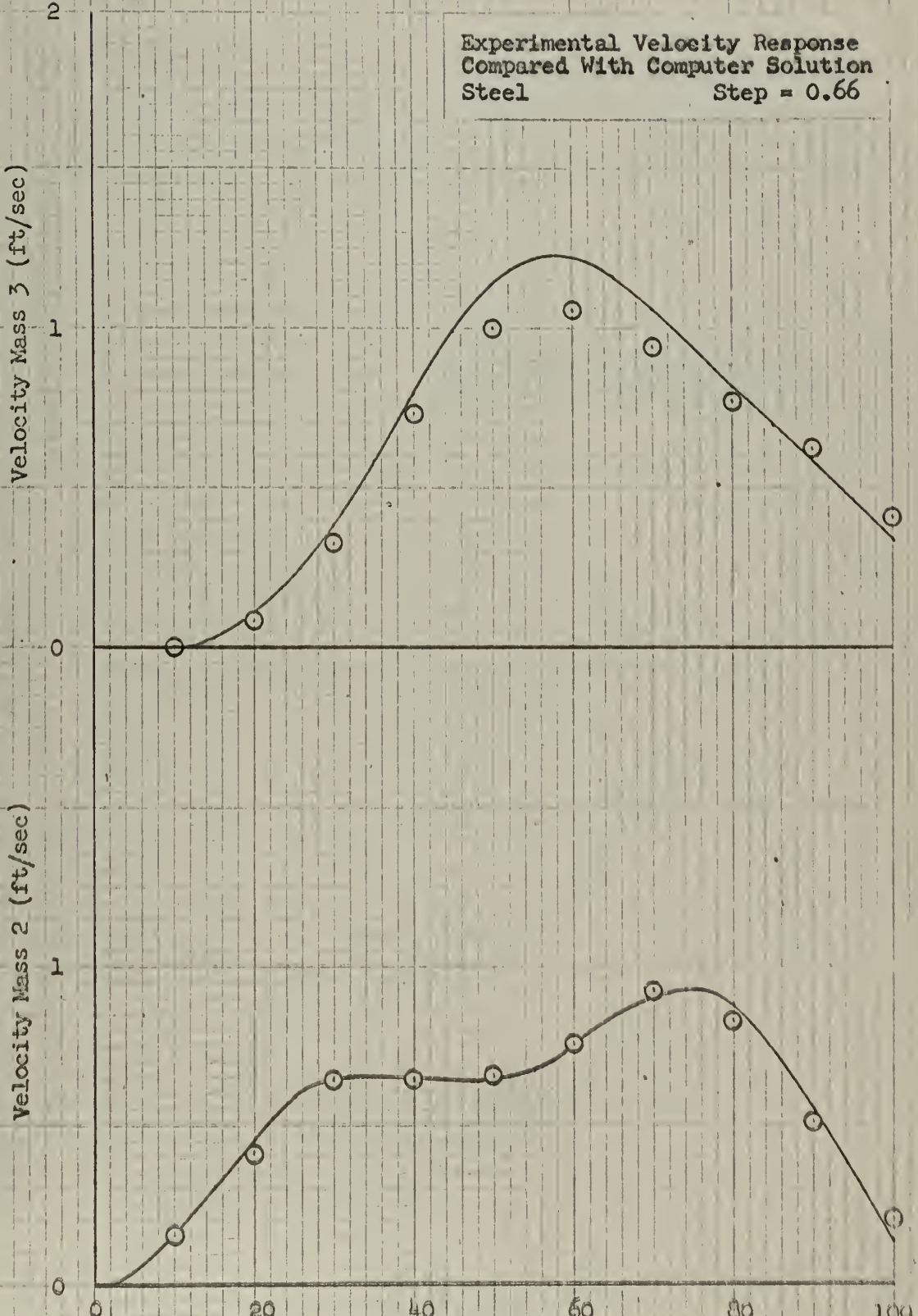
Experimental Velocity Response
Compared With Computer Solution
Steel
Step = 0.66
Velocity Mass 3 (ft/sec)
Velocity Mass 2 (ft/sec)
2
1
0
1
0
0
20
40
60
80
100
Time (MS)

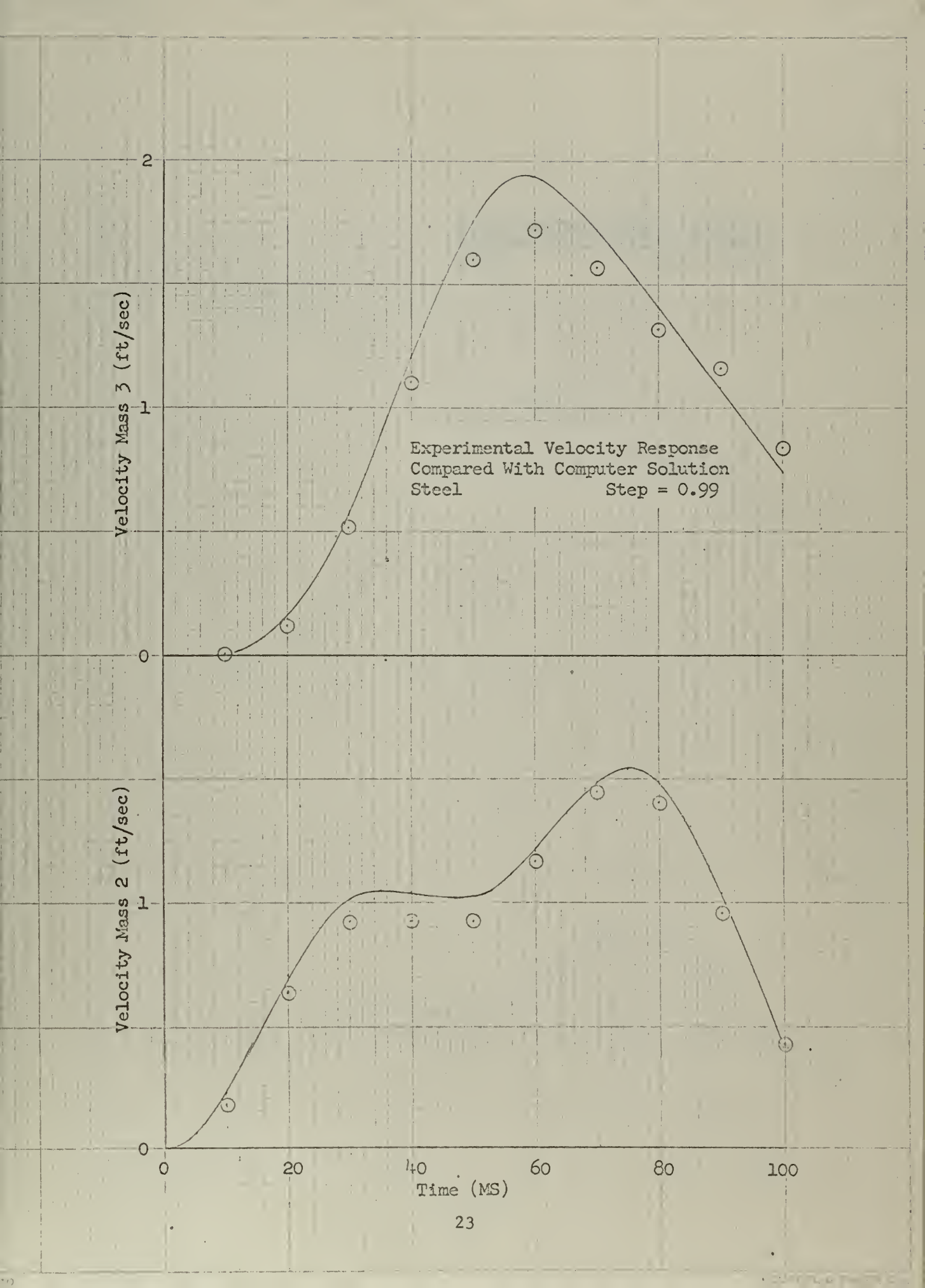
Velocity Mass 3 (ft/sec)
2
1
0
Experimental Velocity Response
Compared With Computer Solution
Steel
Step = 0.99
Velocity Mass 2 (ft/sec)
1
0
0
20
40
60
80
100
Time (MS)

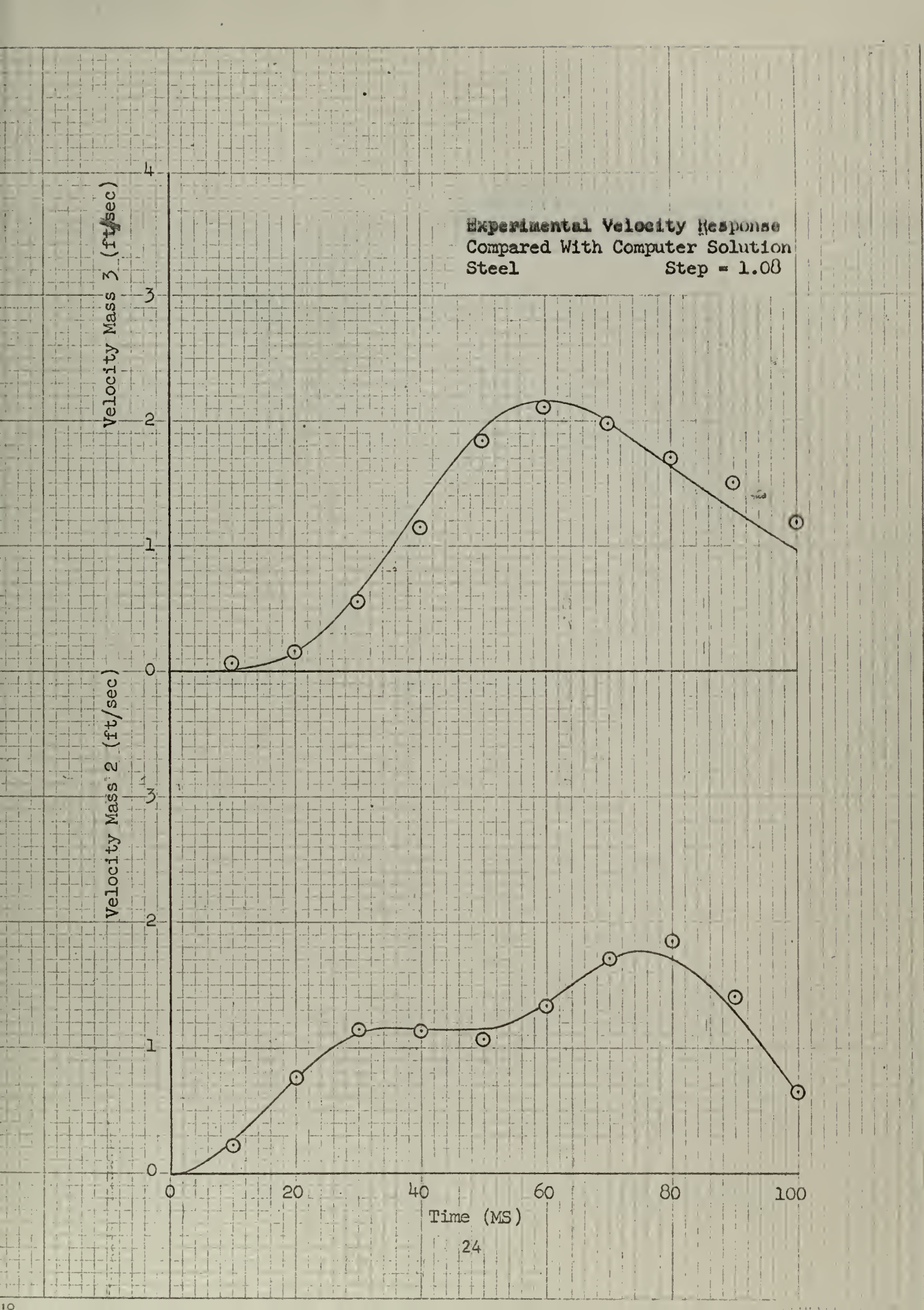
Experimental Velocity Response
Compared With Computer Solution
Steel
Step = 1.08
Velocity Mass 3 (ft/sec)
Velocity Mass 2 (ft/sec)
0
1
2
3
4
0
20
40
60
80
100
Time (MS)

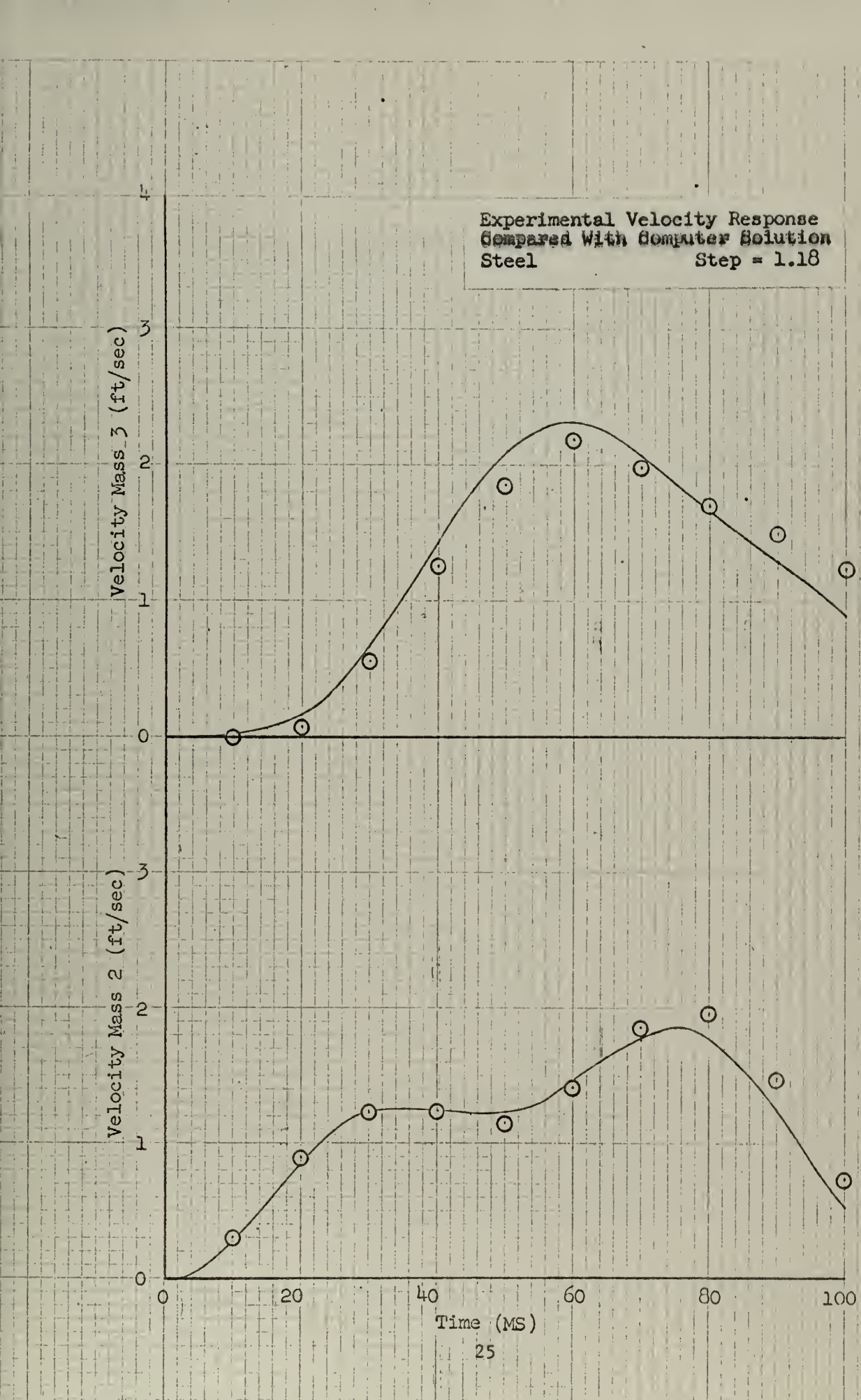
Experimental Velocity Response
Compared With Computer Solution
Steel
Step = 1.18
Velocity Mass 3 (ft/sec)
Velocity Mass 2 (ft/sec)
0
1
2
3
4
0
20
40
60
80
100
Time (MS)

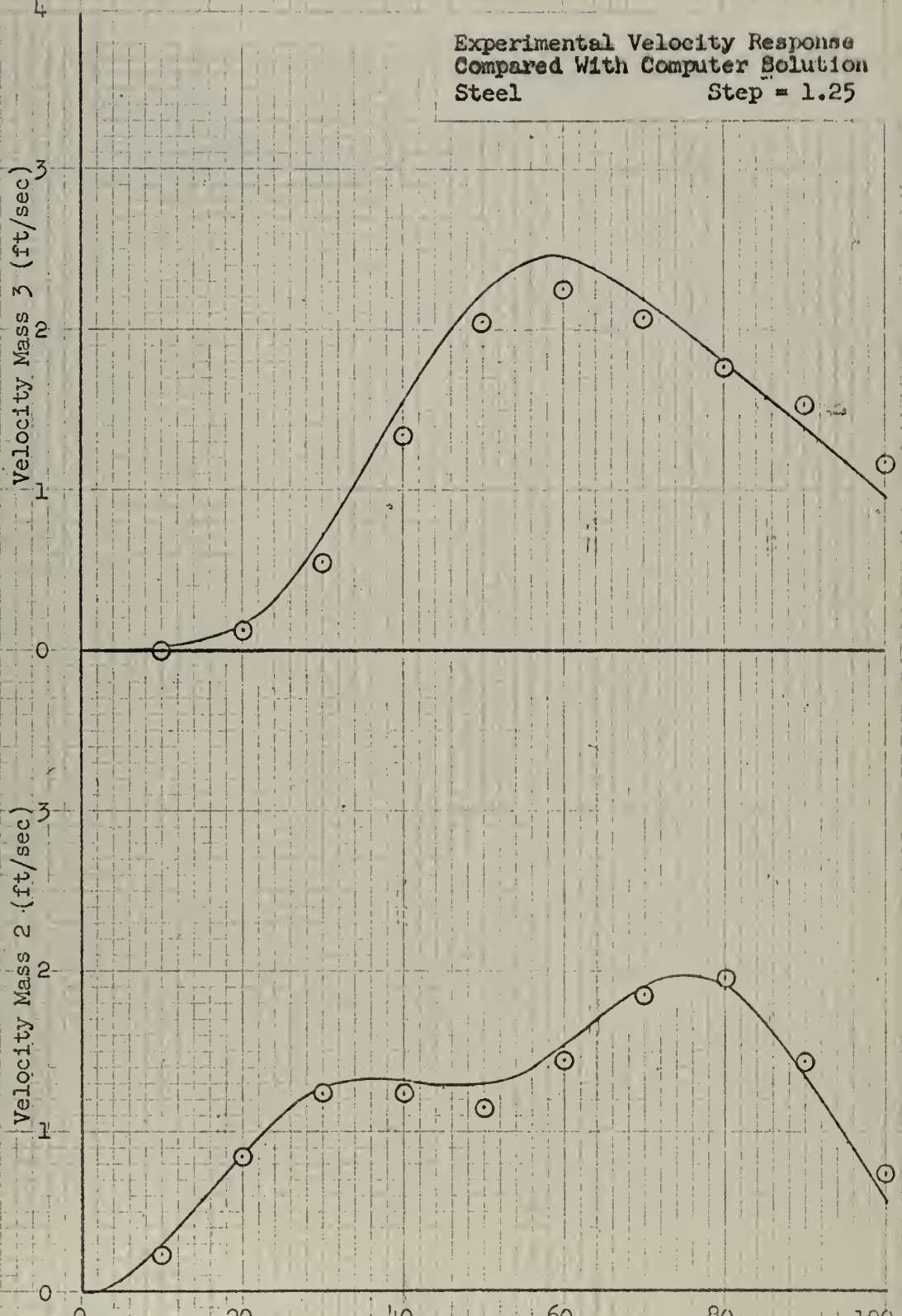
Experimental Velocity Response
Compared With Computer Solution
Steel
Step = 1.25
Velocity Mass 3 (ft/sec)
Velocity Mass 2 (ft/sec)
0
1
2
3
4
0
20
40
60
80
100
Time (MS)

Experimental Velocity Response
Compared With Computer Solution
Steel Step = 1.82

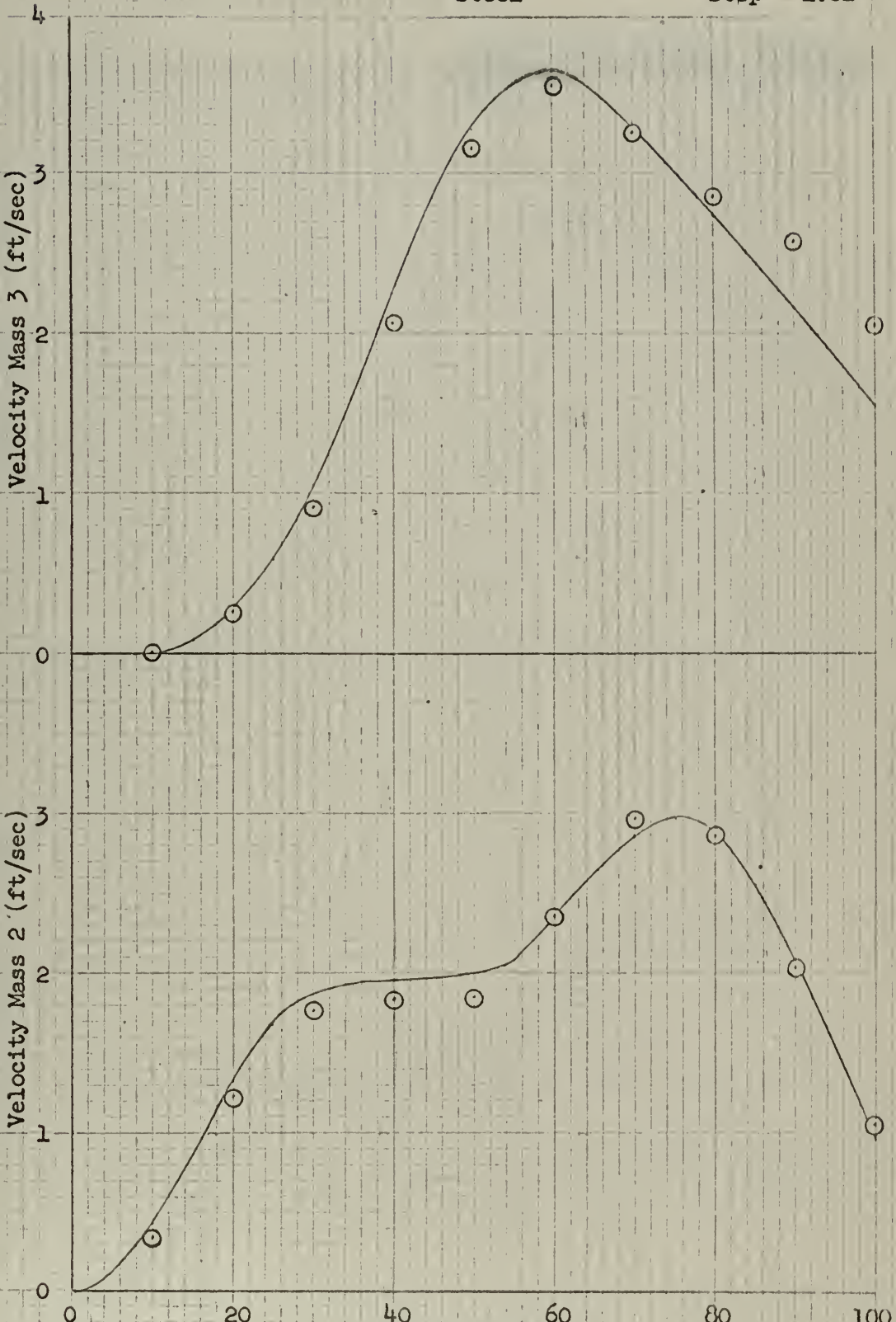

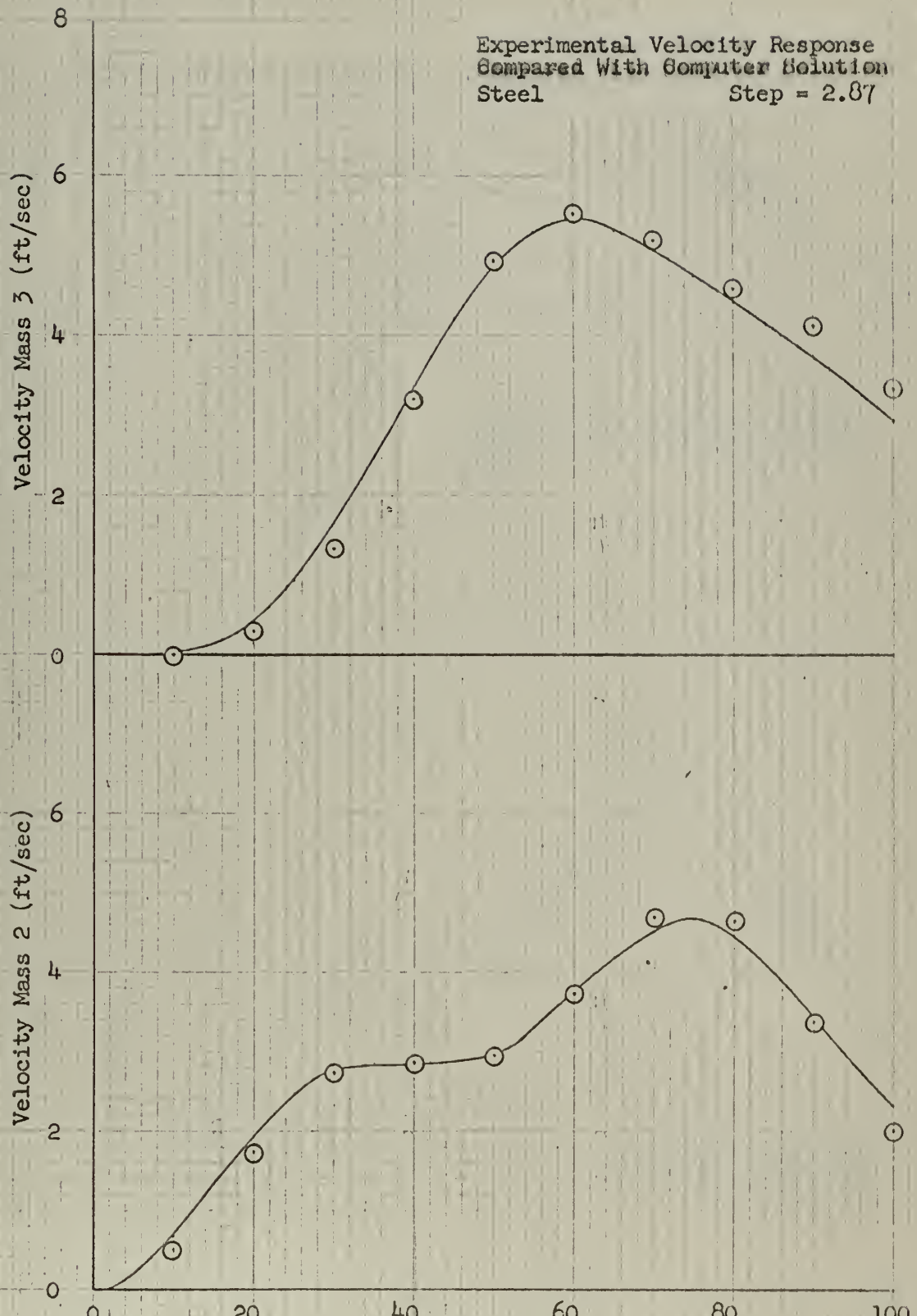
Experimental Velocity Response
Compared With Computer Solution
Steel
Step = 2.87
Velocity Mass 3 (ft/sec)
Velocity Mass 2 (ft/sec)
8
6
4
2
0
0
20
40
60
80
100
Time (MS)

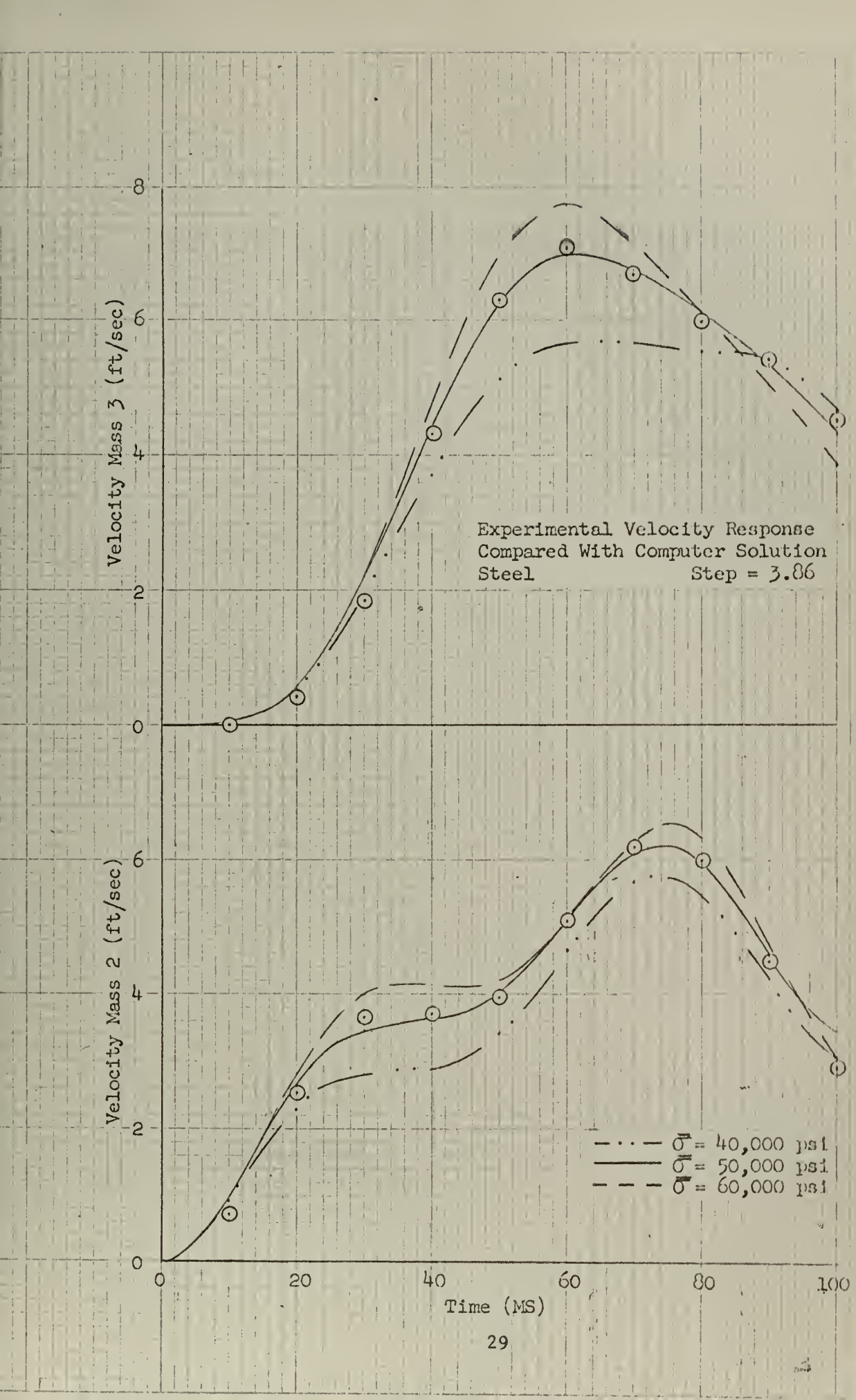
Velocity Mass 3 (ft/sec)
Velocity Mass 2 (ft/sec)
Time (MS)
0
20
40
60
80
100
2
4
6
8
Experimental Velocity Response
Compared With Computer Solution
Steel
Step = 3.86
σ = 40,000 psi
σ = 50,000 psi
σ = 60,000 psi

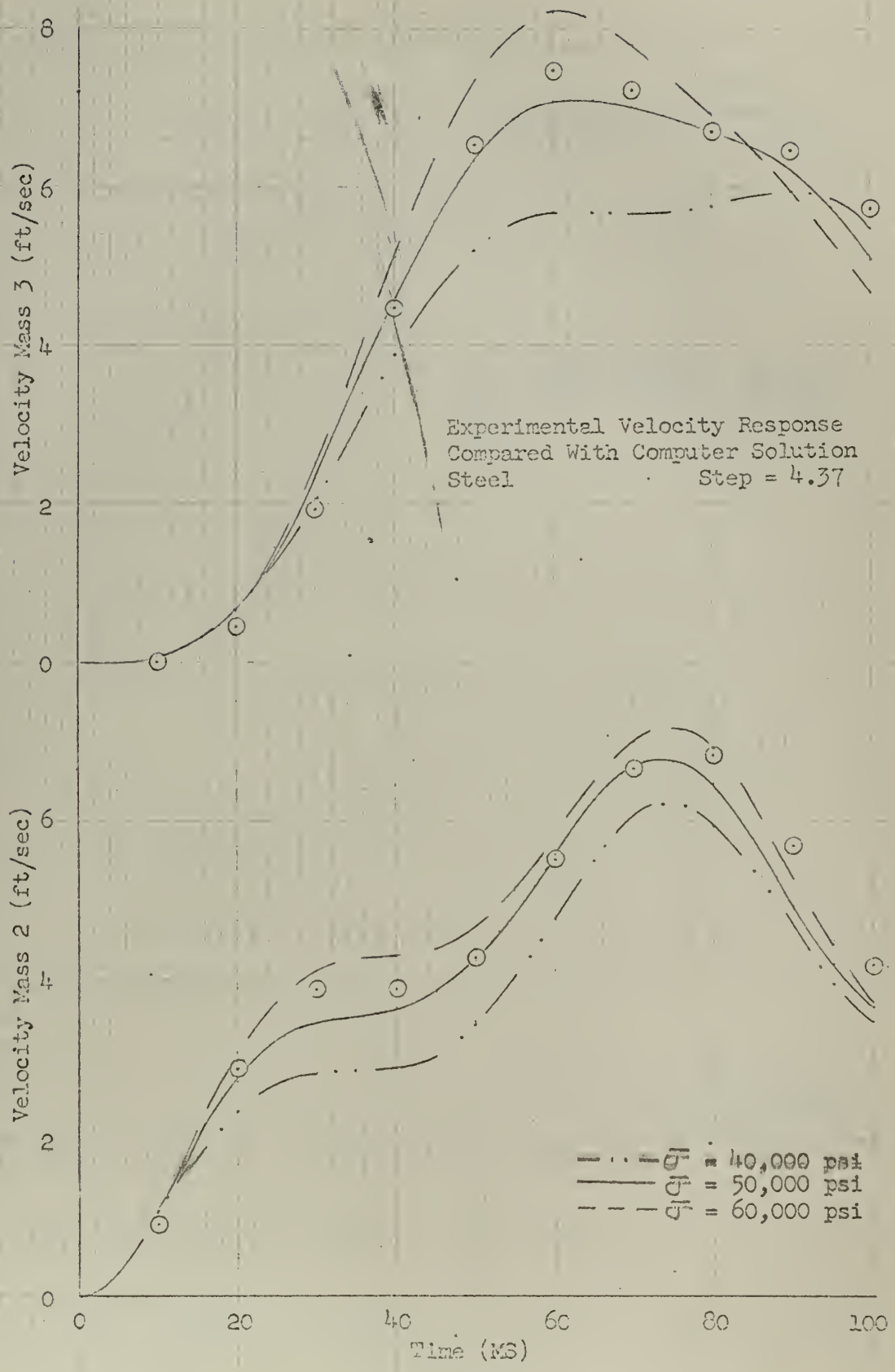
Velocity Mass 3 (ft/sec)
Velocity Mass 2 (ft/sec)
Time (MS)
0
20
40
60
80
100
Experimental Velocity Response
Compared With Computer Solution
Steel
Step = 4.37
σ = 40,000 psi
σ = 50,000 psi
σ = 60,000 psi

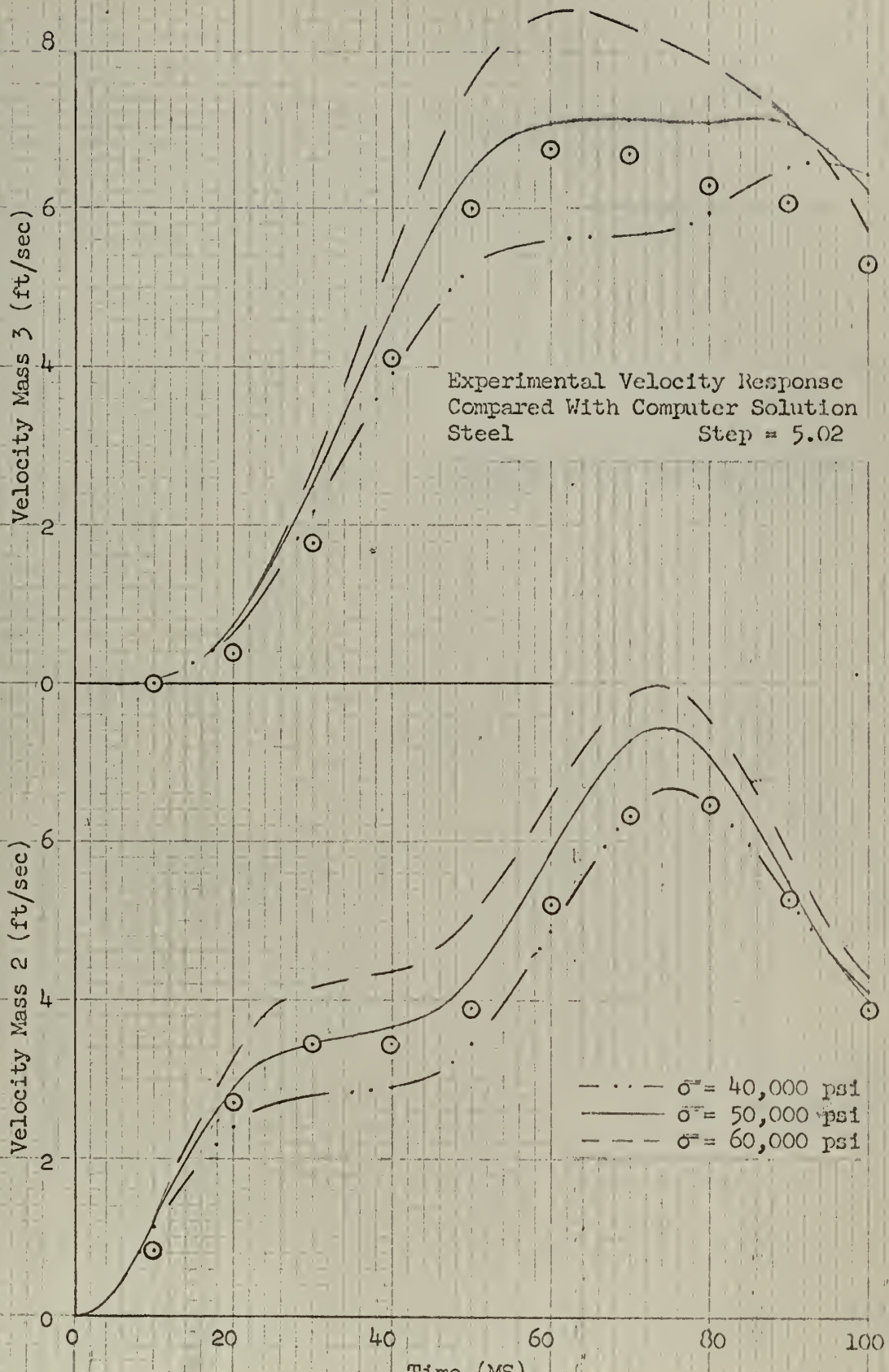
Experimental Velocity Response
Compared With Computer Solution
Steel
Step = 5.02
Velocity Mass 3 (ft/sec)
Velocity Mass 2 (ft/sec)
8
6
4
2
0
6
4
2
0
0
20
40
60
80
100
Time (MS)
σ = 40,000 psi
σ = 50,000 psi
σ = 60,000 psi

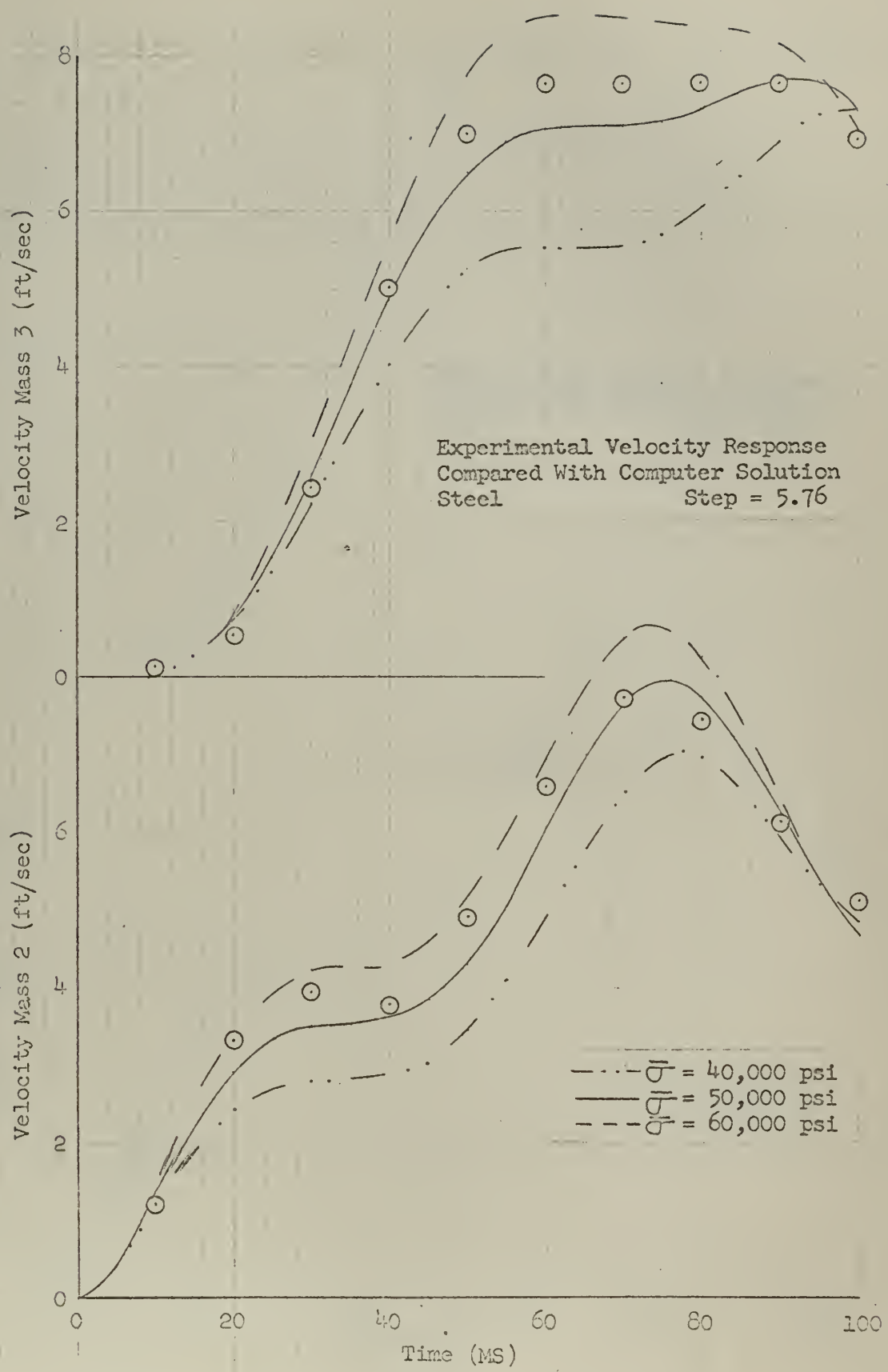
Velocity Mass 3 (ft/sec)
Velocity Mass 2 (ft/sec)
Time (MS)
0
2
4
6
8
0
20
40
60
80
100
Experimental Velocity Response
Compared With Computer Solution
Steel
Step = 5.76
$\bar{\sigma}$ = 40,000 psi
$\bar{\sigma}$ = 50,000 psi
$\bar{\sigma}$ = 60,000 psi

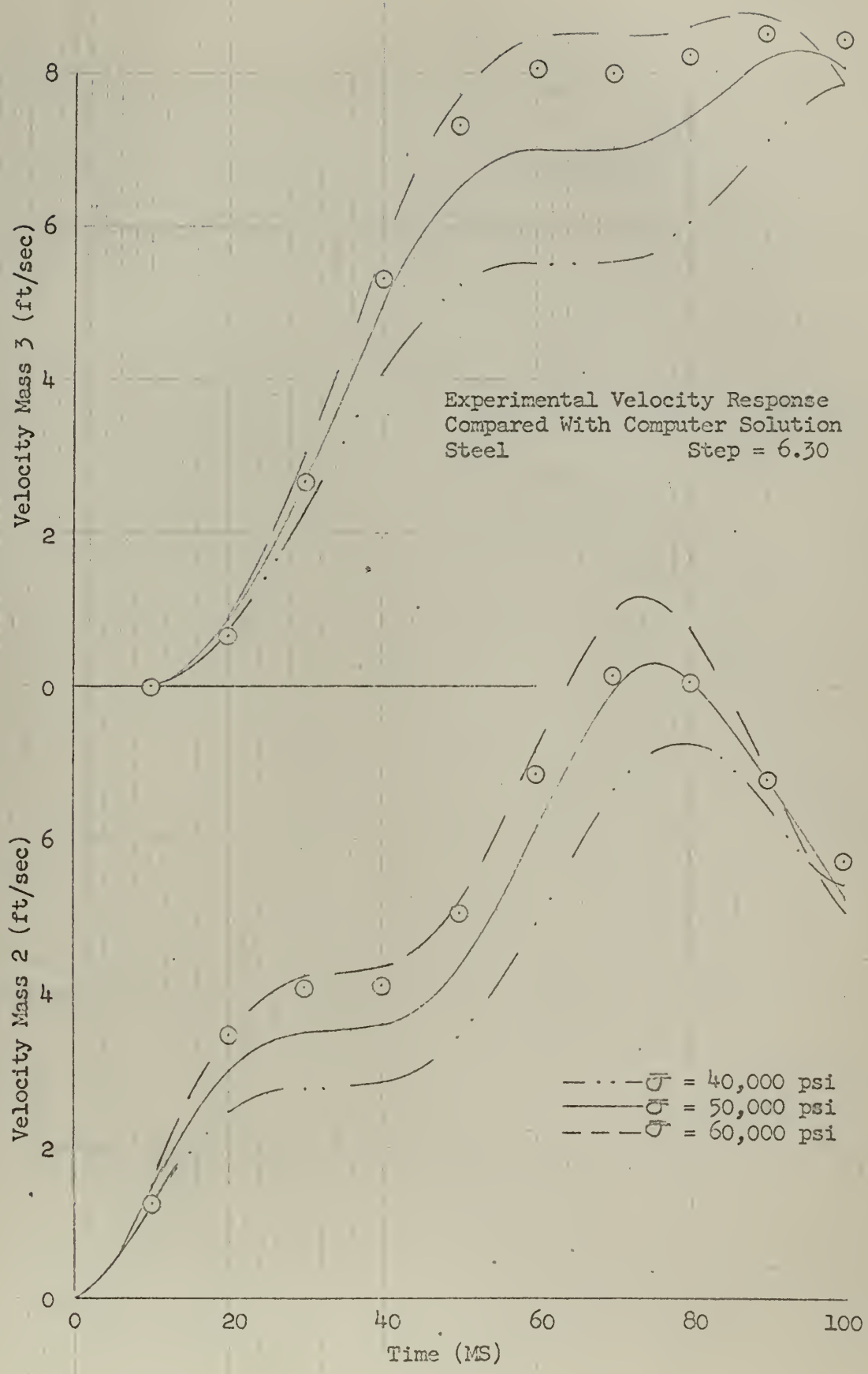
Velocity Mass 3 (ft/sec)
Velocity Mass 2 (ft/sec)
8
6
4
2
0
6
4
2
0
0
20
40
60
80
100
Time (MS)
Experimental Velocity Response
Compared With Computer Solution
Steel
Step = 6.30
— · · — σ = 40,000 psi
——— σ = 50,000 psi
— — — σ = 60,000 psi

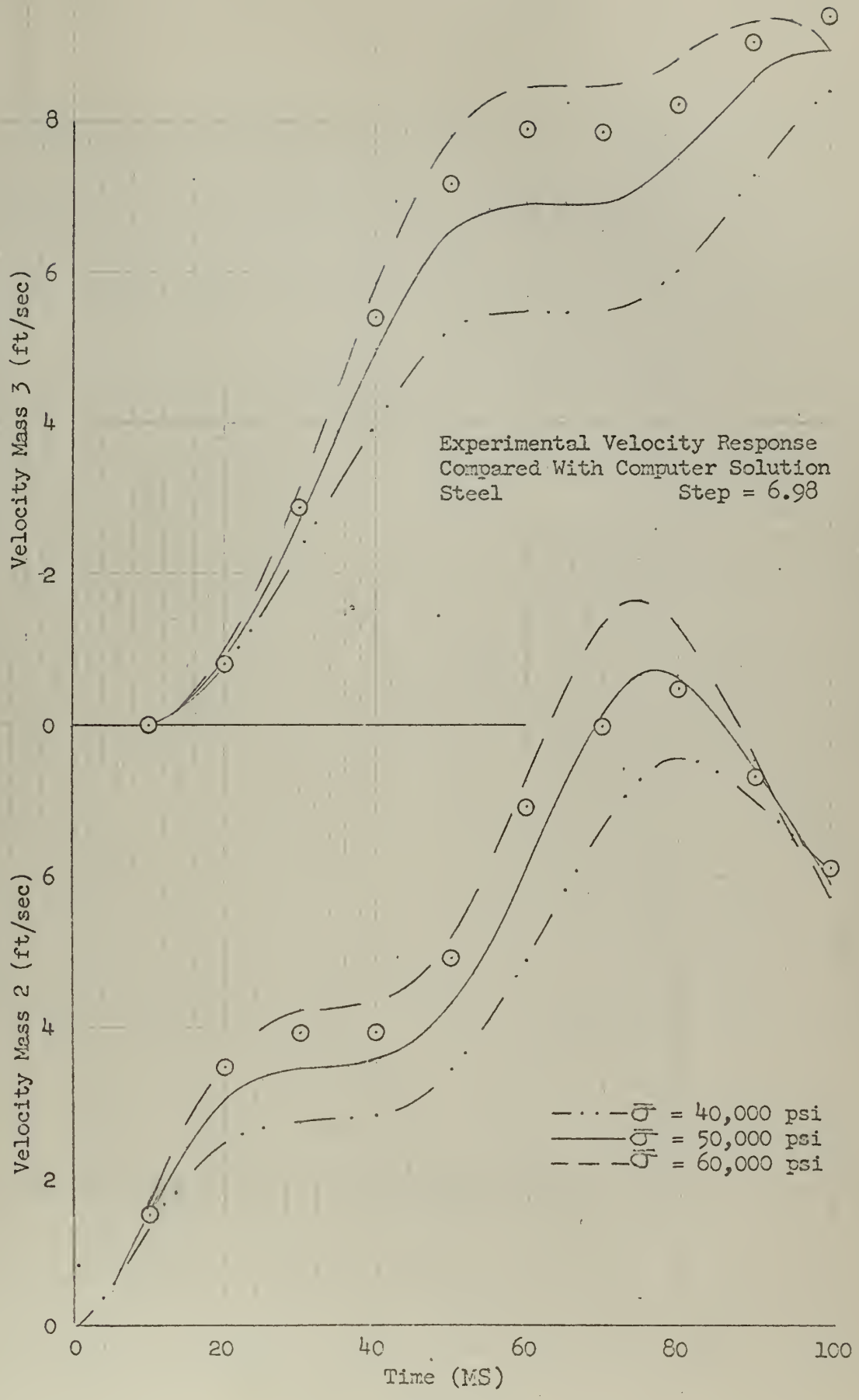
Velocity Mass 3 (ft/sec)
8
6
4
2
0
Experimental Velocity Response
Compared With Computer Solution
Steel
Step = 6.98
Velocity Mass 2 (ft/sec)
6
4
2
0
σ = 40,000 psi
σ = 50,000 psi
σ = 60,000 psi
0
20
40
60
80
100
Time (MS)

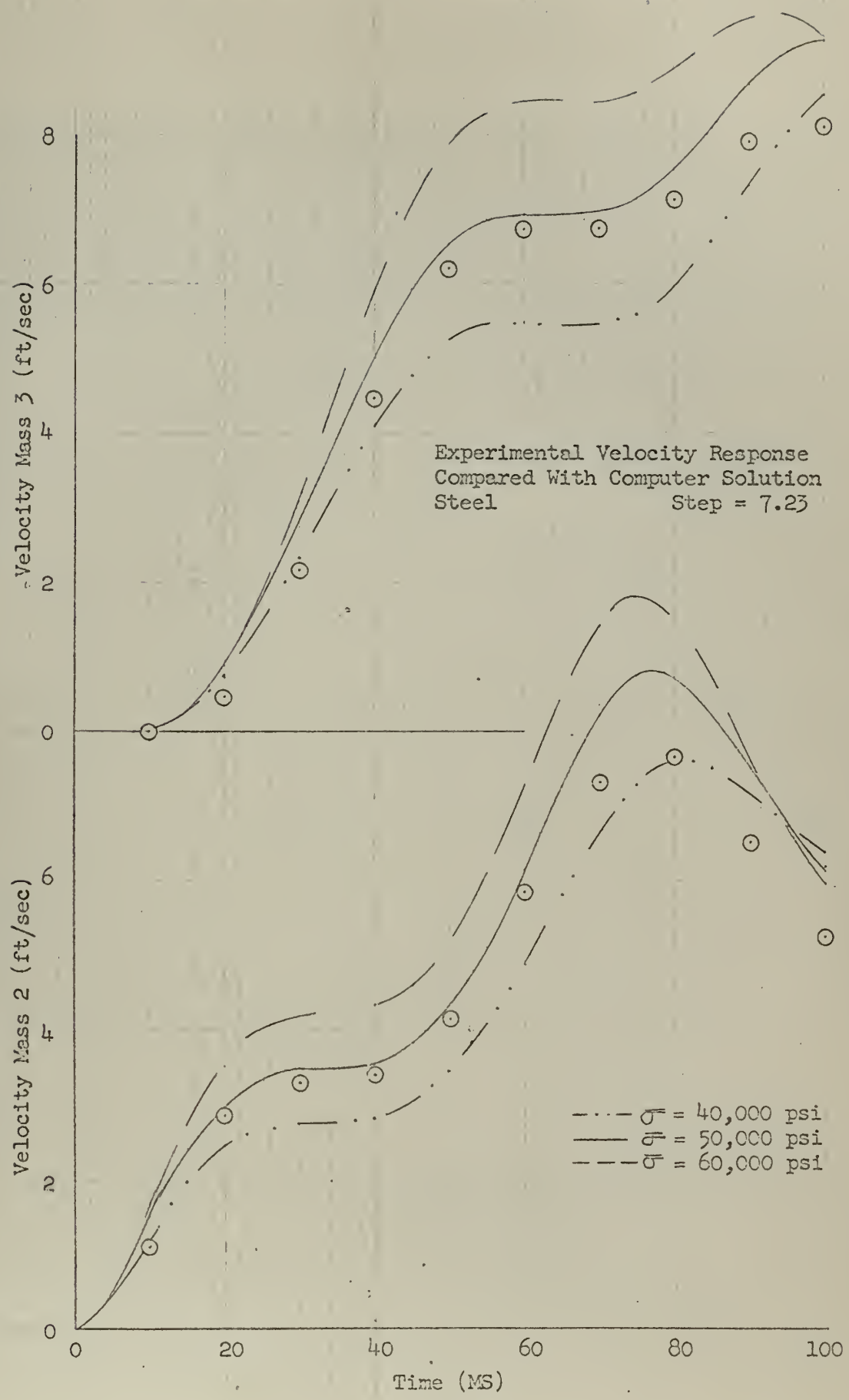
Experimental Velocity Response
Compared With Computer Solution
Steel
Step = 7.23
Velocity Mass 3 (ft/sec)
Velocity Mass 2 (ft/sec)
8
6
4
2
0
6
4
2
0
0
20
40
60
80
100
Time (MS)
σ = 40,000 psi
σ = 50,000 psi
σ = 60,000 psi

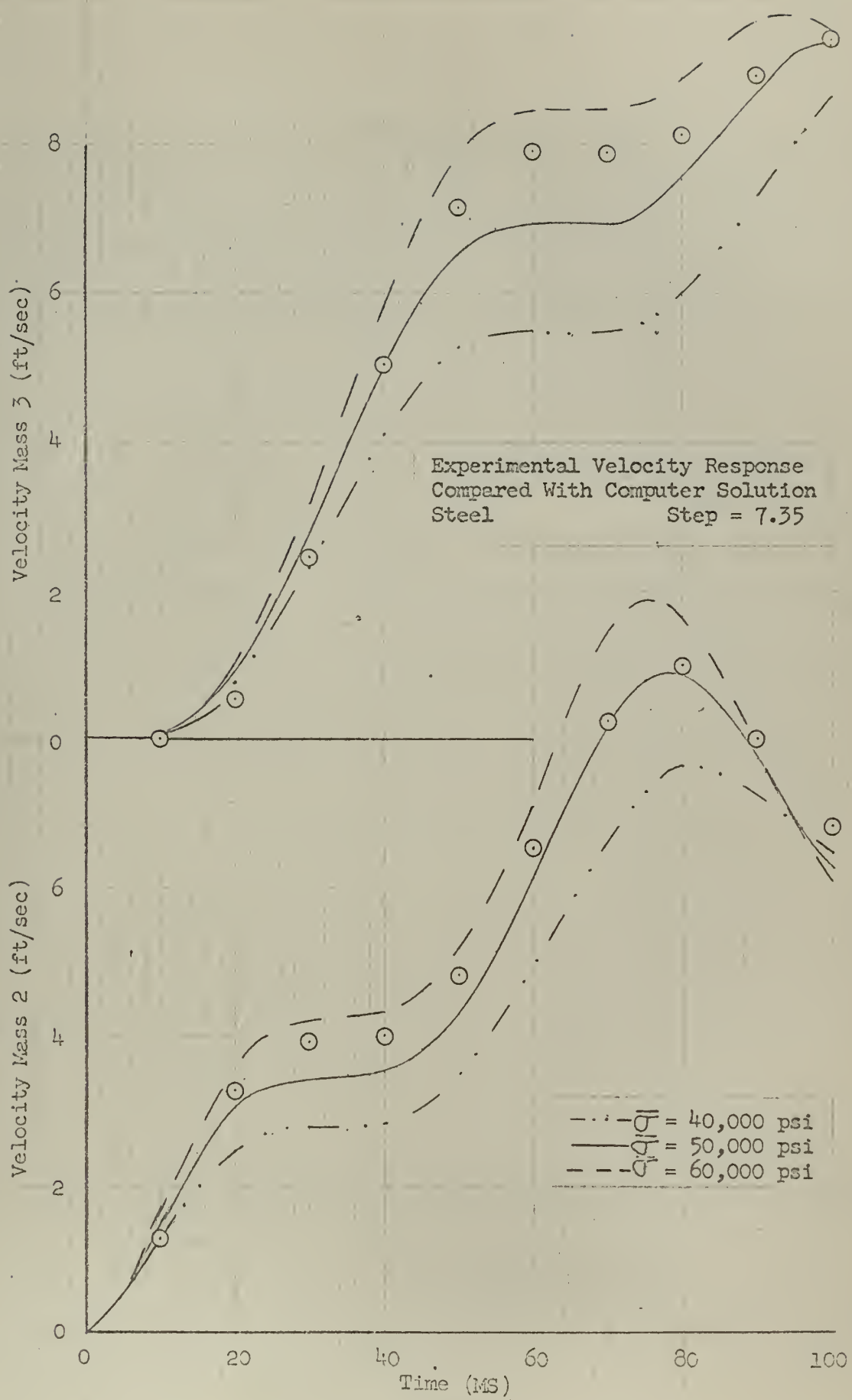
Velocity Mass 3 (ft/sec)
Velocity Mass 2 (ft/sec)
Time (MS)
0
20
40
60
80
100
2
4
6
8
Experimental Velocity Response
Compared With Computer Solution
Steel
Step = 7.35
$\bar{\sigma}$ = 40,000 psi
$\bar{\sigma}$ = 50,000 psi
$\bar{\sigma}$ = 60,000 psi

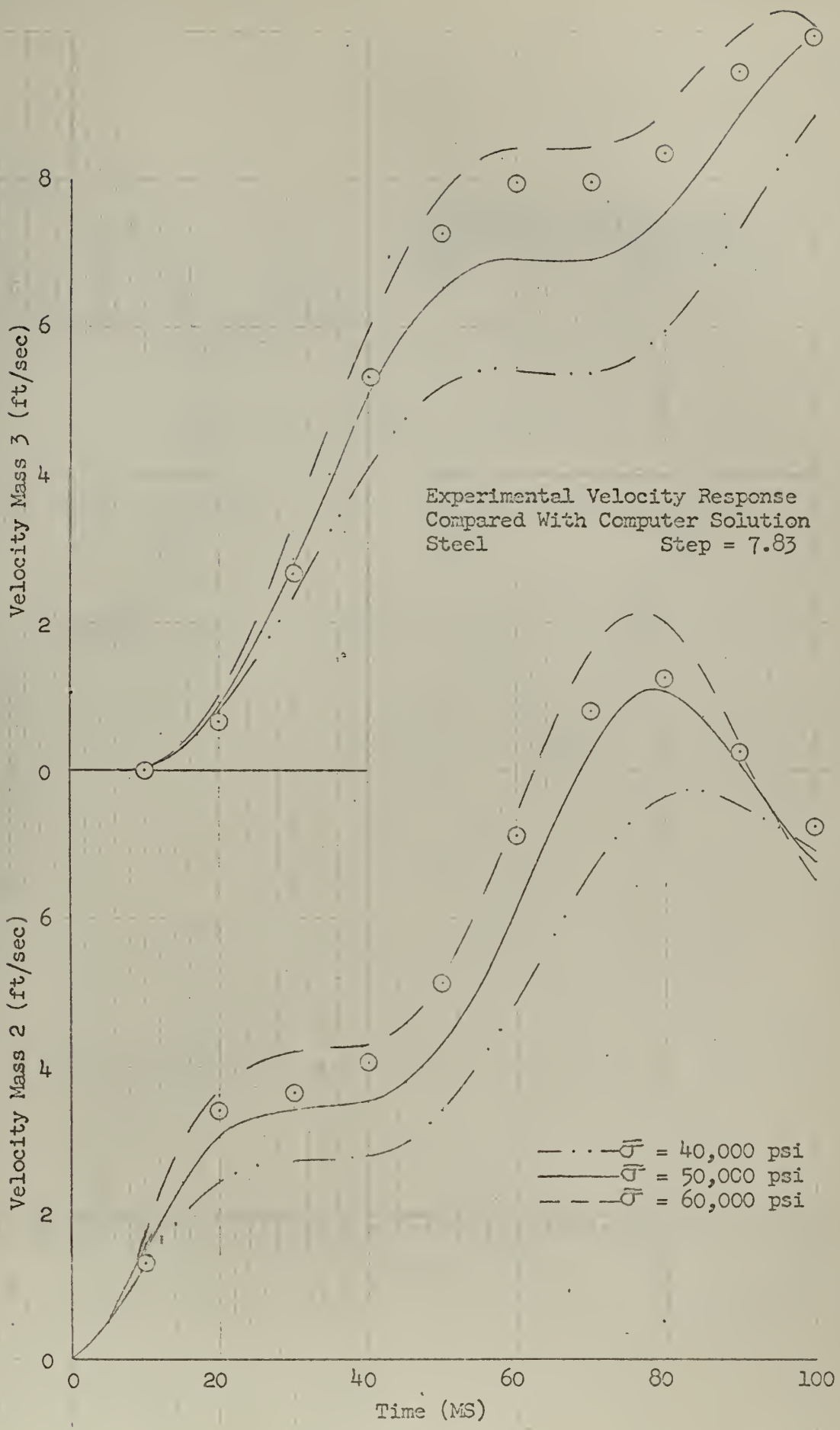
Velocity Mass 3 (ft/sec)
Velocity Mass 2 (ft/sec)
8
6
4
2
0
6
4
2
0
0
20
40
60
80
100
Time (MS)
Experimental Velocity Response
Compared With Computer Solution
Steel
Step = 7.83
$\bar{\sigma}$ = 40,000 psi
$\bar{\sigma}$ = 50,000 psi
$\bar{\sigma}$ = 60,000 psi

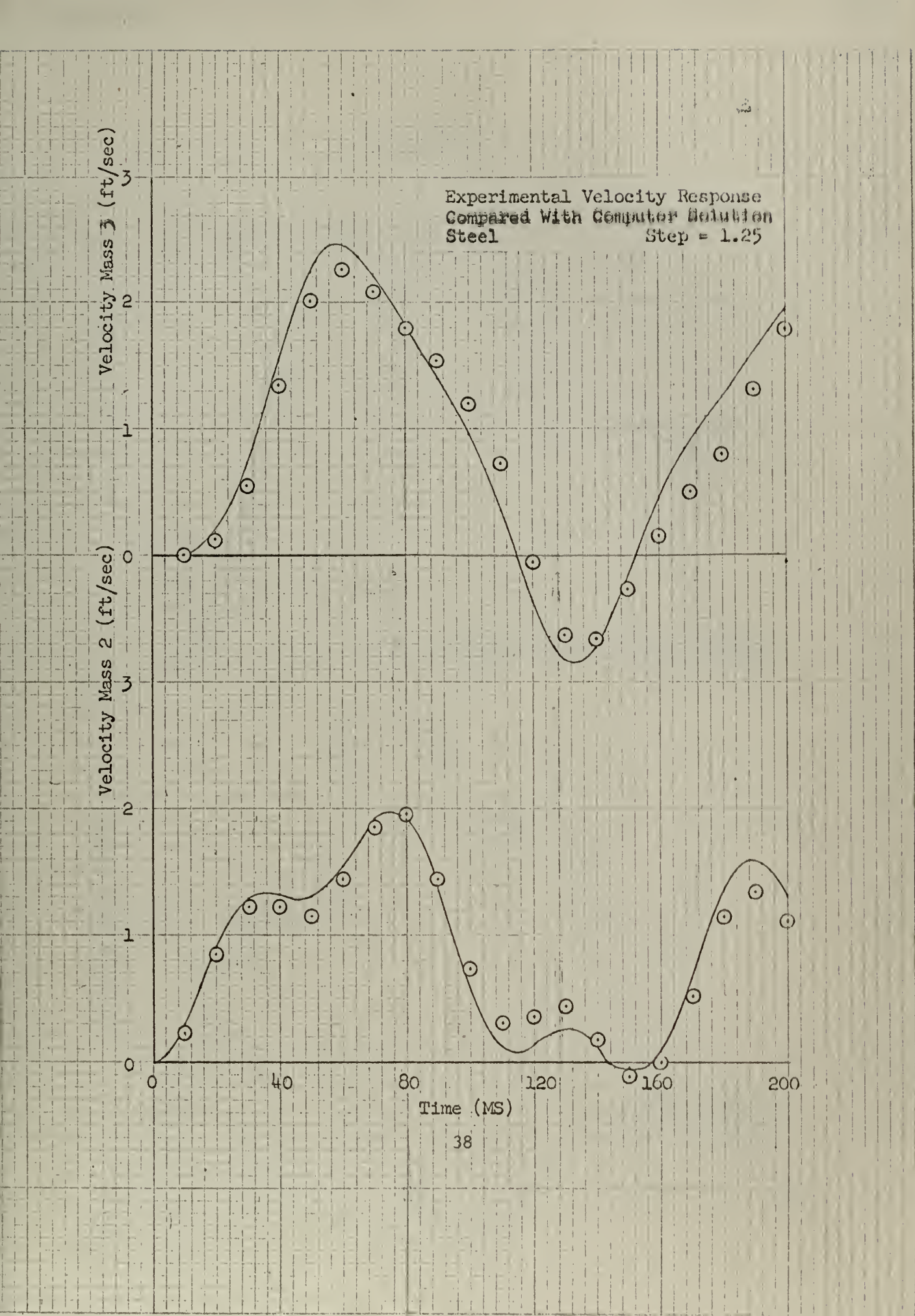
Experimental Velocity Response
Compared With Computer Solution
Steel
Step = 1.25
Velocity Mass 3 (ft/sec)
Velocity Mass 2 (ft/sec)
3
2
1
0
0
40
80
120
160
200
Time (MS)

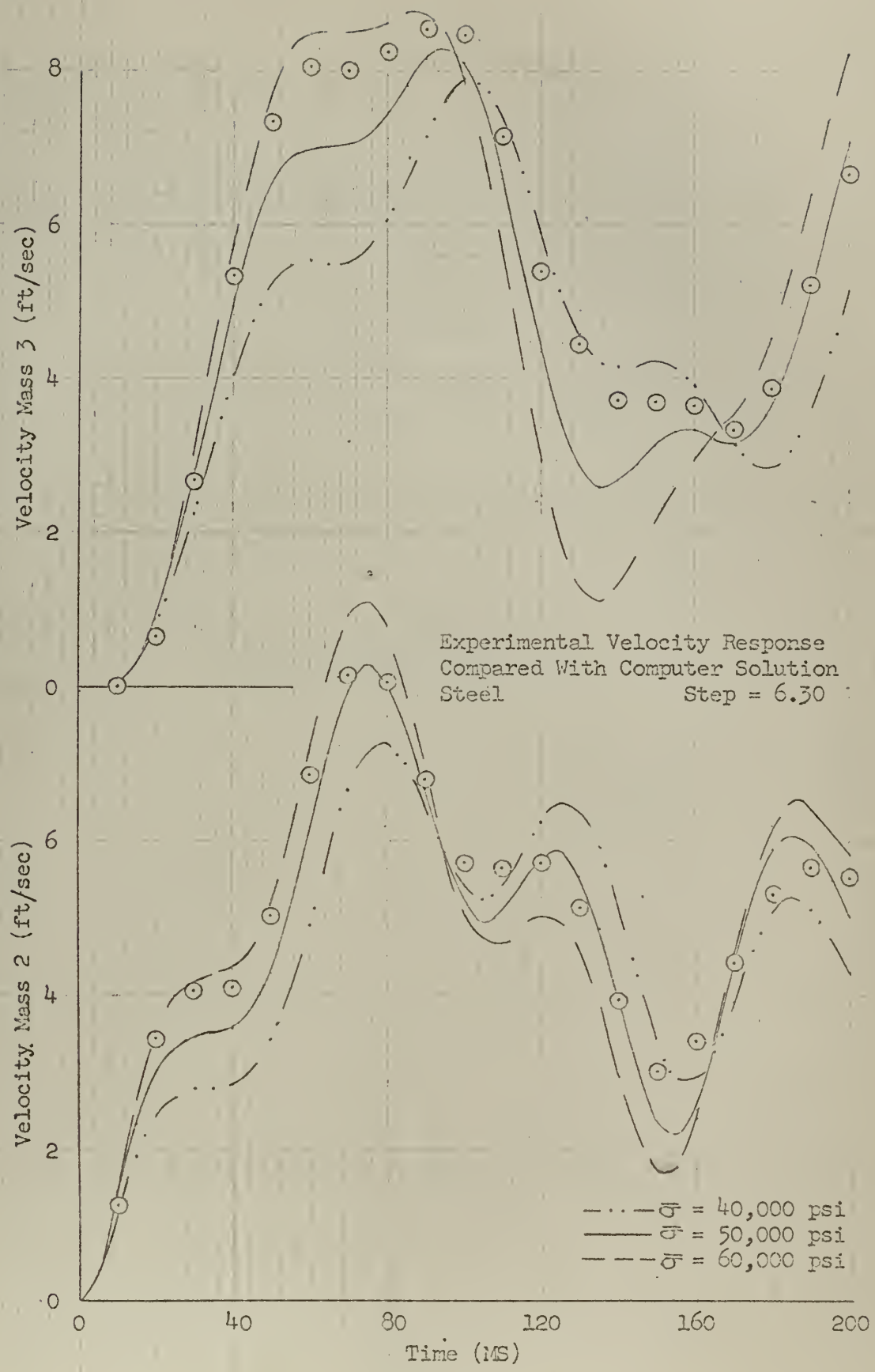
Velocity Mass 3 (ft/sec)
Velocity Mass 2 (ft/sec)
8
6
4
2
0
6
4
2
0
0
40
80
120
160
200
Time (MS)
Experimental Velocity Response
Compared With Computer Solution
Steel
Step = 6.30
σ = 40,000 psi
σ = 50,000 psi
σ = 60,000 psi

Section Two - Aluminum Alloy

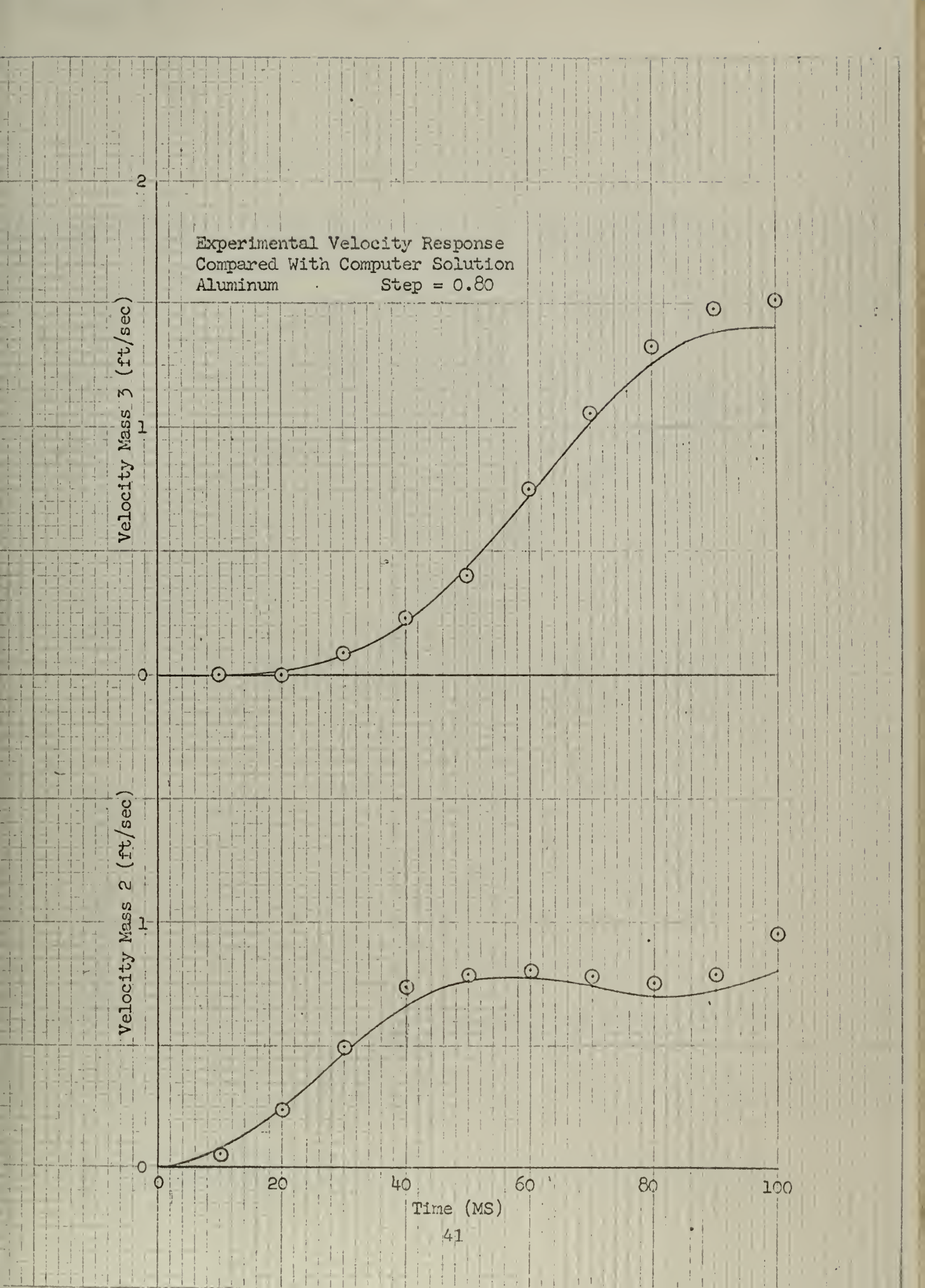
Experimental Velocity Response
Compared With Computer Solution
Aluminum Step = 0.80
Velocity Mass 3 (ft/sec)
Velocity Mass 2 (ft/sec)
2
1
0
1
0
0
20
40
60
80
100
Time (MS)

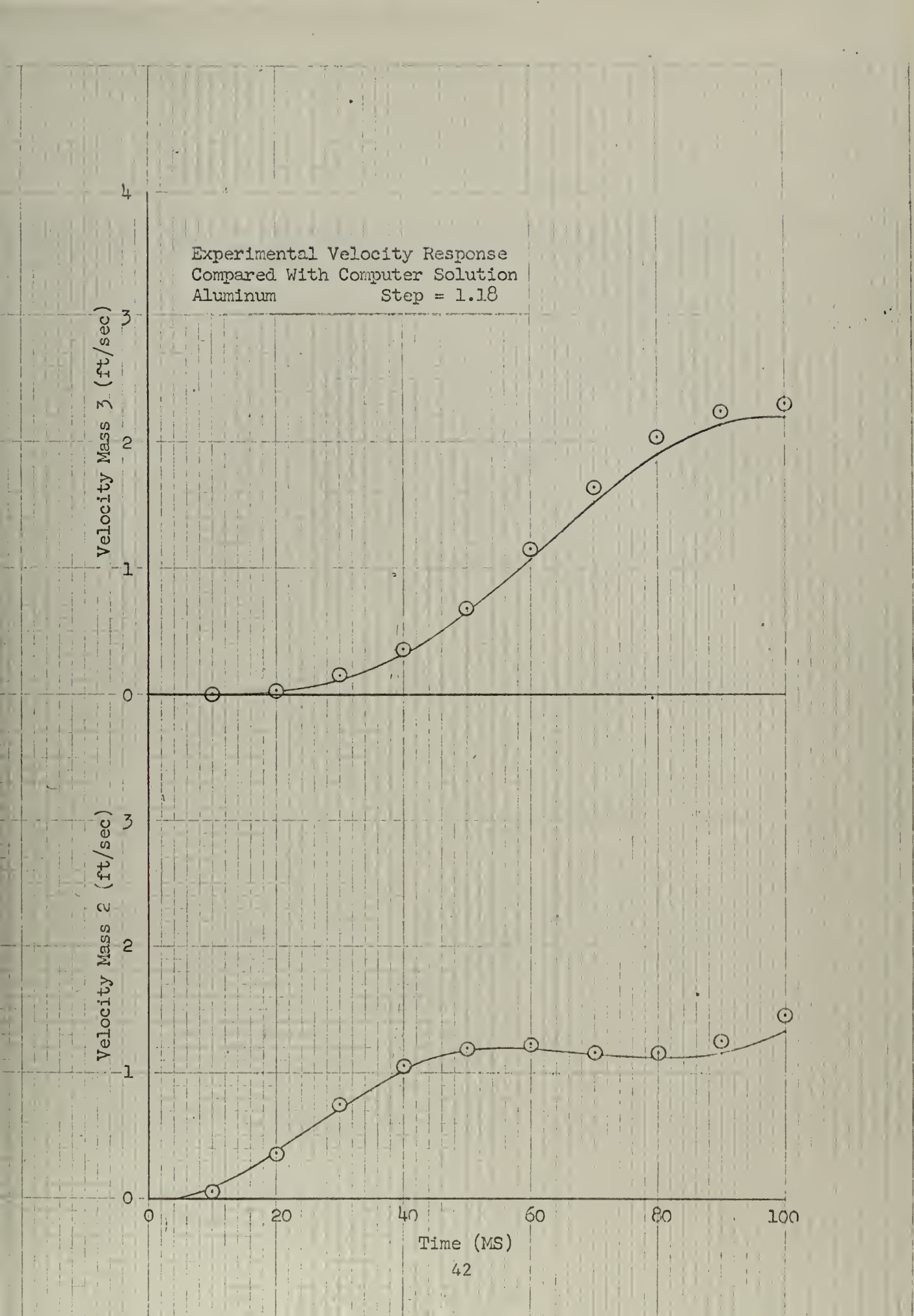
Experimental Velocity Response
Compared With Computer Solution
Aluminum Step = 1.18
Velocity Mass 3 (ft/sec)
Velocity Mass 2 (ft/sec)
0
1
2
3
4
0
20
40
60
80
100
Time (MS)

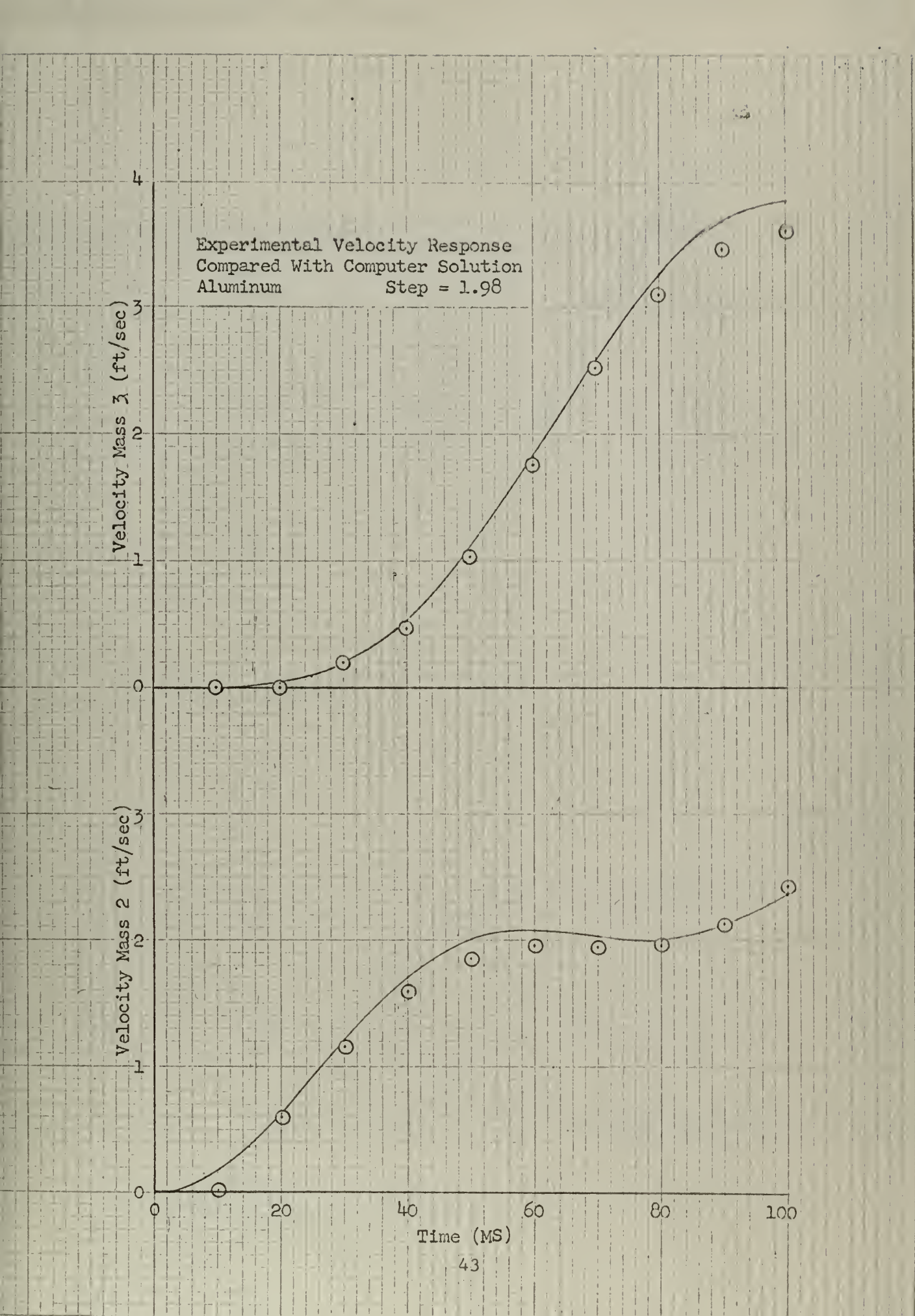
Experimental Velocity Response
Compared With Computer Solution
Aluminum Step = 1.98
Velocity Mass 3 (ft/sec)
Velocity Mass 2 (ft/sec)
0
1
2
3
4
0
20
40
60
80
100
Time (MS)

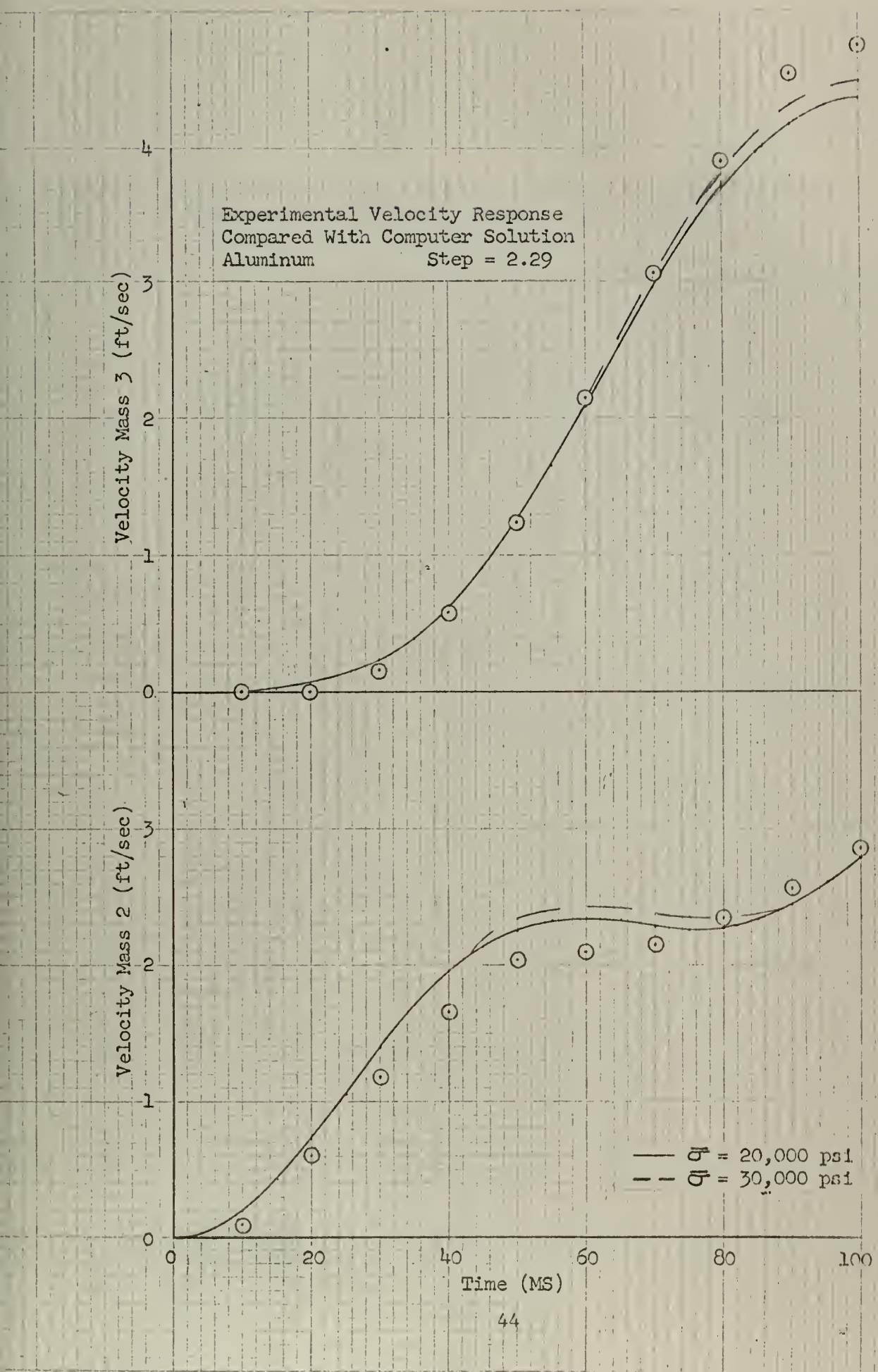
Experimental Velocity Response
Compared With Computer Solution
Aluminum Step = 2.29
Velocity Mass 3 (ft/sec)
Velocity Mass 2 (ft/sec)
0
1
2
3
4
0
20
40
60
80
100
Time (MS)
σ = 20,000 psi
σ = 30,000 psi

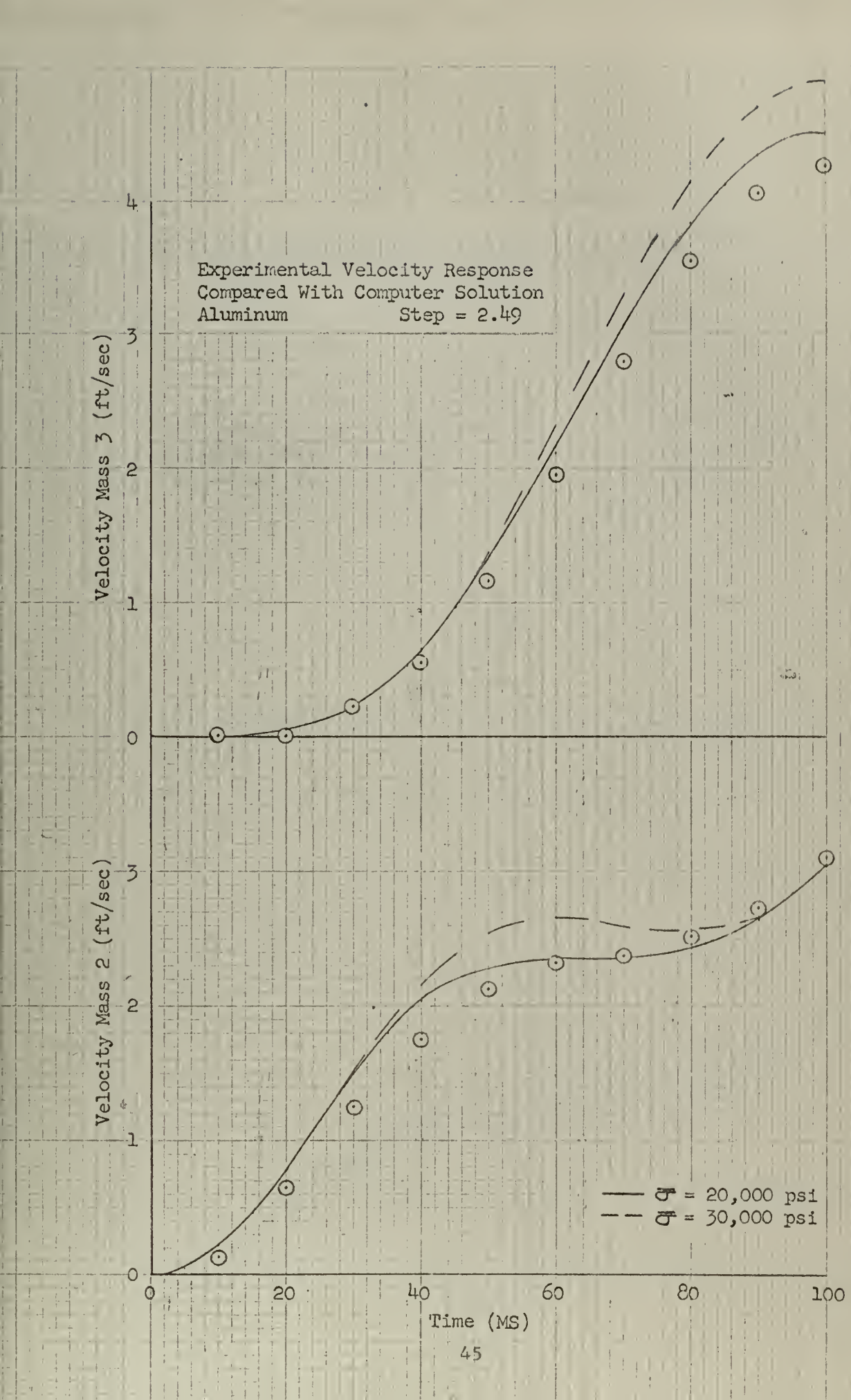
Experimental Velocity Response
Compared With Computer Solution
Aluminum Step = 2.49
Velocity Mass 3 (ft/sec)
Velocity Mass 2 (ft/sec)
0
1
2
3
4
0
20
40
60
80
100
Time (MS)
σ = 20,000 psi
σ = 30,000 psi

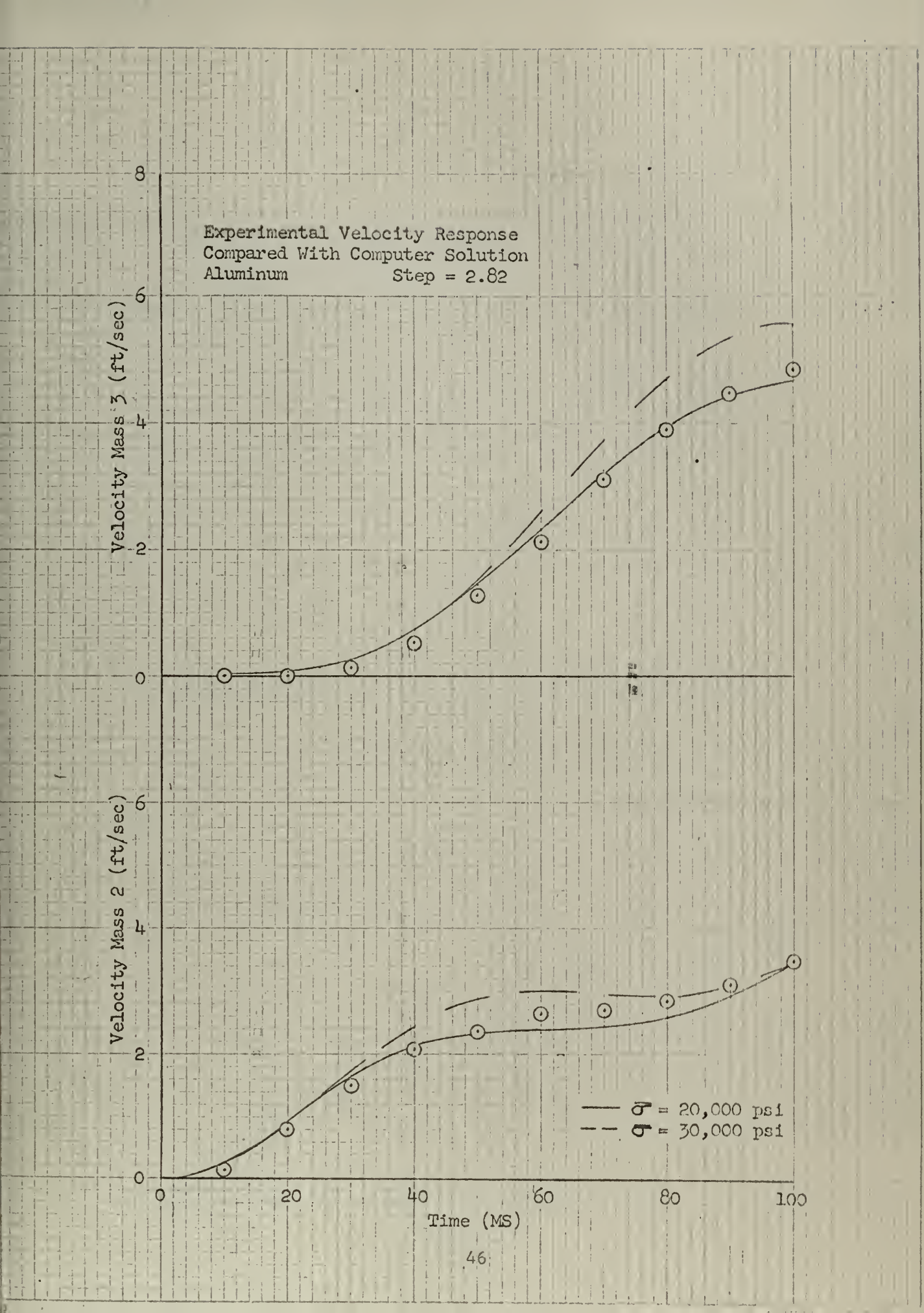
Experimental Velocity Response
Compared With Computer Solution
Aluminum Step = 2.82
Velocity Mass 3 (ft/sec)
Velocity Mass 2 (ft/sec)
8
6
4
2
0
6
4
2
0
0
20
40
60
80
100
Time (MS)
σ = 20,000 psi
σ = 30,000 psi

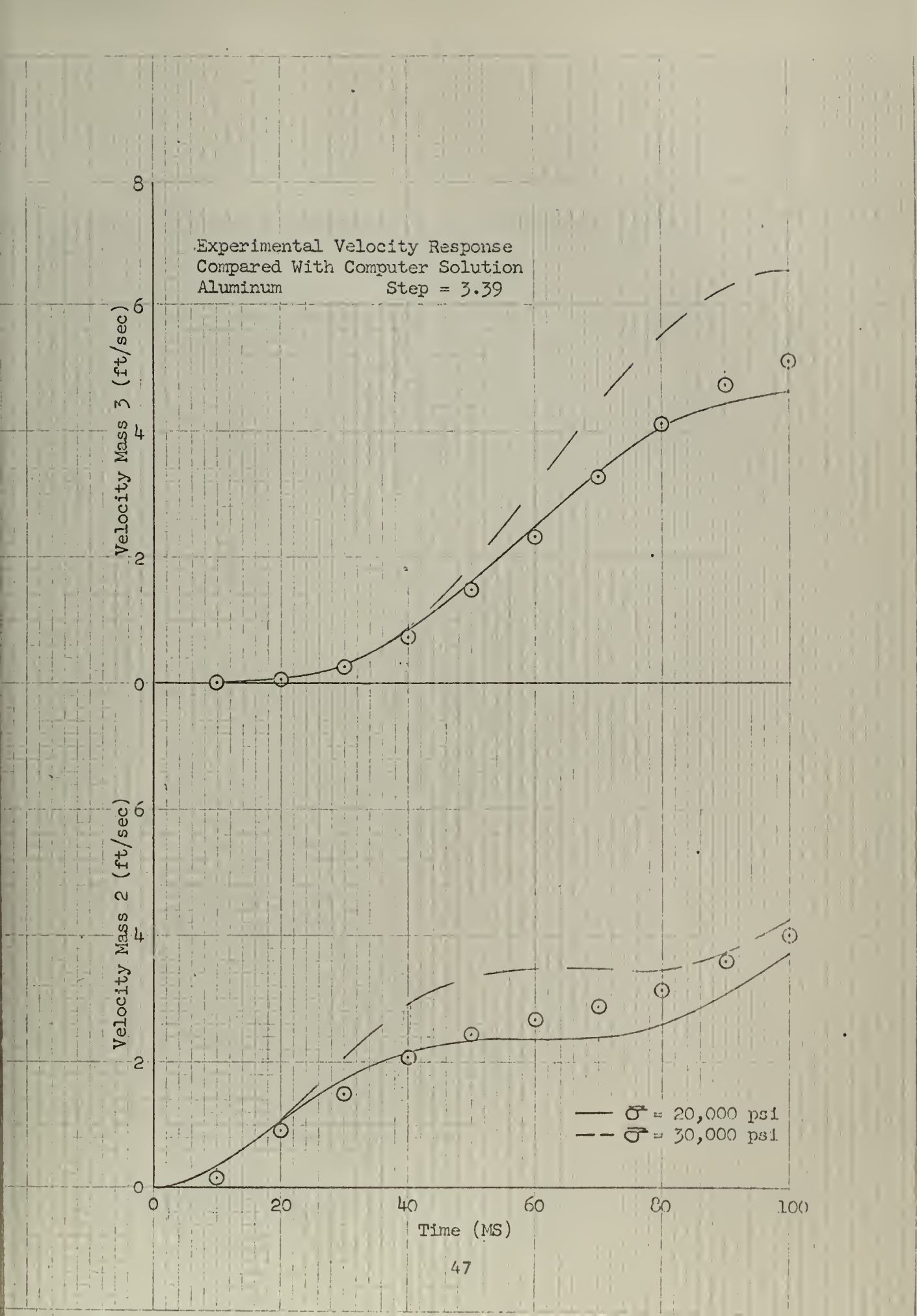
Experimental Velocity Response
Compared With Computer Solution
Aluminum Step = 3.39
Velocity Mass 3 (ft/sec)
Velocity Mass 2 (ft/sec)
0
2
4
6
8
0
20
40
60
80
100
Time (MS)
σ = 20,000 psi
σ = 30,000 psi

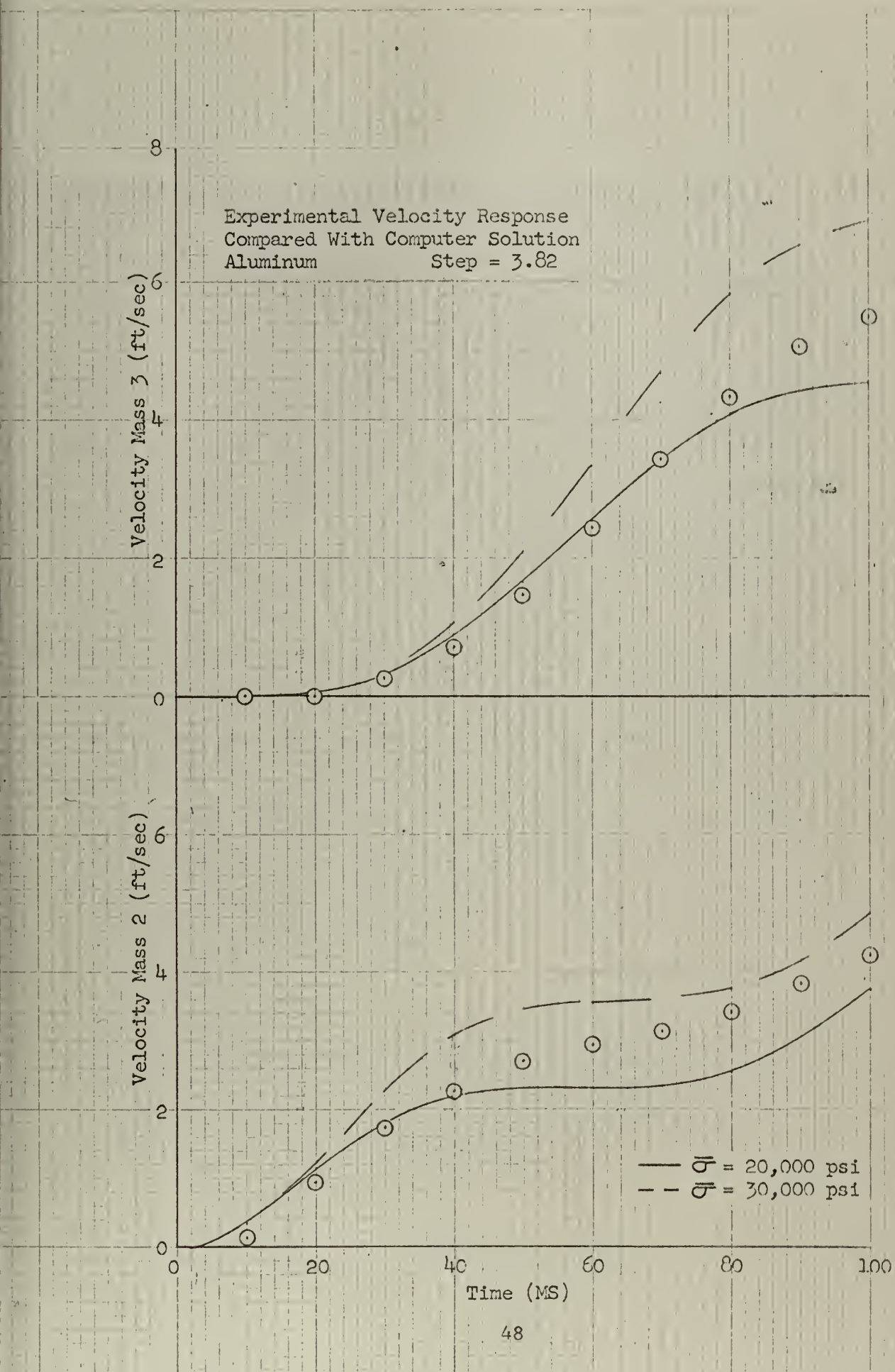
Experimental Velocity Response
Compared With Computer Solution
Aluminum Step = 3.82
Velocity Mass 3 (ft/sec)
Velocity Mass 2 (ft/sec)
0
2
4
6
8
0
20
40
60
80
100
Time (MS)
$\bar{\sigma}$ = 20,000 psi
$\bar{\sigma}$ = 30,000 psi

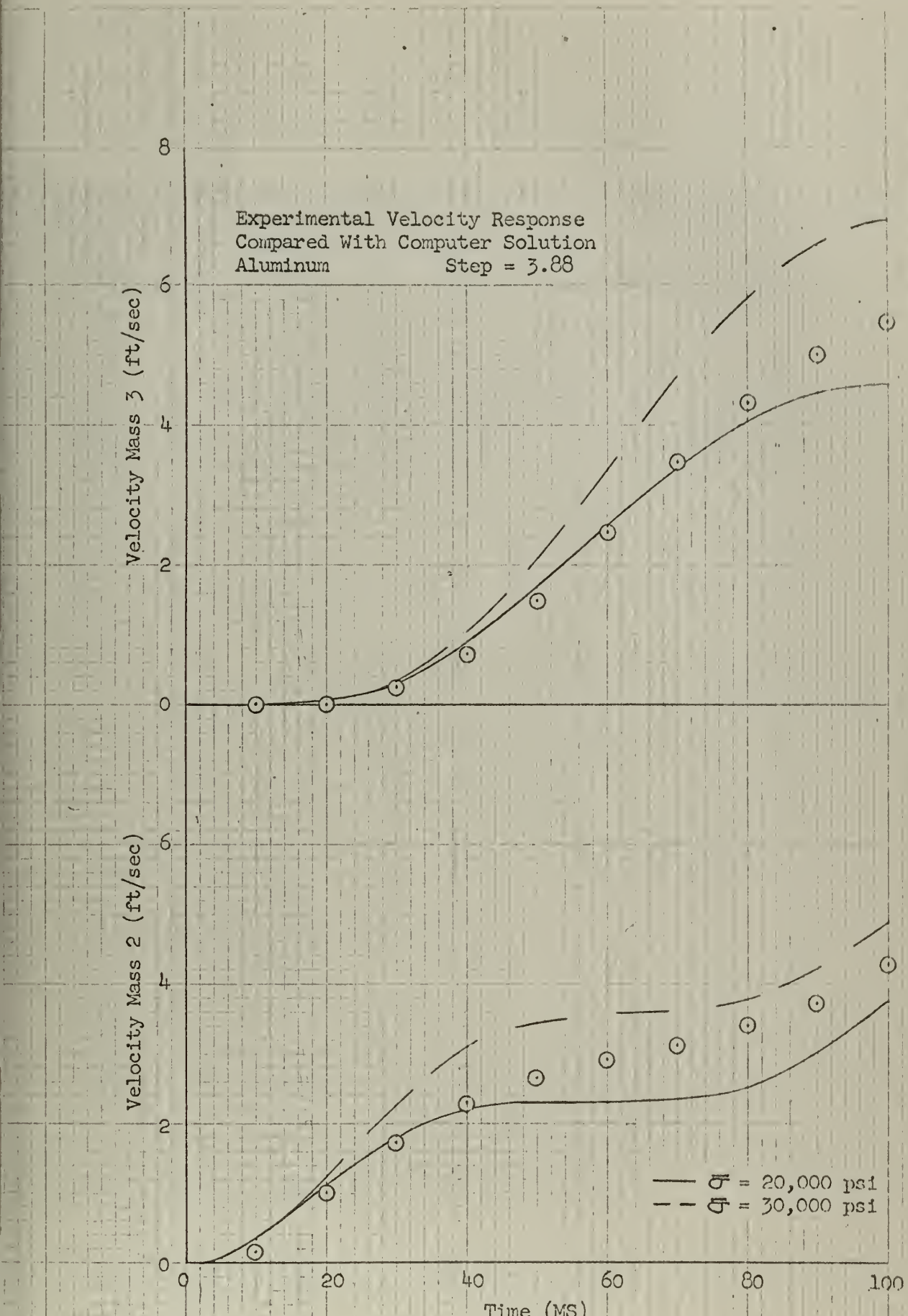
Experimental Velocity Response
Compared With Computer Solution
Aluminum Step = 3.88
Velocity Mass 3 (ft/sec)
Velocity Mass 2 (ft/sec)
0
2
4
6
8
0
20
40
60
80
100
Time (MS)
σ = 20,000 psi
σ = 30,000 psi

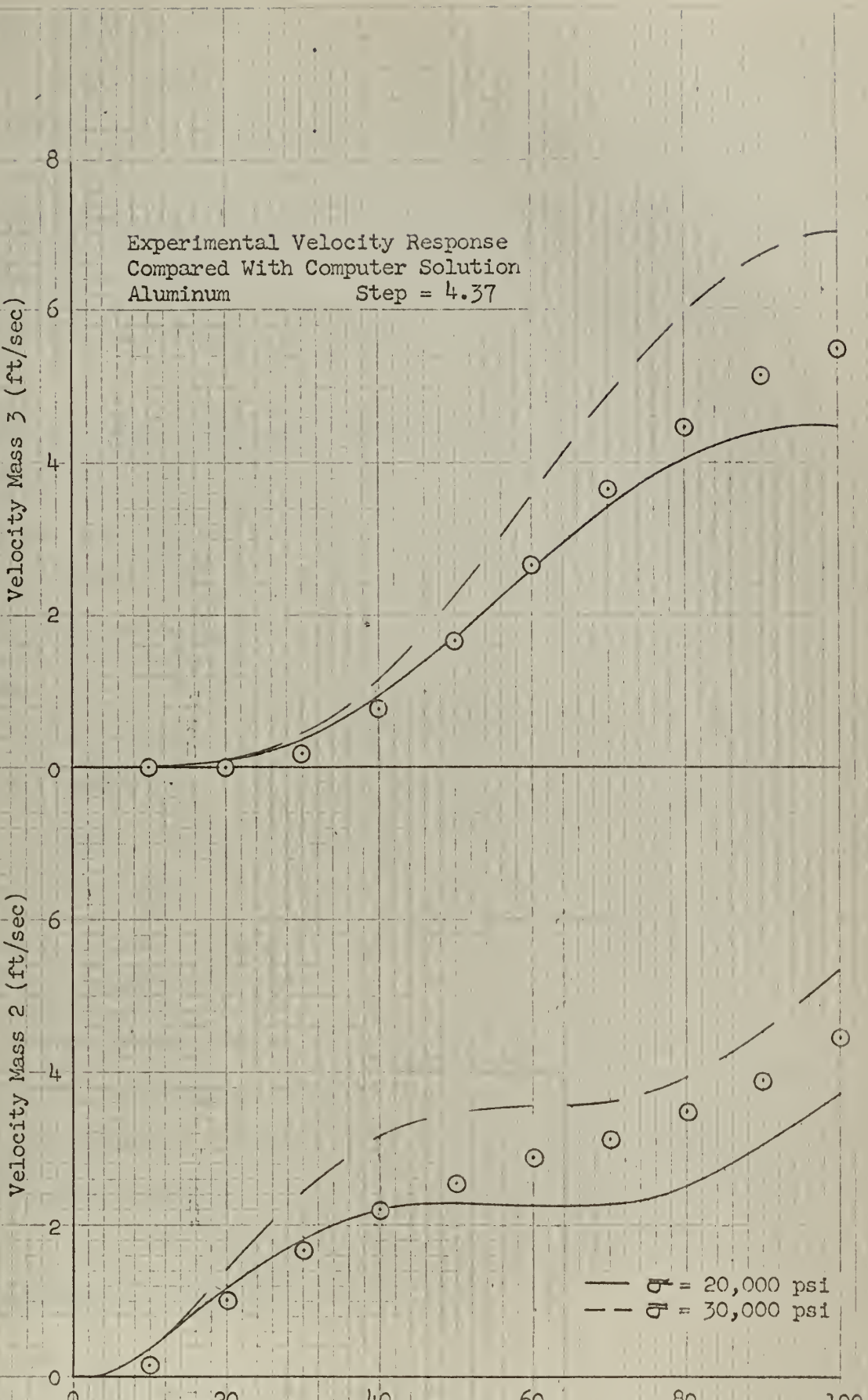
Experimental Velocity Response
Compared With Computer Solution
Aluminum Step = 4.37
Velocity Mass 3 (ft/sec)
Velocity Mass 2 (ft/sec)
8
6
4
2
0
6
4
2
0
0
20
40
60
80
100
Time (MS)
σ = 20,000 psi
σ = 30,000 psi

6. Discussion of Results

1. A complete tabulation of the experimental and theoretical points shown in the graphical comparison is not included in this thesis. Samples of the data are contained in Appendices (II) and (V). The Fortran program used is found in Appendix (I), and, if desired, may be utilized for obtaining additional theoretical results. The experimental results shown on the various plots are as accurate as the values used in plotting.

2. The two major experimental discrepancies, as noted earlier, were the lack of fixity and the failure to record the initial anvil displacement. These two items have been suitably discussed in previous sections; however, an improvement to the test structure is suggested for future tests. The single bolting arrangement used appeared to be inadequate, as far as providing a fixity approaching a cantilever beam. The more rigid connection used by Kurzenhauser [1] in his tests consisted of four 5/16" N. C. socket head cap screws plus a 1/4" clamping plate. The four screws were located near the edges of the clamping plate instead of the centrally located bolt used in this thesis. It is therefore felt that the design of the test structure was poor in this respect, and the use of four holding bolts would have improved the fixity.

Nothing further will be said concerning the failure to record the initial anvil displacement, except that this was vital information that should have been recorded. In any future structural tests utilizing the ballistic pendulum herein described, the test structure should receive the initial impact with the anvil hanging vertically (initial displacement zero), thus eliminating this initial horizontal force.

3. The maximum step velocity (initial anvil velocity upon impact) experienced by the test structure was 7.83 ft/sec. The ballistic pendulum was capable of producing approximately 14.0 ft/sec; however, due to the interference between the test structure and the anvil supporting cables, the maximum of 7.83 ft/sec. was the highest input before interference was experienced.

4. The limiting value of time used for the graphical comparison of results was 100 MS. The reason for cutting off the comparison at this point was due to the fact that in reconstructing the initial anvil displacement (a = 0.7'), the total momentum vs. time plot was used. This plot was limited by the velocity record of the anvil. The velocity meter magnet for the anvil departed the coil after approximately 100 MS, up to a step of 3.86 ft/sec. Above this value for initial velocity, the anvil velocity trace was even shorter, averaging about 50 MS. Since the total momentum vs. time plot was limited to approximately 100 MS, it was felt that use of the predicted anvil displacement beyond 100 MS would not be warrented.

A second reason for using the 100 MS limit was that the two velocity meters mounted on the structural masses produced faulty traces beyond 70 MS for the steel columns, at the higher inputs. These faulty traces were likewise caused by the velocity meter magnets departing their respective coils. The purpose of mounting the accelerometers on the test structure was to allow for a continuation of the velocity plots beyond 70 MS by integration of the acceleration vs. time traces. It was felt that the increased error due to reduction and integration of the acceleration traces would be held to a minimum if the number of points added by this method were small. Three

points were added, producing a total velocity vs. time trace of 100 MS duration. Discrepancies of the order $\pm$ 5% were noted between velocities obtained from the velocity traces directly and by integration of the acceleration traces, over intervals where the velocity traces were considered valid.

5. The graphical comparison of results, for steel columns, found on pages 22 through 37 , consists of approximately seven elastic runs and nine plastic runs. The experimental points for the elastic runs are compared with a single theoretical plot since the theoretical results within this range, are not affected by changes in the dynamic yield strength. The plot for step = 2.87 ft/sec is a borderline case. A slight variation between theoretical values for $\bar{\sigma}$ = 40,000 psi and $\bar{\sigma}$ = 60,000 psi was noted, however the variation was quite small (0.3 ft/sec maximum) and therefore only the theoretical trace for $\bar{\sigma}$ = 40,000 psi is shown. Starting with the value step = 3.86 ft/sec, three theoretical curves are shown for the remainder of the runs. The curves represent dynamic yield strengths of 40,000 psi, 50,000 psi, and 60,000 psi. The general trend in the curves indicates the increased dynamic yield strength with increased initial velocity. The runs for step = 5.02 ft/sec and 7.23 ft/sec do not fit in with the remainder of the plots. The dynamic yield strength for these two runs shows a decrease, whereas, an increase should be indicated to follow the sequence of values previous to and following these respective runs. The cause of the disagreement could possibly be due to an error in the experimental values for initial anvil velocity. The comparison indicates a lower velocity input than the values used. A change of 0.02" in measurement from the oscillograph record produces a change of 0.19 ft/sec. Also a variation in supporting columns from one test structure to another could introduce an appreciable

error. It can be seen in some of the higher input plots, for steel, that the experimental points tend to fall off more rapidly than would be indicated for continuity of plot. As was noted earlier, the last three points for the steel plastic runs were computed using the integrated acceleration vs. time traces. The added error caused by this procedure may account for this discrepancy.

Pages 38 and 39 show an extension of two of the previous runs out to 200 MS. The purpose of these two plots was to give an indication of the agreement beyond the 100 MS limit. As can be seen from the plots, the agreement is very good. This further indicates the validity of the computed value for initial anvil displacement.

6. The graphical comparisons using aluminum columns are likewise limited to 100 MS. The first three plots show the single theoretical trace whereas the remaining seven plots show two theoretical traces, one trace representing $\bar{\sigma}$ = 20,000 psi and a second trace representing $\bar{\sigma}$ = 30,000 psi. For the three runs represented by step = 2.29, 2.49, and 2.82 ft/sec, the theoretical values for $\bar{\sigma}$ = 20,000 psi and $\bar{\sigma}$ = 30,000 psi merge within plotting error between 90 and 100 MS.

The experimental values for the velocity-time plot for the aluminum columns were taken entirely from the velocity trace since the magnets remained in the coils somewhat longer than for the steel columns. For the two highest input velocities the last three points were checked by integrating the acceleration vs. time traces.

7. Massard and Collins [2], in tests of structural metals under rapid loading, demonstrated the time sensitive behavior known as "delayed yield" for structural steel and aluminum. It was found that metals that display

a definite upper and lower yield point, under slow testing procedures, are quite time sensitive and display the delayed yield phenomenon. For metals such as aluminum, where straining under slow tests is not discontinuous, the delayed yield effect is not as prominent. From the graphical presentation of data, the aluminum plots would tend to substantiate this conclusion, since the apparent increase in dynamic yield strength is somewhat smaller relative to that demonstrated for steel.

8. An improvement to the testing procedure used would be to replace the supporting columns before each run. Obviously, this is a requirement for the plastic runs; however, in several instances, the same set of supporting columns was used for one very low input elastic run and then a higher velocity input plastic run. This procedure only involved about three of the runs and was done to save time.

9. As mentioned earlier, the integration routine utilized in this thesis was the Runge-Kutta method. The time interval used was 1/10 MS. This was arrived at by comparison with the results for an exact solution for a similar system contained in reference [4] . The only difference between the two systems was that the exact solution was based upon a system whose base was rigid. The system utilized in this thesis was easily reduced to the above system merely by making M_1 very large. Comparison of the two systems in the elastic range (exact solution was valid for elastic response only) produced answers that were in agreement to about three significant figures. This was considered accurate enough for plotting.

Since the time interval used in the computer program was 1/10 MS, theoretical results could have been obtained for every 1/10 MS; however,

this would have produced an excessive amount of output data and the values were therefore printed every MS or every tenth time interval. The theoretical curves shown in the graphical presentation of results were plotted using points every five milliseconds.

One inherent difficulty with the Runge-Kutta method, as pointed out by Newmark and Chan [5], is that "the amplitude will gradually damp itself out even in the case of an undamped system, and the method is therefore not desirable for a long period of time." No explanation was given as to what constituted "a long period of time"; however, the time limit imposed in this problem was undoubtedly short enough to prevent this from affecting the results.

10. Perhaps the greatest source of error involved in the experiment was the reduction of the experimental data. The data reduction involved first of all a determination of a zero reference level for the various traces. This was accomplished by using the edge of the oscillograph record as a reference and then comparing this with the 1000 cycle trace for straightness. In all cases the straight line formed by the 1000 cycle trace agreed with the paper edge reference. Amplitudes for the various parameters were measured from the respective reference lines using a six inch steel scale. A magnifying glass was used for greater accuracy. The scale was read to the nearest 0.01".

As noted earlier, the sensitivity of the velocity meters varied $\pm$ 3% during a 4" sweep. The response of the accelerometers was good; the only drawback in their use was the high frequency pick-up in the first 30 MS. This completely obliterated the trace for the first 30 or 40 MS, preventing any real comparison of the compatibility between velocity and acceleration traces.

The integration of the acceleration vs. time plots was accomplished by using a K & E 4236 Compensating Polar Planimeter, serial number 6098. It is estimated that an error of about 2% was possible using this instrument since the areas involved were of the order 0.1 sq. in.

Since the values obtained in the data reduction were accurate to about two or three significant figures, the values put into the computer were limited to the same precision, which was also utilized in presenting the graphical comparison of results.

11. It is to be noted that the parameters chosen for the comparison of the results could have been force vs. deflection, acceleration vs. time, or some other comparison. The velocity vs. time comparison was chosen because it offered the quickest comparison with the least manipulation of numbers. The other comparisons mentioned above, would have involved extensive reduction, which would have introduced the possibility of increased error.

7. Conclusions and Recommendations

The gratifyingly close comparisons between experimentally observed behavior and theoretically predicted behavior of the three mass structure considered herein permits the conclusion that the response of similar structures may be predicted by mathematical analysis using digital computer calculations and involving force-deflection relations for the elastic and plastic regimes which involve prior deformation history in the manner described in Appendix I. The analysis in the present case was complicated by a feature of the experimental set-up which would probably have no counterpart in actual practice. There should be no essential difficulty in analysing cases where the excitation comes from lateral forces having specified variations with time rather than from a velocity step of one of the masses, although the latter case is certainly of primary interest in considering response to explosive loadings. Similarly, there should be no difficulty in incorporating further refinements regarding "large" geometry in the analysis should it be desired to follow the deflection history into ranges where the present restrictions to "small" geometry might not be sufficiently accurate.

The present experiments show that for the higher response velocities that accompany the larger input velocity steps, the value of $\bar{\sigma}$ that gives the best theoretical prediction of the response also increases. For reasons cited by Kurzenhauser [1], no attempt was made in this thesis to make a quantitative evaluation of this relation.

The predicted response depends greatly on the details of the load-deflection relations which depend, in turn, upon a knowledge of the dynamic behavior of the material as it is loaded and unloaded in both the elastic and plastic regime. It would be of great advantage to have better information than seems to be available presently about structural materials loaded

in such a manner; including the variability of $\bar{\sigma}$ with strain-rate.

Future experimental investigations should employ apparatus in which a closer control over or knowledge of column fixity is available. Also, if a ballistic pendulum type of apparatus is to be used, it is clear that the masses should be hanging freely before impact so as to avoid the complications introduced in the present experiments by the presence of the hold-back cable. Finally, it would clearly be quite advantageous to have a single instrumentation capable of reporting the response of the structure beyond the 100 MS cut-off without the necessity of augmenting the response with a second instrumentation as was necessary in this investigation, wherein velocity meter data was extended by use of integrated accelerometer data.

Bibliography

1. Alfred Kurzenhauser, Portal Frame Under Impact Loading, Thesis, U. S. Naval Postgraduate School, Monterey, California, 1961.

2. J. M. Massard and R. A. Collins, The Engineering Behavior of Structural Metals Under Slow and Rapid Loading, Structural Research Series No. 161, University of Illinois, October 1958.

3. A. H. Keil, The Response of Ships to Underwater Explosions, Structural Mechanics Laboratory, Report 1576, David Taylor Model Basin, November 1961.

4. G. L. O'Hara, Shock Spectra and Design Shock Spectra, Structures Branch Mechanics Division, U. S. Naval Research Laboratory, November 12, 1959.

5. N. M. Newmark and S. P. Chan, A Comparison of Numerical Methods for Analyzing the Dynamic Response of Structures, Structural Research Series No. 36, University of Illinois, October 1952.

6. S. Timoshenko, Strength of Materials - Part I, 3rd Edition, p. 267, D. Von Nostrand Co., Inc., New York, N. Y., 1955.

7. Alcoa Aluminum Handbook, Aluminum Company of America, 1957.

8. W. E. Milne, Numerical Solution of Differential Equations, John Wiley & Sons, 1953.

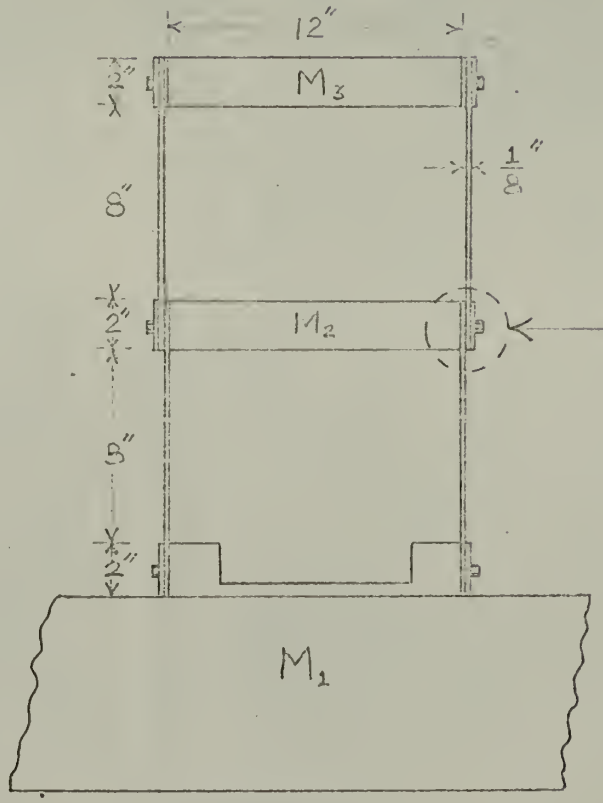

Figure 1a

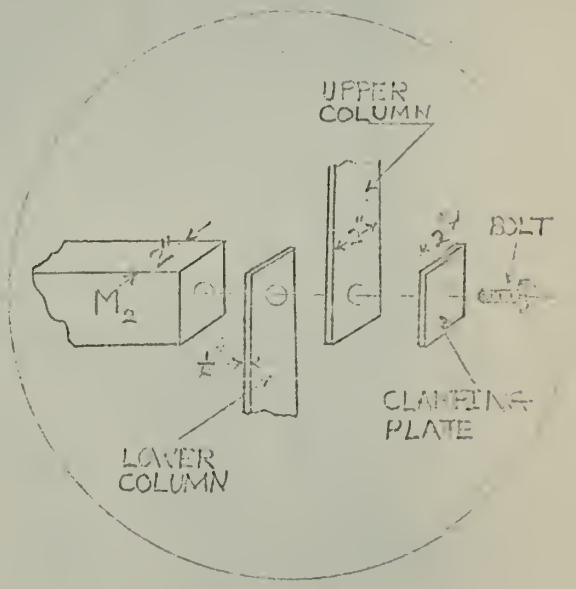

Figure 1b

Figure 2

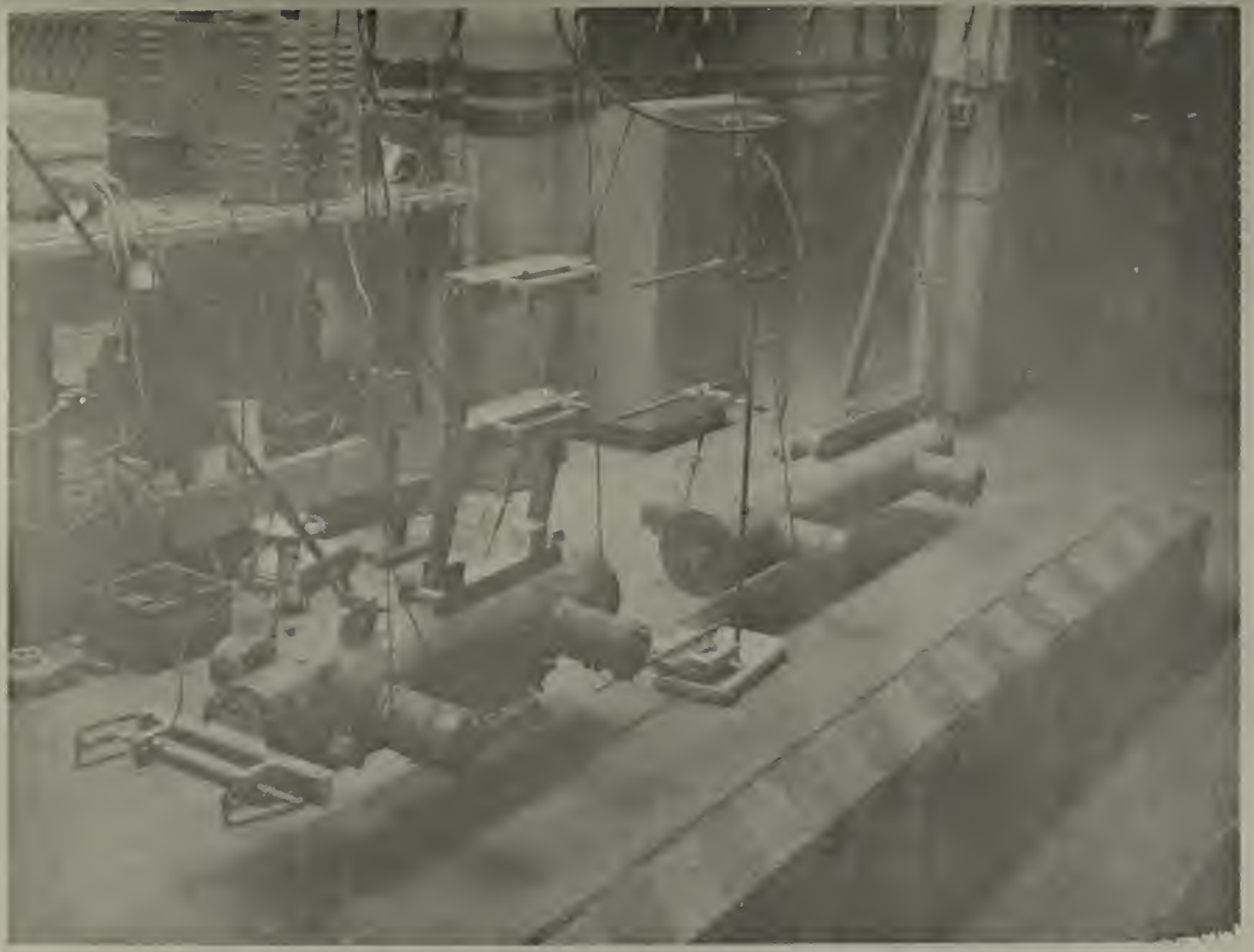

Figure 3

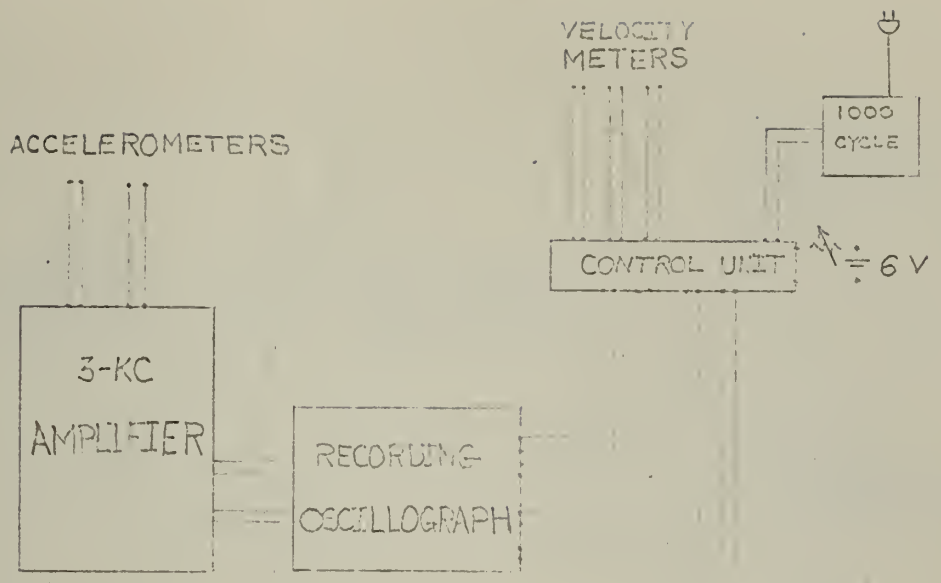

Figure 4

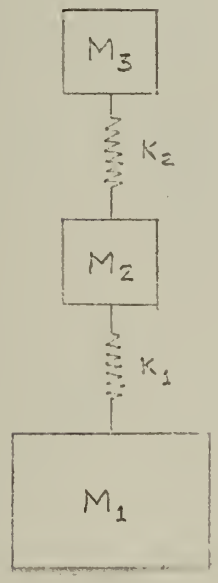

Figure 5a

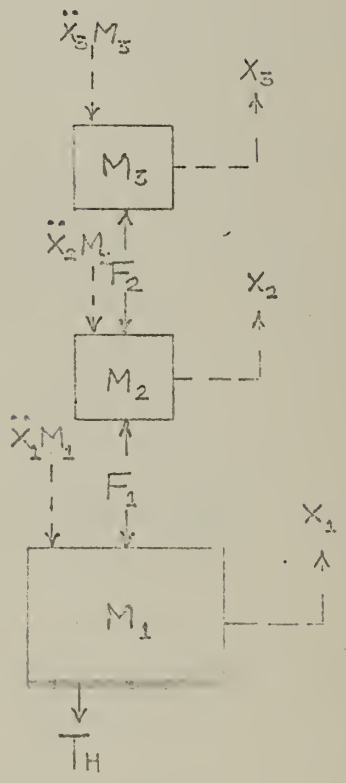

Figure 5b

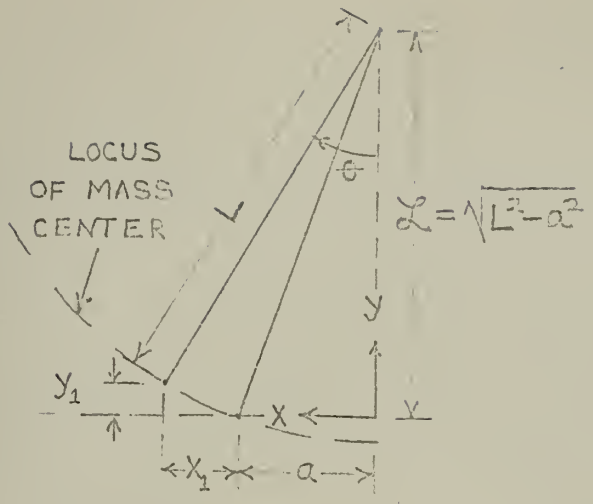

Figure 6a

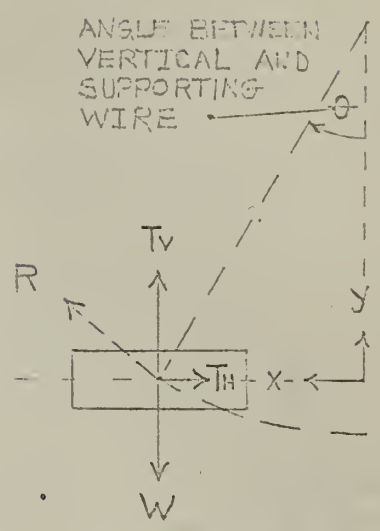

Figure 6b

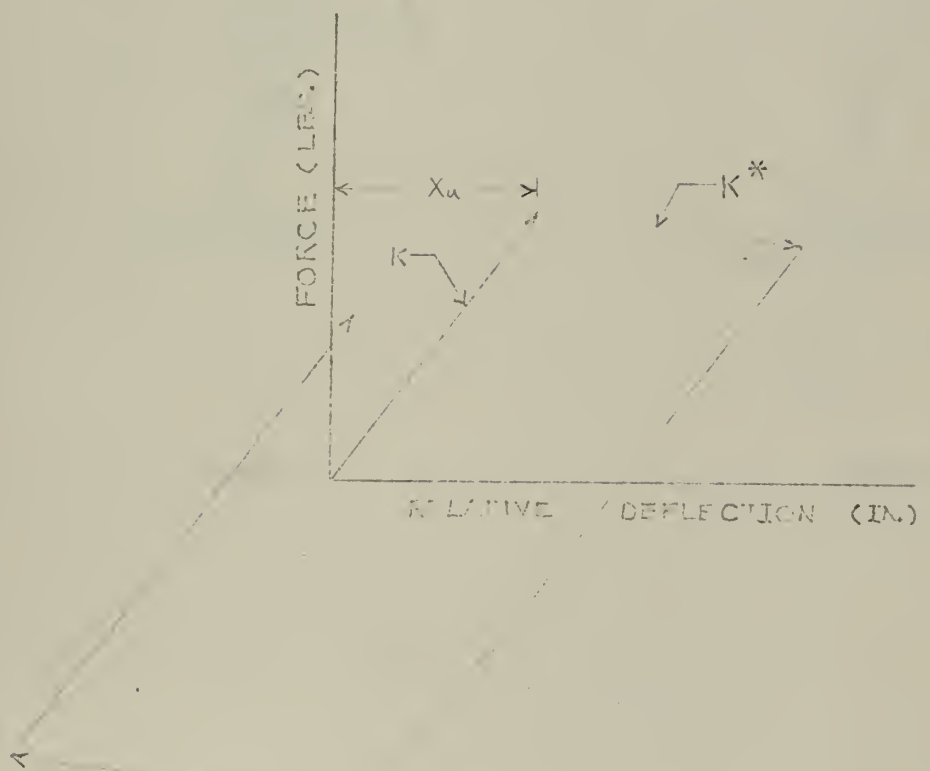

Figure 7

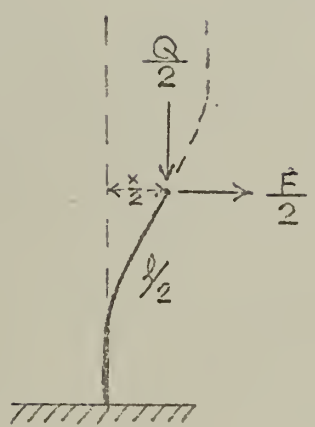

Figure 8a

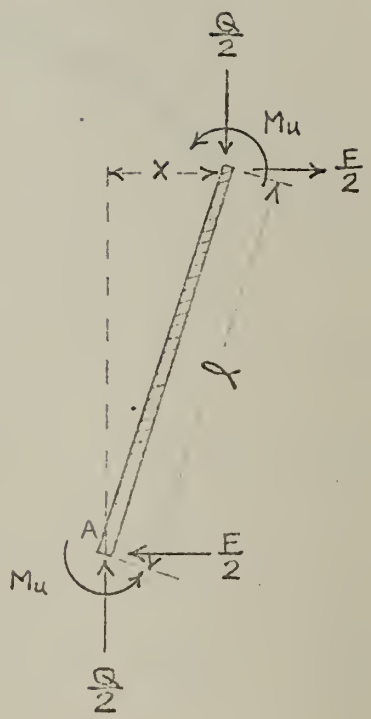

Figure 8b

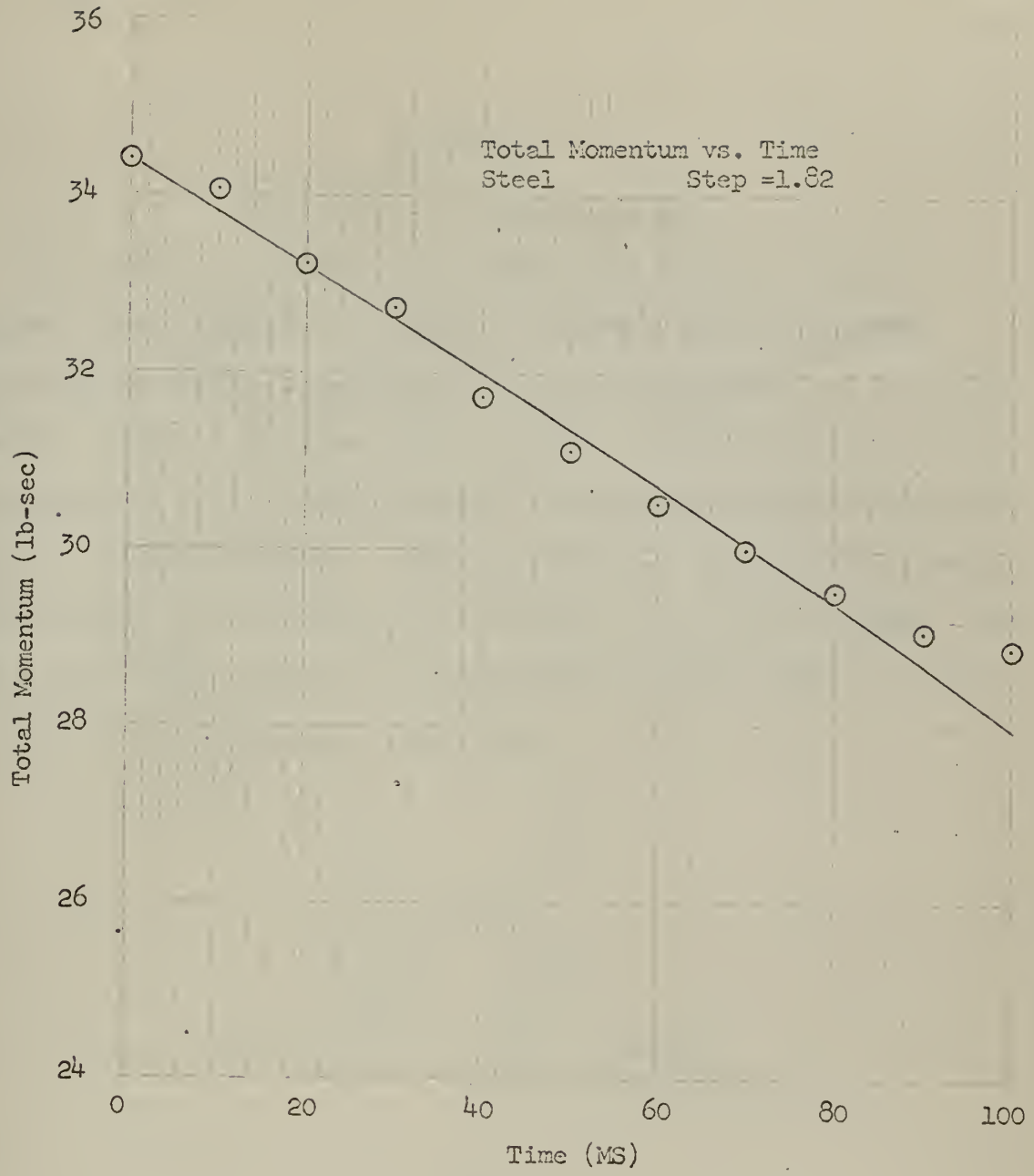

Figure 9
Plot of total momentum vs. time for an initial velocity input (Step) of 1.82 ft/sec. The symbol ⊙ denotes experimental points and the solid curve represents theoretical values for an initial anvil displacement of 0.7 ft.

APPENDIX I

FLOW CHARTS AND COMPUTER PROGRAM

This section contains a very general flow chart for the main program, a more detailed flow chart of the force versus deflection routine which was the controlling routine of the program, and the actual computer program. The force versus relative deflection routine permitted the evaluation of the spring forces as the mathematical model experienced elastic - plastic response. A list of symbols is included, since several symbol changes were necessary in conversion to the Fortran language. The figure shown below and the force-deflection flow chart shown on page 74 explain the force-deflection subroutine.

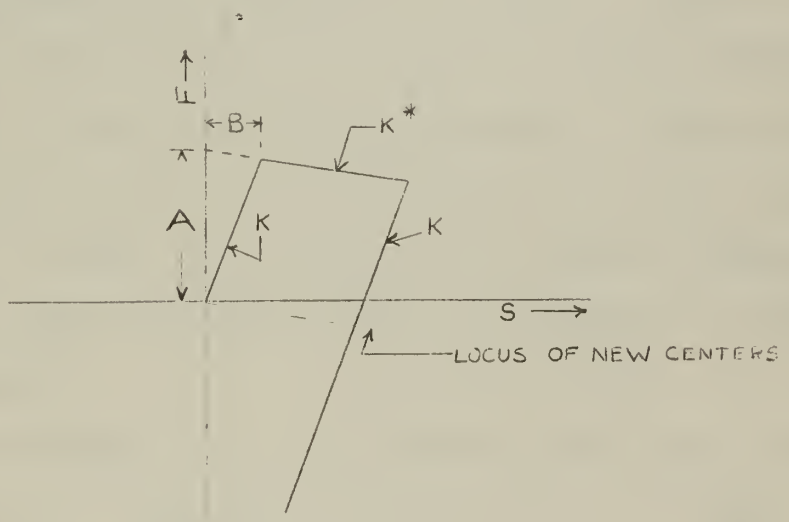

The subroutine is entered from the main program shown by the box labeled MP. Several parameters are picked up such as the relative displacement of the columns, denoted by S, the abscissa B of the knee-point, the elastic and plastic spring constants k and k*, the value for F where the extension of the line represented by k* crosses the vertical or force axis (denoted by A), and the coordinates (P,G) of the present location of the origin of

the force-deflection plot. Note that k* is negative as derived on page 15 . This is indicated in the figure above. The symbol R is the value of displacement used throughout the routine. This value is continually corrected for the changing origin. The location of the origin is determined from the previous history of the response. The first time that the subroutine is entered the values of P and G are zero, that is the origin is at (0,0). If the relative displacement S is less than the knee-point value B, then the force will be equal to the elastic spring constant k times the relative displacement R, where R = S - P or R = S since P = zero. When the value of R builds up to exceed the knee-point value B, a check is made to see if the column is loading or unloading. The check used is a displacement check denoted by the symbol U, where U is equal to the present relative displacement S minus the previous relative displacement SS. As long as the present displacement is larger, the forcing function is equal to A + k*R. The above routine is followed until the columns begin to unload. The present value of relative displacement becomes smaller than the previous value and a new origin is computed from the relations: P = O + H - B and G = k*(P) where O is the horizontal value of the previous origin and H is the last recorded value of R. The routine loops back to R = S - P where R will now be less than the knee-point value B. The value for force will be computed from F = G + kR or for values greater than B by F = A + G + k*R. The above described routine continues until the problem ends and a new step input is introduced whereupon all parameters are initialized. The same type of routine is also included for the case where the relative displacement or forcing function or both become negative. This can be seen by following the same type of analysis used above.

The force-deflection routine is found inside the subroutine labeled SUBROUTINE DERIV statement number 77 of the program listing.

STEP - the initial input velocity to anvil (ft/sec)

V - time increment (sec)

XE - time limit of problem (sec)

DE - end value of step input (ft/sec)

DD - initial anvil displacement [a]* (ft)

CHG - correction factor to allow for variable initial anvil displacement

DC - $[\text{anvil cable length}]^2 - [DD]^2$ (ft^2)

YD_i - displacement corresponding to ultimate bending moment $[X_u]$ (in)

SL_i - elastic spring constant [k] $(\#/in^2)$

STR_i - plastic spring constant [k*] $(\#/in^2)$

FBR_i - intersection of plastic force-deflection line with the vertical axis (lbs)

ANS - output printing interval (sec)

SP(I)- step input values for I different values (ft/sec)

Y_i - independent variables

D_i - dependent variables

F - forcing function in columns (lbs)

S - present relative displacement

SS - previous relative displacement

X - time variable

TAB - time expired between print intervals

O - last value for relative displacement of origin of force-deflection plot

H - last value for force origin of force-deflection plot

*Symbols in [ ] refer to previously defined terms.

G - new force coordinate for force-deflection plot

P - new relative displacement coordinate for force-deflection plot

R - Relative deflection of the columns

U - S —SS

SUM - total momentum of the structure

Main Flow Chart

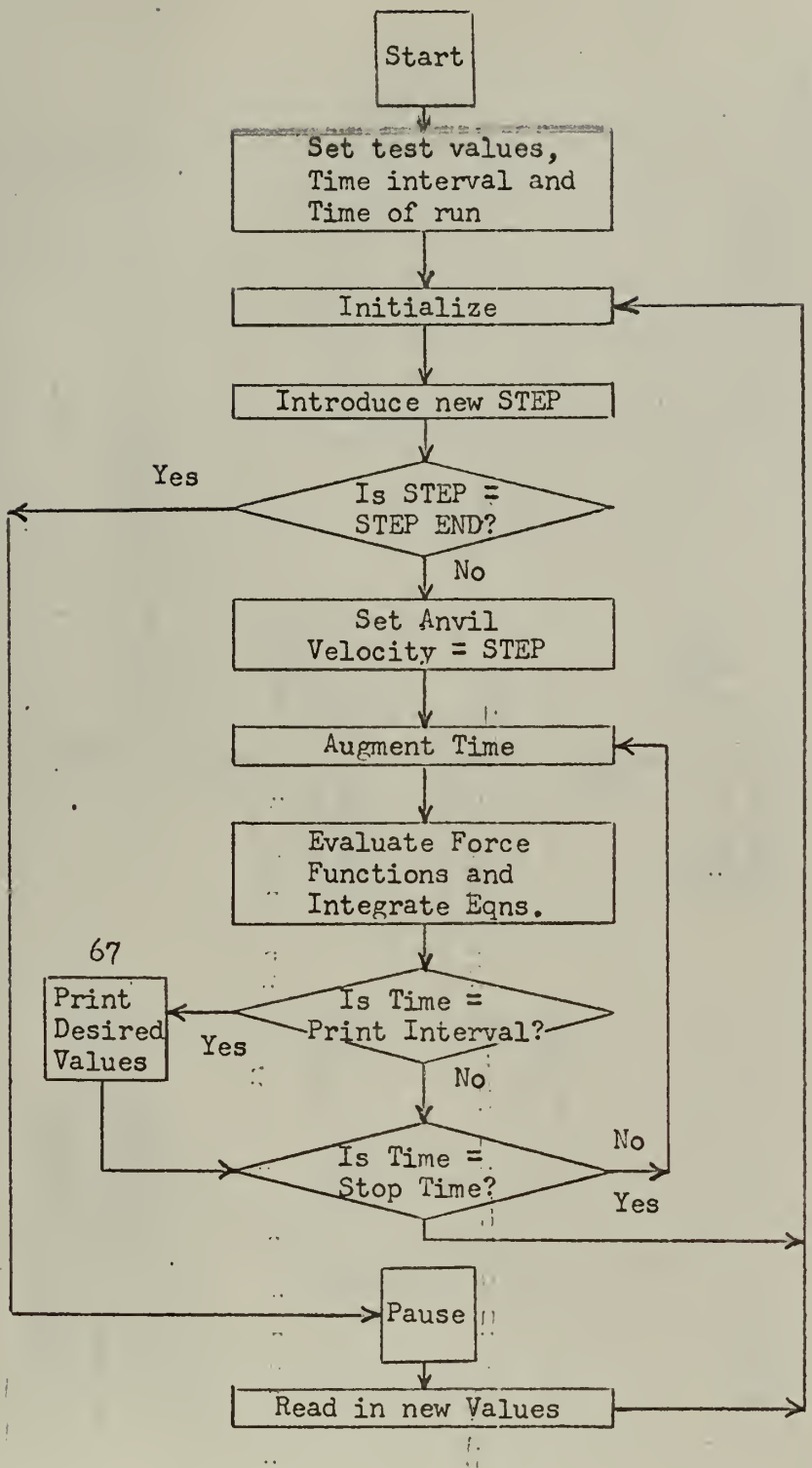

** Statement numbers are sequential starting with PROGRAM KENBOB as statement number one. Continued statements count as one statement.

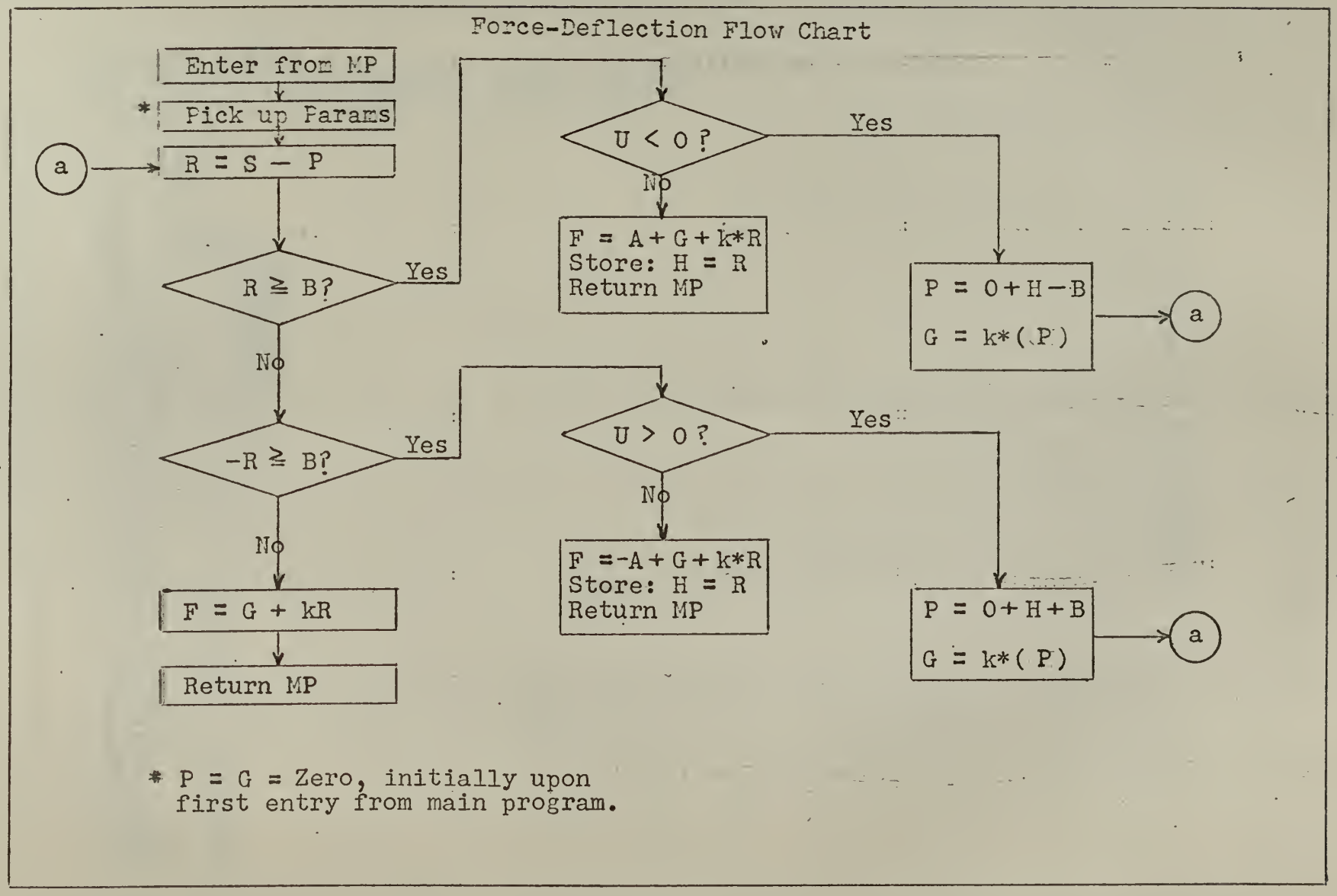
Force-Deflection Flow Chart
Enter from MP
* Pick up Params
a
R = S − P
R ≧ B?
Yes
No
-R ≧ B?
Yes
No
F = G + kR
Return MP
U < 0 ?
Yes
No
F = A + G + k*R
Store: H = R
Return MP
P = 0 + H − B
G = k*(P)
a
U > 0 ?
Yes
No
F = -A + G + k*R
Store: H = R
Return MP
P = 0 + H + B
G = k*(P)
a
* P = G = Zero, initially upon
first entry from main program.

Computer Program for Steel Columns*

```
      PROGRAM KENBOB
     0DIMENSION D(6),Y(6),R(2),S(2),F(2),O(2),G(2),H(2),P(2),U(2),
     1YD(2),SL(2),STR(2),FBR(2),SS(2),SP(6)
        COMMON YD,SL,STR,FBR,F,SS,O,G,H,S,DD,DC
          STEP = 0.1
            V = 0.001
           XE = 0.1
           DE = 2.0
          CHG = 0.4
           DD = 63.84
           DC = 0.500
        YD(1) = 0.500
        YD(2) = 1.000
        SL(1) = 12.000
        SL(2) = 12.000
       STR(1) = 2.500
       STR(2) = 2.500
       FBR(1) = 0.01
       FBR(2) = 1.00
       ANS = 0.
      SP(1) = 2.0000
      SP(2) = 0.
      SP(3) = 0.
      SP(4) = 0.
      SP(5) = 0.
      SP(6) = 0.
         I = 1
      Y(1) = 0.000000
      Y(2) = 0.
      Y(3) = 0.
      Y(4) = 0.
      Y(5) = 0.
      Y(6) = 0.
      F(1) = 0.
      F(2) = 0.
     SS(1) = 0.00
     SS(2) = 0.
     XTAB = 0.
     O(1) = 0.000000
     O(2) = 0.
     G(1) = 0.
     G(2) = 0.
     H(1) = 0.
     H(2) = 0.
        I = I + 1
       15 CONTINUE
```

*The program for aluminum columns is identical except for slightly different values for M_2 and M_3.

```
      STEP = SP(I)
      IF(STEP-DE)35,16,16
35    IF(SENSE SWITCH 1)33,34
33    PRINT 31,STEP
  310 FORMAT(7H STEP = F5.2/// 101H       TIME            X(1)
     1 V(1)              F(1)          F(2)          S(1)          S(2))
      GO TO 32
34    PRINT 30,STEP
 30 0 FORMAT(7H STEP = F5.2/// 101H       TIME            SUM
     1 DD                V(2)          V(3)          A(2)          A(3))
32    Y(4) = STEP
  10  X = X + V
      CALL RKUTTA(6,X,Y,V)
      D(5) = (F(1)-F(2))/0.743
      D(6) = F(2)/0.717
      SUM = 18.90*Y(4) + 0.743*Y(5) + 0.717*Y(6)
      DD = DD + CHG
      DC = 64.00 - DD**2
      TAB = TAB + V
      IF(TAB-ANS) 12,18,18
  18  TAB = 0.
      IF(SENSE SWITCH 1 )13,14
13    PRINT 19,X,Y(1),Y(4),F(1),F(2),S(1),S(2)
      GO TO 19
14    PRINT 19,X,SUM ,DD  ,Y(5),Y(6),D(5),D(6)
  19  FORMAT ( 1PE 15.4 , 6E 15.3)
12    IF(X-XE) 10,15,15
16    I = 0

      PAUSE
     OREAD 17,CHG ,V,XE,DE,DD,YD(1),YD(2),SL(1),SL(2),STR(1),STR(2),
     1FBR(1),FBR(2),ANS,SP(1),SP(2),SP(3),SP(4),SP(5),SP(6)
17    FORMAT(10E8.2)
      DC = 64.00 - DD**2
      GO TO 15
      END
      SUBROUTINE DERIV (D,Y,X)
     DDIMENSION D(6),Y(6),R(2),S(2),F(2),O(2),G(2),H(2),P(2),U(2),
     1YD(2),SL(2),STR(2),FBR(2)  ,SS(2)
      COMMON YD,SL,STR,FBR,F,SS,O,G,H,S,DD,DC
      D(1) = Y(4)
      D(2) = Y(5)
      D(3) = Y(6)
      S(1) = (Y(1) - Y(2)) * 12.
      S(2) = (Y(2) - Y(3)) * 12.
      U(1) = S(1) - SS(1)
      U(2) = S(2) - SS(2)
```

```
    9 R(1) = S(1) - O(1)
      IF(R(1)-YD(1))1,3,3
1     IF(R(1)+YD(1))5,5,2
2     F(1) = G(1) + SL(1)*R(1)
      SS(1) = S(1)
      GO TO 11
    3 IF(U(1)) 7,4,4
4     F(1) = FBR(1) + G(1) + STR(1)*R(1)
      H(1) = R(1)
      SS(1) = S(1)
      GO TO 11
    5 IF(U(1)) 6,6,8
6     F(1) = -FBR(1) + G(1) + STR(1)*R(1)
      H(1) = R(1)
      SS(1) = S(1)
      GO TO 11
7     P(1) = O(1) + H(1) - YD(1)
      G(1) = STR(1)*P(1)
      O(1) = P(1)
      GO TO  9
8     P(1) = O(1) + H(1) + YD(1)
      G(1) = STR(1)*P(1)
      O(1) = P(1)
      GO TO  9
   11 R(2) = S(2) - O(2)
      IF(R(2)-YD(2))21,23,23
21    IF(R(2)+YD(2))25,25,22
22    F(2) = G(2) + SL(2)*R(2)
      SS(2) = S(2)
      GO TO 29
   23 IF(U(2)) 27,24,24
24    F(2) = FBR(2) + G(2) + STR(2)*R(2)
      H(2) = R(2)
      SS(2) = S(2)
      GO TO 29
   25 IF(U(2)) 26,26,28
26    F(2) = -FBR(2) + G(2) + STR(2)*R(2)
      H(2) = R(2)
      SS(2) = S(2)
      GO TO  29
27    P(2) = O(2) + H(2) - YD(2)
      G(2) = STR(2)*P(2)
      O(2) = P(2)
      GO TO 11
28    P(2) = O(2) + H(2) + YD(2)
      G(2) = STR(2)*P(2)
```

```
      O(2) = P(2)
      GO TO 11
   29 CC = DD + Y(1)
      YX = 8.00 - SQRTF(DC-CC**2)
      CK = 8.00 - YX
      YV = (CC*Y(4))/CK
     OD(4) = (-F(1)-(CC/CK)*656.*(1.+(Y(4)**2+YV**2)/(32.20*CK)))/( 18.9
     1+(656./32.20)*(CC/CK)**2)
      D(5) = (F(1)-F(2))/0.743

      D(6) = F(2)/0.717
      END
      SUBROUTINE RKUTTA(NUMBER,XVAR,YVARS,STEP)
      DIMENSION YVARS(30),AK(4,30),            DY(30),YC(30),C(3)
      C(1)=0.5
      C(2)=0.5
      C(3)=1.0
      CALL DERIV(DY,    YVARS,XVAR)
      DO 1 J=1,NUMBER
    1 AK(1,J)=STEP*DY(J)
      DO 2 I=2,4
      XC=XVAR +C(I-1)*STEP
      DO 3 J=1,NUMBER
    3 YC(J)= YVARS(J) + C(I-1)*AK(I-1,J)
      CALL DERIV(DY,YC,XC)
      DO 2 J=1,NUMBER
    2 AK(I,J)=STEP *DY(J)
      DO 4 J=1,NUMBER
    4 YVARS(J)=YVARS(J)+(AK(1,J)+2.*AK(2,J)+2.*AK(3,J)+AK(4,J))/6.0
      RETURN
      END
      END
```

APPENDIX II

REDUCTION OF DATA

This section contains a complete set of calculations for one run. Also included is a tracing of the oscillograph record for the same run. A photograph of the actual record was not possible due to the lack of contrast between the trace and the paper. It is to be noted that the 1000 cycle trace, mentioned earlier, is not shown. This particular trace was omitted to prevent cluttering of the other tracings and also because of the tedious tracing job required to accurately reproduce this trace.

The data reduction consisted of the following steps:

1. Establishing reference lines on oscillograph record
2. Measuring trace amplitudes for velocity parameters
3. Integrating the acceleration vs. time trace
4. Computing conversion factors
5. Converting measured parameters to proper units.

The run in question was for steel columns and a step input of 5.02 ft/sec.

Computation of the necessary spring constants, and other input parameters are also shown.

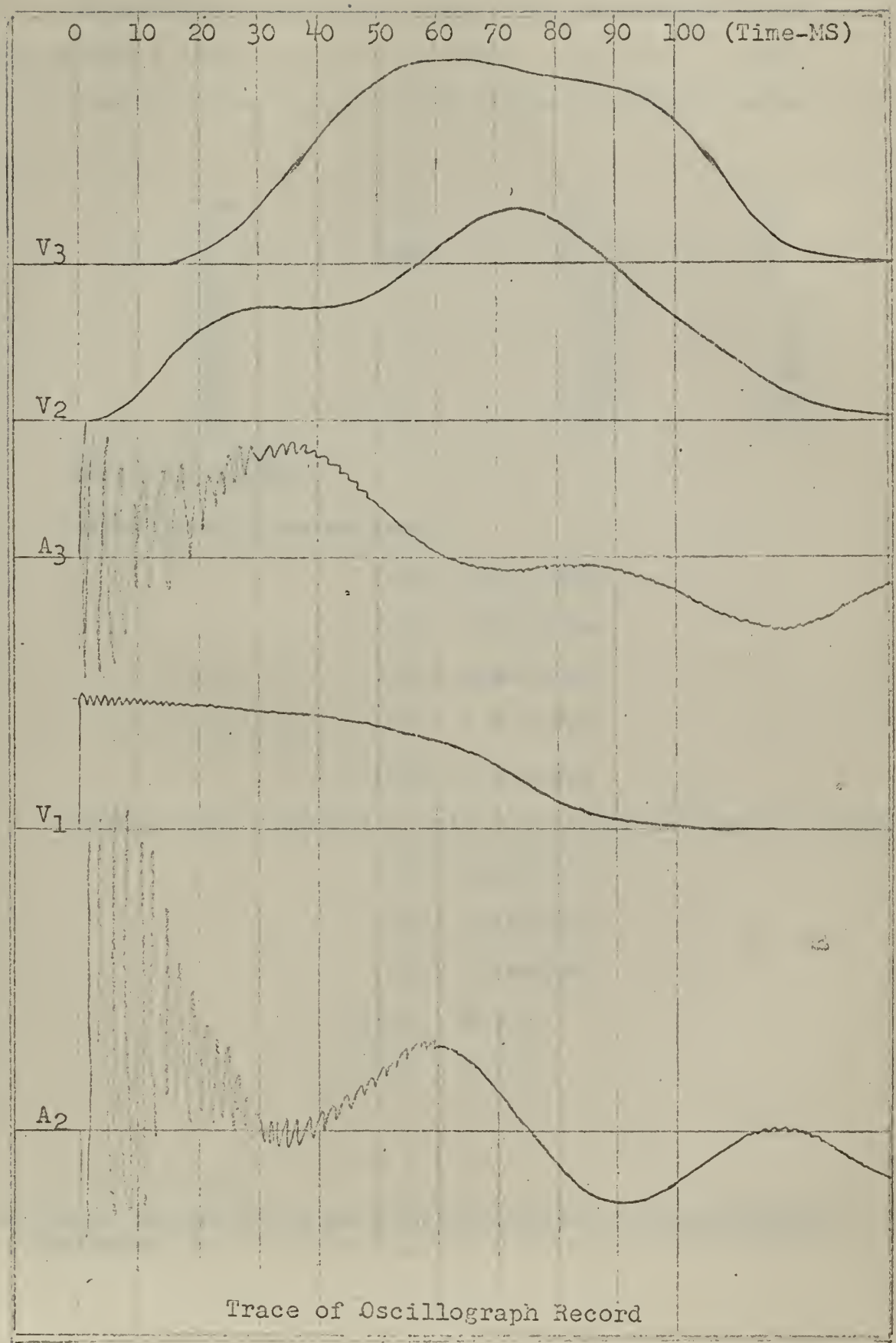

Trace of Oscillograph Record

The preceding figure shows traces of the oscillograph record. The symbols V denote velocity and A denote acceleration. Direct measurements from the figure gives the following values in inches:

Time	V(1)	V(2)	V(3)
0	0.88	0	0
10	*	.18	0
20	*	.59	.08
30	*	.75	.37
40	*	.75	.85
50	*	.86	1.24
60	*	1.14	1.40
70	*	1.39	1.37

*values not measured

Calibration pulse measurements:

V(1) - 0.720 inches

V(2) - 0.785 inches

V(3) - 0.820 inches

A(2) - 1.24 inches

A(3) - 1.12 inches

Velocity meter sensitivities and accelerometer calibration constants:

V(1) - 146 mv/fps

V(2) - 167 mv/fps

V(3) - 151 mv/fps

**A(2) - 70.7 g

**A(3) - 78.0 g

** values obtained by the David Taylor Model Basin using calibration resistance.

Instrument settings:

a. Calibration

Amplifier gain set at 30 for accelerometers, paper speed set at 4"/sec
Battery voltage for velocity meters set at 0.6 volts

b. Run

Amplifier gain set at 5 for accelerometers, paper speed set at 40"/sec

Combination of the above information gives the following conversion factors:

a. for velocity conversion

$$V_{FACTOR} = \frac{\text{CALIB. VOLTAGE (v)}}{\text{SENSITIVITY (V/fps)}} \cdot \frac{1}{\text{PULSE HT.}}$$

SAMPLE:

$$V_{1\,FACTOR} = \frac{0.6\ V}{0.146\ V/fps} \cdot \frac{1}{0.720\ in} = 5.71\ fps/in$$

$$V_{2\,FACTOR} = 4.57\ fps/in.$$

$$V_{3\,FACTOR} = 4.84\ fps/in.$$

b. for acceleration factors

$$A_{FACTOR} = \frac{\text{CALIB. CONSTANT}}{\text{CALIB PULSE HT.}} \cdot \frac{\text{RUN GAIN}}{\text{CALIB. GAIN}}$$

SAMPLE:

$$A_{2\,FACTOR} = \frac{(70.7)(32.2)\ ft/sec^2}{1.24\ in.} \cdot \frac{5}{30} = 306\ ft/sec\text{-}in.$$

$$A_{3\,FACTOR} = 374\ ft/sec\text{-}in.$$

c. conversion for integration constant

$$V_{c\text{-}FACTOR} = A_{FACTOR} \cdot TIME_{FACTOR} \cdot AREA$$

$$V_{2c\text{-}FACTOR} = 306\left(\frac{ft/sec}{in}\right) \cdot 0.025\left(\frac{sec}{in}\right) \cdot AREA\ (in^2)$$

$$V_{2c\text{-}FACTOR} = 7.65 \cdot AREA\ (ft/sec)$$

$$V_{3c\text{-}FACTOR} = 9.35 \cdot AREA\ (ft/sec)$$

Areas under acceleration trace:

Time range (MS)	Area V(2) (in^2)	Area V(3) (in^2)
70-80	0.01	-0.04
70-90	-0.14	-0.06
70-100	-0.32	-0.14

From the above information:

Time (MS)	V(1) (ft/sec)	V(2) (ft/sec)	V(3) (ft/sec)
0	5.02	0	0
10	*	0.82	0
20	*	2.70	0.39
30	*	3.43	1.79
40	*	3.43	4.12
50	*	3.92	6.00
60	*	5.21	6.78
70	*	6.35	6.63
80	*	6.43	6.26
90	*	5.28	6.07
100	*	3.90	5.32

*Not measured

Evaluation of spring constants - steel

Column thickness = h = 0.128"
Column width = b = 1.95"
Effective length = l_{eff} = 90."

*modulus of elasticity = E = 29.4 x 10^6 psi

Weight on upper columns = Q_2 = 23.1 lbs

Weight on lower columns = Q_1 = 47.0 lbs

*Value obtained from actual tension test of sample column. See Appendix III

$$I = \frac{bh^3}{12} = \frac{(1.95)(0.128)^3}{12} = 341 \times 10^{-6} \text{ in.}^4$$

$$Q_e = \frac{2\pi^2 EI}{\ell^2} = \frac{2\pi^2(29.4)(341)}{81} = 2440 \text{ lbs.}$$

$$K_1 = \frac{24EI}{\ell^3}\left[1 - \frac{Q_1}{Q_e}\right] = \frac{(24)(29.4)(341)}{9^3}\left[1 - \frac{47.0}{2440}\right]$$

$$K_1 = 324 \text{ lb./in}$$

$$K_2 = 327 \text{ lb./in}$$

$$K_1^* = -\frac{Q_1}{\ell} = -\frac{47.0}{9} = -5.22 \text{ lb./in.}$$

$$K_2^* = -2.57 \text{ lb./in}$$

Evaluation of force-deflection knee points

(a.) $\bar{\sigma} = 40{,}000$ psi

$$4M_u = \bar{\sigma} b h^2 = (40{,}000)(1.95)(0.128)^2 = 1278 \text{ in-lb}$$

$$K_1 X_{u1} = \frac{4M_u - Q_1 X_{u1}}{\ell}$$

$$324 X_{u1} = \frac{1278 - 47.0 X_{u1}}{9}$$

$$X_{u1} = \frac{1278}{2963} = 0.431 \text{ in}$$

$$X_{u2} = \frac{1278}{2966} = 0.430 \text{ in}$$

$$A = \frac{4M_u}{\ell} = \frac{1278}{9} = 142 \text{ lb}$$

(b) $\bar{\sigma} = 50,000$ psi

$x_{u_1} = 0.539$ in

$x_{u_2} = 0.538$ in

$A = 177$ lb.

(c) $\bar{\sigma} = 60,000$ psi

$x_{u_1} = 0.646$ in

$x_{u_2} = 0.645$ in.

$A = 213$ lb.

Using the same procedure for 3003-H14 aluminum:

$K_1 = 109$ lb/in.

$K_2 = 112$ lb/in.

$K_1^* = -5.21$ lb./in.

$K_2^* = -2.59$ lb./in.

WHERE: $h = 0.125''$
$b = 1.98''$
$l_{EFF} = 8.75''$
* $E = 10.0 \times 10^6$ psi
$Q_1 = 22.8$ lbs
$Q_2 = 11.4$ lbs.

KNEE POINTS:

(a) $\sigma = 20,000$ psi

$x_{u_1} = 0.619$ in

$x_{u_2} = 0.616$ in

$A = 70.8$ lb.

(b) $\sigma = 30,000$ psi

$x_{u_1} = 0.928$ in.

$x_{u_2} = 0.923$ in

$A = 106$ lb.

---

*value taken from Alcoa Aluminum Handbook for 3003-H14 Aluminum reference [7].

APPENDIX III

COLUMN MATERIALS, TENSION TESTS, AND EFFECTIVE MASSES

Column Materials

As noted earlier, two different materials were utilized in the test columns; hot rolled steel, with properties similar to those of the steel used by Kurzenhauser, and 3003 - H14 aluminum. The aluminum sheet used had a yield strength of 21,000 psi and an ultimate strength of 22,000 psi, as listed by the Alcoa Aluminum Handbook [7] . A 6061 T6 aluminum used by Massard and Collins [2] , would have been more representative of the aluminum used in structural work; however, this was not available at the time the experimentation was conducted.

Tension Tests

Three samples of each of the column materials used were selected and shaped into standard tensile test specimens with a 2" gage length to meet ASTM Standard E8-54T. A Baldwin Universal Testing machine, along with a Riehle extensometer were utilized in making the tension tests. The results are tabulated in Table 1 below:

Table 1

	Steel	Aluminum
Modulus of Elasticity	29.4×10^6 psi	10.2×10^6 psi
Yield Point	40,800 psi	20,300 psi
Ultimate Strength	59,300 psi	22,250 psi

Effective Masses

A very simple approximation of the effective weights of the structure was made by including one half of the weight of two supporting columns with the upper mass and the weight of two full supporting columns with the center mass. The remaining two halves of the lower columns were included with the anvil mass. The figure below shows this procedure.

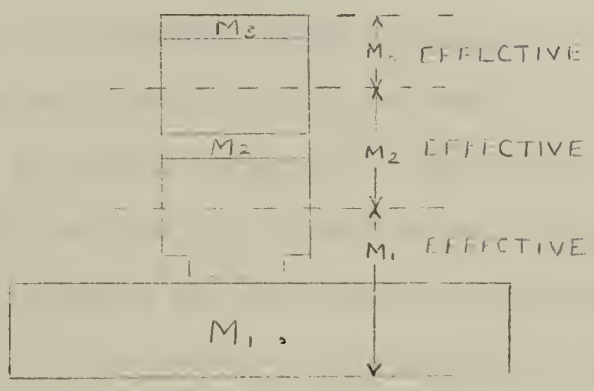

The values of the above effective masses are listed in table 2. The units are $lb\text{-}sec^2/ft$.

Table 2

Mass Number	Steel effective	Al effective
1	18.9	18.9
2	0.743	0.711
3	0.717	0.705

APPENDIX IV

FURTHER PROGRAM MODIFICATIONS CONSIDERED

Two further modifications to the computer solution were considered. One modification was the determination of the effect of vertical acceleration upon the structure's columns. The fact that the anvil experiences a vertical acceleration upon impact, produces a force in addition to the structure's static weight. This vertical acceleration was obtained for several runs and found not to exceed about $5 ft/sec^2$. This would have resulted in a variable correction to the effective value of Q of not more than 16%, and the Q/Q_e correction was itself rather small, of the order of 2%. Thus it was not considered of sufficient importance to make this correction which would have greatly complicated the theoretical analysis and would have resulted in considerably more cumbersome differential equations to work with.

The second modification was an attempt to force the theoretical and experimental total momentum vs. time curves to agree exactly, by varying the value of initial anvil displacement during the run in such a manner as to retain the proper momentum relation. This was tried for several runs, resulting in perfect agreement in the plots of total momentum vs. time; however, practically no change in the velocity response was noted. This modification was likewise not included since the constant value of $a = 0.7'$ produced essentially the same results.

APPENDIX V

TYPICAL COMPUTER OUTPUT

The tabulation of theoretical values for a typical run shows the time in MS, velocities V(2) and V(3) in ft/sec, and the total momentum in lb-sec designated by the term SUM.

Computer Solution STEP = 5.02

$\bar{\sigma}$ = 40,000 psi Steel

TIME	SUM	V(2)	V(3)
1.0000E-03	9.481E+01	1.312E-02	5.986E-06
2.0000E-03	9.475E+01	5.233E-02	9.561E-05
3.0000E-03	9.469E+01	1.172E-01	4.827E-04
4.0000E-03	9.462E+01	2.070E-01	1.519E-03
5.0000E-03	9.456E+01	3.207E-01	3.691E-03
6.0000E-03	9.449E+01	4.573E-01	7.608E-03
7.0000E-03	9.443E+01	6.150E-01	1.399E-02
8.0000E-03	9.437E+01	7.902E-01	2.368E-02
9.0000E-03	9.430E+01	9.645E-01	3.755E-02
1.0000E-02	9.423E+01	1.134E+00	5.649E-02
1.1000E-02	9.417E+01	1.297E+00	8.133E-02
1.2000E-02	9.410E+01	1.453E+00	1.128E-01
1.3000E-02	9.403E+01	1.602E+00	1.516E-01
1.4000E-02	9.397E+01	1.743E+00	1.983E-01
1.5000E-02	9.390E+01	1.876E+00	2.535E-01
1.6000E-02	9.383E+01	2.000E+00	3.176E-01
1.7000E-02	9.376E+01	2.119E+00	3.908E-01
1.8000E-02	9.369E+01	2.220E+00	4.735E-01
1.9000E-02	9.362E+01	2.316E+00	5.657E-01
2.0000E-02	9.355E+01	2.402E+00	6.675E-01
2.1000E-02	9.348E+01	2.479E+00	7.788E-01
2.2000E-02	9.341E+01	2.547E+00	8.993E-01
2.3000E-02	9.334E+01	2.606E+00	1.029E+00
2.4000E-02	9.327E+01	2.657E+00	1.167E+00
2.5000E-02	9.320E+01	2.699E+00	1.313E+00
2.6000E-02	9.313E+01	2.734E+00	1.467E+00
2.7000E-02	9.306E+01	2.763E+00	1.628E+00
2.8000E-02	9.298E+01	2.785E+00	1.795E+00
2.9000E-02	9.291E+01	2.801E+00	1.968E+00
3.0000E-02	9.284E+01	2.813E+00	2.145E+00
3.1000E-02	9.276E+01	2.822E+00	2.325E+00
3.2000E-02	9.269E+01	2.827E+00	2.509E+00
3.3000E-02	9.261E+01	2.831E+00	2.694E+00
3.4000E-02	9.254E+01	2.834E+00	2.880E+00
3.5000E-02	9.246E+01	2.837E+00	3.066E+00
3.6000E-02	9.239E+01	2.841E+00	3.250E+00
3.7000E-02	9.231E+01	2.847E+00	3.432E+00
3.8000E-02	9.223E+01	2.856E+00	3.611E+00
3.9000E-02	9.216E+01	2.869E+00	3.786E+00
4.0000E-02	9.208E+01	2.887E+00	3.956E+00
4.1000E-02	9.200E+01	2.910E+00	4.120E+00
4.2000E-02	9.193E+01	2.939E+00	4.277E+00
4.3000E-02	9.185E+01	2.978E+00	4.427E+00
4.4000E-02	9.177E+01	3.019E+00	4.569E+00
4.5000E-02	9.169E+01	3.071E+00	4.703E+00
4.6000E-02	9.161E+01	3.131E+00	4.827E+00
4.7000E-02	9.153E+01	3.200E+00	4.943E+00
4.8000E-02	9.145E+01	3.278E+00	5.049E+00
4.9000E-02	9.137E+01	3.366E+00	5.145E+00
5.0000E-02	9.129E+01	3.462E+00	5.232E+00
5.1000E-02	9.121E+01	3.568E+00	5.308E+00
5.2000E-02	9.113E+01	3.683E+00	5.376E+00
5.3000E-02	9.105E+01	3.807E+00	5.434E+00
5.4000E-02	9.096E+01	3.940E+00	5.483E+00
5.5000E-02	9.088E+01	4.080E+00	5.524E+00
5.6000E-02	9.080E+01	4.228E+00	5.556E+00
5.7000E-02	9.072E+01	4.383E+00	5.582E+00
5.8000E-02	9.063E+01	4.545E+00	5.601E+00
5.9000E-02	9.055E+01	4.711E+00	5.614E+00
6.0000E-02	9.047E+01	4.880E+00	5.622E+00

TIME	SUM	V(2)	V(3)
6.1000E-02	9.038E+01	5.050E+00	5.627E+00
6.2000E-02	9.030E+01	5.220E+00	5.628E+00
6.3000E-02	9.021E+01	5.388E+00	5.627E+00
6.4000E-02	9.013E+01	5.552E+00	5.624E+00
6.5000E-02	9.004E+01	5.709E+00	5.621E+00
6.6000E-02	8.995E+01	5.859E+00	5.619E+00
6.7000E-02	8.987E+01	5.999E+00	5.618E+00
6.8000E-02	8.978E+01	6.129E+00	5.619E+00
6.9000E-02	8.969E+01	6.246E+00	5.623E+00
7.0000E-02	8.960E+01	6.350E+00	5.630E+00
7.1000E-02	8.951E+01	6.439E+00	5.641E+00
7.2000E-02	8.943E+01	6.513E+00	5.656E+00
7.3000E-02	8.934E+01	6.570E+00	5.677E+00
7.4000E-02	8.925E+01	6.611E+00	5.702E+00
7.5000E-02	8.916E+01	6.634E+00	5.732E+00
7.6000E-02	8.906E+01	6.640E+00	5.767E+00
7.7000E-02	8.897E+01	6.629E+00	5.806E+00
7.8000E-02	8.888E+01	6.601E+00	5.851E+00
7.9000E-02	8.879E+01	6.556E+00	5.899E+00
8.0000E-02	8.869E+01	6.496E+00	5.951E+00
8.1000E-02	8.860E+01	6.421E+00	6.006E+00
8.2000E-02	8.851E+01	6.332E+00	6.063E+00
8.3000E-02	8.841E+01	6.231E+00	6.121E+00
8.4000E-02	8.832E+01	6.119E+00	6.180E+00
8.5000E-02	8.822E+01	5.997E+00	6.239E+00
8.6000E-02	8.812E+01	5.866E+00	6.297E+00
8.7000E-02	8.803E+01	5.729E+00	6.352E+00
8.8000E-02	8.793E+01	5.588E+00	6.404E+00
8.9000E-02	8.783E+01	5.443E+00	6.451E+00
9.0000E-02	8.773E+01	5.297E+00	6.493E+00
9.1000E-02	8.764E+01	5.152E+00	6.528E+00
9.2000E-02	8.754E+01	5.009E+00	6.556E+00
9.3000E-02	8.744E+01	4.870E+00	6.575E+00
9.4000E-02	8.734E+01	4.736E+00	6.585E+00
9.5000E-02	8.724E+01	4.609E+00	6.585E+00
9.6000E-02	8.714E+01	4.490E+00	6.574E+00
9.7000E-02	8.703E+01	4.381E+00	6.551E+00
9.8000E-02	8.693E+01	4.282E+00	6.517E+00
9.9000E-02	8.683E+01	4.194E+00	6.471E+00
1.0000E-01	8.673E+01	4.119E+00	6.412E+00

Computer Solution STEP = 5.02

$\bar{\sigma}$ = 50,000 psi Steel

TIME	SUM	V(2)	V(3)
1.0000E-03	9.481E+01	1.312E-02	5.986E-06
2.0000E-03	9.475E+01	5.233E-02	9.561E-05
3.0000E-03	9.469E+01	1.172E-01	4.827E-04
4.0000E-03	9.462E+01	2.070E-01	1.519E-03
5.0000E-03	9.456E+01	3.207E-01	3.691E-03
6.0000E-03	9.449E+01	4.573E-01	7.608E-03
7.0000E-03	9.443E+01	6.150E-01	1.399E-02
8.0000E-03	9.437E+01	7.924E-01	2.368E-02
9.0000E-03	9.430E+01	9.876E-01	3.757E-02
1.0000E-02	9.423E+01	1.198E+00	5.667E-02
1.1000E-02	9.417E+01	1.408E+00	8.201E-02
1.2000E-02	9.410E+01	1.611E+00	1.146E-01
1.3000E-02	9.404E+01	1.805E+00	1.554E-01
1.4000E-02	9.397E+01	1.991E+00	2.052E-01
1.5000E-02	9.390E+01	2.167E+00	2.647E-01
1.6000E-02	9.383E+01	2.333E+00	3.347E-01
1.7000E-02	9.377E+01	2.488E+00	4.156E-01
1.8000E-02	9.370E+01	2.631E+00	5.078E-01
1.9000E-02	9.363E+01	2.764E+00	6.116E-01
2.0000E-02	9.356E+01	2.885E+00	7.272E-01
2.1000E-02	9.349E+01	2.994E+00	8.546E-01
2.2000E-02	9.342E+01	3.092E+00	9.937E-01
2.3000E-02	9.335E+01	3.179E+00	1.144E+00
2.4000E-02	9.328E+01	3.254E+00	1.306E+00
2.5000E-02	9.321E+01	3.320E+00	1.478E+00
2.6000E-02	9.314E+01	3.375E+00	1.661E+00
2.7000E-02	9.306E+01	3.422E+00	1.852E+00
2.8000E-02	9.299E+01	3.460E+00	2.053E+00
2.9000E-02	9.292E+01	3.490E+00	2.261E+00
3.0000E-02	9.285E+01	3.514E+00	2.476E+00
3.1000E-02	9.277E+01	3.533E+00	2.696E+00
3.2000E-02	9.270E+01	3.546E+00	2.921E+00
3.3000E-02	9.262E+01	3.557E+00	3.150E+00
3.4000E-02	9.255E+01	3.565E+00	3.380E+00
3.5000E-02	9.248E+01	3.572E+00	3.612E+00
3.6000E-02	9.240E+01	3.579E+00	3.843E+00
3.7000E-02	9.233E+01	3.588E+00	4.073E+00
3.8000E-02	9.225E+01	3.599E+00	4.301E+00
3.9000E-02	9.217E+01	3.614E+00	4.524E+00
4.0000E-02	9.210E+01	3.633E+00	4.743E+00
4.1000E-02	9.202E+01	3.658E+00	4.955E+00
4.2000E-02	9.194E+01	3.690E+00	5.161E+00
4.3000E-02	9.187E+01	3.730E+00	5.358E+00
4.4000E-02	9.179E+01	3.778E+00	5.547E+00
4.5000E-02	9.171E+01	3.835E+00	5.725E+00
4.6000E-02	9.163E+01	3.903E+00	5.894E+00
4.7000E-02	9.155E+01	3.980E+00	6.051E+00
4.8000E-02	9.147E+01	4.069E+00	6.198E+00
4.9000E-02	9.139E+01	4.169E+00	6.332E+00
5.0000E-02	9.131E+01	4.280E+00	6.455E+00
5.1000E-02	9.123E+01	4.403E+00	6.566E+00
5.2000E-02	9.115E+01	4.537E+00	6.665E+00
5.3000E-02	9.107E+01	4.682E+00	6.752E+00
5.4000E-02	9.099E+01	4.836E+00	6.828E+00
5.5000E-02	9.091E+01	4.998E+00	6.893E+00
5.6000E-02	9.083E+01	5.167E+00	6.948E+00
5.7000E-02	9.075E+01	5.341E+00	6.993E+00
5.8000E-02	9.066E+01	5.518E+00	7.029E+00
5.9000E-02	9.058E+01	5.697E+00	7.057E+00
6.0000E-02	9.050E+01	5.876E+00	7.078E+00

TIME	SUM	V(2)	V(3)
6.1000E-02	9.041E+01	6.653E+00	7.091E+00
6.2000E-02	9.033E+01	6.226E+00	7.099E+00
6.3000E-02	9.025E+01	6.393E+00	7.103E+00
6.4000E-02	9.016E+01	6.553E+00	7.102E+00
6.5000E-02	9.007E+01	6.704E+00	7.099E+00
6.6000E-02	8.998E+01	6.844E+00	7.093E+00
6.7000E-02	8.990E+01	6.971E+00	7.086E+00
6.8000E-02	8.982E+01	7.085E+00	7.078E+00
6.9000E-02	8.973E+01	7.184E+00	7.070E+00
7.0000E-02	8.964E+01	7.269E+00	7.063E+00
7.1000E-02	8.955E+01	7.331E+00	7.057E+00
7.2000E-02	8.946E+01	7.379E+00	7.053E+00
7.3000E-02	8.937E+01	7.408E+00	7.050E+00
7.4000E-02	8.928E+01	7.418E+00	7.049E+00
7.5000E-02	8.919E+01	7.409E+00	7.050E+00
7.6000E-02	8.910E+01	7.381E+00	7.053E+00
7.7000E-02	8.901E+01	7.335E+00	7.058E+00
7.8000E-02	8.891E+01	7.270E+00	7.065E+00
7.9000E-02	8.882E+01	7.189E+00	7.072E+00
8.0000E-02	8.873E+01	7.090E+00	7.081E+00
8.1000E-02	8.863E+01	6.976E+00	7.089E+00
8.2000E-02	8.854E+01	6.848E+00	7.097E+00
8.3000E-02	8.844E+01	6.708E+00	7.103E+00
8.4000E-02	8.835E+01	6.556E+00	7.107E+00
8.5000E-02	8.825E+01	6.394E+00	7.108E+00
8.6000E-02	8.815E+01	6.224E+00	7.105E+00
8.7000E-02	8.805E+01	6.048E+00	7.098E+00
8.8000E-02	8.796E+01	5.868E+00	7.084E+00
8.9000E-02	8.786E+01	5.685E+00	7.064E+00
9.0000E-02	8.776E+01	5.501E+00	7.037E+00
9.1000E-02	8.766E+01	5.319E+00	7.001E+00
9.2000E-02	8.756E+01	5.139E+00	6.955E+00
9.3000E-02	8.746E+01	4.964E+00	6.900E+00
9.4000E-02	8.736E+01	4.795E+00	6.834E+00
9.5000E-02	8.725E+01	4.633E+00	6.758E+00
9.6000E-02	8.715E+01	4.480E+00	6.669E+00
9.7000E-02	8.705E+01	4.338E+00	6.569E+00
9.8000E-02	8.695E+01	4.207E+00	6.456E+00
9.9000E-02	8.684E+01	4.087E+00	6.331E+00
1.0000E-01	8.674E+01	3.980E+00	6.194E+00

Computer Solution STEP = 5.02

$\bar{\sigma}$ = 60,000 psi Steel

TIME	SUM	V(2)	V(3)
1.0000E-03	9.481E+01	1.312E-02	5.986E-06
2.0000E-03	9.475E+01	5.253E-02	9.561E-05
3.0000E-03	9.469E+01	1.172E-01	4.827E-04
4.0000E-03	9.462E+01	2.070E-01	1.519E-03
5.0000E-03	9.456E+01	3.207E-01	3.671E-03
6.0000E-03	9.449E+01	4.573E-01	7.608E-03
7.0000E-03	9.443E+01	6.150E-01	1.399E-02
8.0000E-03	9.437E+01	7.924E-01	2.368E-02
9.0000E-03	9.430E+01	9.876E-01	3.757E-02
1.0000E-02	9.423E+01	1.198E+00	5.667E-02
1.1000E-02	9.417E+01	1.423E+00	8.202E-02
1.2000E-02	9.410E+01	1.658E+00	1.147E-01
1.3000E-02	9.404E+01	1.899E+00	1.559E-01
1.4000E-02	9.397E+01	2.132E+00	2.065E-01
1.5000E-02	9.390E+01	2.355E+00	2.677E-01
1.6000E-02	9.384E+01	2.566E+00	3.403E-01
1.7000E-02	9.377E+01	2.765E+00	4.251E-01
1.8000E-02	9.370E+01	2.952E+00	5.227E-01
1.9000E-02	9.363E+01	3.125E+00	6.336E-01
2.0000E-02	9.356E+01	3.286E+00	7.580E-01
2.1000E-02	9.349E+01	3.433E+00	8.963E-01
2.2000E-02	9.342E+01	3.566E+00	1.049E+00
2.3000E-02	9.335E+01	3.686E+00	1.216E+00
2.4000E-02	9.328E+01	3.793E+00	1.394E+00
2.5000E-02	9.321E+01	3.887E+00	1.586E+00
2.6000E-02	9.314E+01	3.969E+00	1.792E+00
2.7000E-02	9.307E+01	4.040E+00	2.009E+00
2.8000E-02	9.300E+01	4.100E+00	2.237E+00
2.9000E-02	9.293E+01	4.149E+00	2.475E+00
3.0000E-02	9.285E+01	4.190E+00	2.723E+00
3.1000E-02	9.278E+01	4.223E+00	2.978E+00
3.2000E-02	9.271E+01	4.250E+00	3.241E+00
3.3000E-02	9.263E+01	4.271E+00	3.508E+00
3.4000E-02	9.256E+01	4.288E+00	3.780E+00
3.5000E-02	9.249E+01	4.303E+00	4.055E+00
3.6000E-02	9.241E+01	4.316E+00	4.331E+00
3.7000E-02	9.234E+01	4.329E+00	4.608E+00
3.8000E-02	9.226E+01	4.344E+00	4.882E+00
3.9000E-02	9.219E+01	4.361E+00	5.154E+00
4.0000E-02	9.211E+01	4.383E+00	5.421E+00
4.1000E-02	9.204E+01	4.410E+00	5.683E+00
4.2000E-02	9.196E+01	4.444E+00	5.937E+00
4.3000E-02	9.188E+01	4.485E+00	6.184E+00
4.4000E-02	9.181E+01	4.535E+00	6.421E+00
4.5000E-02	9.173E+01	4.595E+00	6.648E+00
4.6000E-02	9.165E+01	4.665E+00	6.863E+00
4.7000E-02	9.157E+01	4.744E+00	7.067E+00
4.8000E-02	9.149E+01	4.834E+00	7.258E+00
4.9000E-02	9.142E+01	4.935E+00	7.436E+00
5.0000E-02	9.134E+01	5.046E+00	7.600E+00
5.1000E-02	9.126E+01	5.166E+00	7.750E+00
5.2000E-02	9.118E+01	5.296E+00	7.886E+00
5.3000E-02	9.110E+01	5.434E+00	8.007E+00
5.4000E-02	9.102E+01	5.580E+00	8.115E+00
5.5000E-02	9.094E+01	5.733E+00	8.209E+00
5.6000E-02	9.085E+01	5.891E+00	8.289E+00
5.7000E-02	9.077E+01	6.053E+00	8.356E+00
5.8000E-02	9.069E+01	6.218E+00	8.411E+00
5.9000E-02	9.061E+01	6.384E+00	8.453E+00
6.0000E-02	9.053E+01	6.550E+00	8.485E+00

TIME	SUM	V(2)	V(3)
6.1000E-02	9.044E+01	6.713E+00	8.505E+00
6.2000E-02	9.036E+01	6.873E+00	8.516E+00
6.3000E-02	9.027E+01	7.025E+00	8.518E+00
6.4000E-02	9.019E+01	7.175E+00	8.512E+00
6.5000E-02	9.010E+01	7.314E+00	8.498E+00
6.6000E-02	9.002E+01	7.443E+00	8.478E+00
6.7000E-02	8.993E+01	7.560E+00	8.452E+00
6.8000E-02	8.984E+01	7.663E+00	8.422E+00
6.9000E-02	8.976E+01	7.753E+00	8.387E+00
7.0000E-02	8.967E+01	7.826E+00	8.348E+00
7.1000E-02	8.959E+01	7.883E+00	8.307E+00
7.2000E-02	8.949E+01	7.923E+00	8.264E+00
7.3000E-02	8.940E+01	7.944E+00	8.219E+00
7.4000E-02	8.931E+01	7.947E+00	8.172E+00
7.5000E-02	8.922E+01	7.931E+00	8.124E+00
7.6000E-02	8.913E+01	7.895E+00	8.074E+00
7.7000E-02	8.903E+01	7.841E+00	8.024E+00
7.8000E-02	8.894E+01	7.769E+00	7.973E+00
7.9000E-02	8.885E+01	7.678E+00	7.921E+00
8.0000E-02	8.875E+01	7.570E+00	7.867E+00
8.1000E-02	8.866E+01	7.445E+00	7.812E+00
8.2000E-02	8.856E+01	7.305E+00	7.755E+00
8.3000E-02	8.847E+01	7.150E+00	7.695E+00
8.4000E-02	8.837E+01	6.982E+00	7.632E+00
8.5000E-02	8.827E+01	6.803E+00	7.566E+00
8.6000E-02	8.817E+01	6.614E+00	7.495E+00
8.7000E-02	8.808E+01	6.416E+00	7.420E+00
8.8000E-02	8.798E+01	6.212E+00	7.339E+00
8.9000E-02	8.788E+01	6.002E+00	7.252E+00
9.0000E-02	8.778E+01	5.818E+00	7.159E+00
9.1000E-02	8.768E+01	5.632E+00	7.058E+00
9.2000E-02	8.758E+01	5.453E+00	6.949E+00
9.3000E-02	8.747E+01	5.282E+00	6.832E+00
9.4000E-02	8.737E+01	5.119E+00	6.706E+00
9.5000E-02	8.727E+01	4.965E+00	6.572E+00
9.6000E-02	8.717E+01	4.820E+00	6.429E+00
9.7000E-02	8.706E+01	4.683E+00	6.277E+00
9.8000E-02	8.696E+01	4.554E+00	6.117E+00
9.9000E-02	8.686E+01	4.434E+00	5.948E+00
1.0000E-01	8.675E+01	4.322E+00	5.770E+00

APPENDIX VI

INSTRUMENTATION SERIAL AND MODEL NUMBERS

Component	Model	Serial
Velocity meter on M_1	*	159
Velocity meter on M_2	*	222
Velocity meter on M_3	*	109
Accelerometer on M_2	A5A-300-500	4369
Accelerometer on M_3	A5A-300-500	4012
Velocity Meter Control Unit	122C	101
Oscillograph	5-119	109025
Amplifier #1	1-113B	198BL10
Amplifier #2	1-113B	641BD09
Power Supply	2-105	245R4
1000 cycle	723-C	2326

*None available